DEPARTMENT FOR INTERNATIONAL DEVELOPMENT

STRATEGY FOR RESEARCH ON RENEWABLE NATURAL RESOURCES

NATURAL RESOURCES SYSTEMS PROGRAMME

FINAL TECHNICAL REPORT

DFID Project Number

R6750

Project title

Modelling soil organic matter transformations and nitrogen availability in periodically flooded soils

Project Leader

Jon Arah [1,3] and John Gaunt [2]

Organisation

[1] AAT Consultants, 15 Clerk Street, Edinburgh EH8 9JH
[2] Institute for Arable Crop Research, Rothamsted Experimental Station, Harpenden, Herts AL5 2JQ
[3] International Rice Research Institute, MCPO Box 3127, 1271 Makati City, Philippines

NRSP Production System

High Potential

Date

May 22nd 2000

Contents page

1. Executive summary

This project was contributes to the development and promotion of strategies to halt and reverse long-term yield decline in irrigated systems.

The project aimed to produce a model of soil organic matter (SOM) cycling in periodically flooded fields – such as those used for rice production – in order to predict the consequences on SOM "quality" and nutrient availability of anticipated changes in management (*eg* intensification of cropping, fertilizer addition and irrigation, alterations to the handling of residues).

The model was necessary because the available alternatives do not (i) specifically take into account the effects of variable oxygen (O_2) availability which mark these systems out as special; and (ii) are based on measurable rather than hypothetical SOM fractions and are therefore explanatory rather than predictive. The possible uses of such a model are many, extending beyond considerations of productivity and management – as prioritised here – to carbon (C) sequestration and climate change, and from predominantly to occasionally flooded soils.

In order to parameterise our model(s), we conducted a number of controlled-redox incubations. We also made field measurements designed to test our primary hypotheses that management affects soil redox potential E_h and E_h affects SOM cycling.

The major outputs of the project are the models SOMO and SUMO, the former providing a framework within which the transformations of measurable SOM fractions can be related to O_2 availability, the latter – which contains the former – integrating this framework within a larger one representing field-scale properties and crop growth. These models, written in the easy-to-understand ModelMaker^{TM} language, are freely available on request.

In addition, we examined the possibility – thrown up by the fact that 20 individual measurements (changes in the C, ^{13}C, N and ^{15}N compositions of 5 measured SOM fractions) might in principle serve to fix 20 individual unknowns (the fluxes between the fractions) – of *measuring* individual inter-fraction fluxes and hence reactivities. The analytical program SOMA– again freely available – automates this process. Success depends critically on the quality of the input data.

Field measurements were made in order to evaluate our hypothesis that management affects soil redox potential (E_h) and might therefore affect SOM cycling. Section 5.8 demonstrates that this is indeed the case.

Sensitivity analysis of SUMO demonstrates that system-level management affects SOM cycling and "quality". In the face of an indeterminate range of potential future management options, a model like SUMO is essential to evaluate their likely impacts.

2. Background

At the time (1996) this project was undertaken, it was feared that the N-use efficiency of intensively-irrigated rice production systems might be declining all over Asia (Cassmann *et al*, 1995). It was thought that this decline might be caused by changes in SOM "quality" brought about by prolonged periods of flooding-induced anoxia (Olk *et al*, 1996). No SOM transformation model was capable, even in principle, of reflecting such a phenomenon, since none took O_2-availability explicitly into account.

Thus the demand addressed by this project was the strategic need for fundamental understanding of soil organic matter (SOM) transformations necessary to evaluate the impact of changes in riceland management on soil fertility, and to identify ways to maintain or enhance that fertility.

Since 1996 the evidence for a widespread "yield decline" in intensively-irrigated rice has recently become less persuasive (Dobermann and Witt, 2000) but concerns still exist. Duxbury *et al*'s (2000) examination of yields in long term rice-wheat experiments showed rice yields declining in 8 out of 11 experiments, whilst wheat yields declined at only 3 sites. However, Dawe *et al* (2000) analysed long term yield trends in 47 long-term experiments in rice-rice and rice wheat systems in Asia and argued that yield declines are not very common, particularly at yield levels of 4-7t ha^{-1}.

However, it is universally accepted that anoxic decomposition pathways differ from oxic ones. The balance between oxic and anoxic processes depends on such variables as flooding and residue incorporation, most under some degree of human control. Management therefore affects the pattern of SOM cycling, and thereby controls SOM "quality", N supply, trace gas exchange and many other (agro)ecosystem properties of interest. The balance between oxic and anoxic processes depends on such variables as flooding and residue incorporation, most under some degree of human control. Thus whilst the project was originally justified in the context of concerns of declining fertility, the case for an improved treatment of SOM transformation in periodically-flooded soil remains compelling.

Jenkinson and Rayner (1977), and many others since, have modelled the turnover of soil organic matter (SOM) in terms of discrete conceptual pools, each with characteristic properties and a measure of reactivity (*eg* the first-order reaction constant *k)*. However, it is impossible to devise a procedure that will reliably extract SOM with a particular reaction constant. Thus such models can only be parameterised against system level outputs (eg. total soil C). Successful description at the system level does not guarantee process level accuracy. For the same reason it is not possible to make a measurement in an unknown field and predict future SOM decomposition. Recognition of these limitations has fuelled a debate as to whether we should aim to "model the measurable" rather than "measure the modelable" (Elliot *et al*, 1996; Magid *et al*, 1997).

If a model is based on measurable fractions, SOM pools are defined as fractions isolated by a specified experimental procedure rather than by their reactivity. This has the enormous potential advantage that the size of a SOM pool can be measured in any soil at any time. It has the corresponding drawback that the reactivity of a SOM fraction cannot simply be assumed to be constant (*eg* Smith *et al*, 1997).

We proposed to create an improved SOM transformation model differing from the established models (*eg Century*: Parton *et al*, 1987; *RothC*: Coleman & Jenkinson, 1996) in two critical respects:

i) rates and pathways of SOM decomposition should depend explicitly on O_2 concentration;

ii) the model should feature measurable SOM fractions (defined in terms of a specific extraction procedure) rather than hypothetical (un-measurable) SOM pools (defined in terms of first-order decay constants).

Given the strategic nature of this project, the uptake pathway for its outputs was the CGIAR (specifically, the International Rice Research Institute and an eco-regional programme, the Rice Wheat Consortium for the Indo Gangetic Plains), and national agencies in the region.

References

Cassman KG, de Datta SK, Olk DC, Alcantara J, Samson M, Descalsota J & Dizon M (1995) Yield decline and the nitrogen economy of long-term experiments on continuous irrigated rice systems in the tropics. In: *Soil Management: Experimental Basis for Sustainability and Environmental Quality* (Lal R & Stewart BA, eds) CRC/Lewis Publishers, Boca Raton, Florida, pp. 181-222.

Coleman K & Jenkinson DS (1996) RothC-26.3 – A model for the turnover of carbon in soil. In: *Evaluation of soil organic matter models using existing long-term datasets* (DS Powlson, P Smith & JU Smith, eds) NATO ASI series I 38, Springer-Verlag, Berlin Heidelberg, pp. 237-246.

Dawe D, Dobermann A, Moya P, Abdulrachman S, Lal P, Li SY, Lin B, Panaullah G, Sariam O, Singh Y, Swarup A, Tan PS, Zhen QX. (2000) How widespread are yield declines in long-term rice experiments in Asia? *Field Crops Research* 66: 175-193

Dobermann A & Witt C (2000) The potential impact of crop intensification on carbon and nitrogen cycling in intensive rice systems. In: *Carbon and Nitrogen Dynamics in Flooded Soils (*Kirk GJD and Olk DC, eds) International Rice Research Institute, Philippines, pp. 1-25.

Elliot E, Paustien K, Frey S. 1996. Modeling the measurable or measuring the modelable: a hierachical approach to isolating meaningful soil organic matter fractionations. In: *Evaluation of soil organic models using long-term datasets* (Powlson DS, Smith P and Smith JU, eds). NATO ASI Series I: Global Environmental Change 38: Springer-Verlag, Berlin Heidelberg. pp 161-181.

Duxbury JM, Abrol IP, Gupta RK & Bronson K. (2000) Analysis of soil fertility experiments in rice wheat rotations in S. Asia. RWC paper series no. 5. New Delhi. Rice wheat consortium for the Indo-Gangetic Plains and CIMMYT.

Jenkinson D, Rayner J. 1977. The turnover of soil organic matter in some of the Rothamsted Classical Experiments. *Soil Sci.* 123: 298-305

Magid J., Mueller T., Jensen L.S and Nielsen N.E. (1997) Modelling the measurable: Interpretation of field-scale CO_2 and N-mineralisation, soil microbial biomass and light fractions as indicators of oilsed rape, maize and barley straw decomposition. *In*: Driven by nature: Plant litter quality and decomposition. Eds. G Cadisch and K.E. Giller. pp 349-362.

Parton WJ, Schimel DS, Cole CV & Ojima DS (1987) Analysis of factors controlling soil organic matter levels in Great Plains grasslands. *Soil Science Society of America Journal* 51:1173-1179.

Olk DC, Cassman KG, Randall EW, Kinchesh P, Sanger LJ & Anderson JM (1996) Changes in chemical properties of organic matter with intensified rice cropping in tropical lowland soil. *European Journal of Soil Science* 47:293-303.

Smith P, Smith JU, Powlson DS, McGill WB, Arah JRM, Chertov OG, Coleman K, Franko U, Frolking S, Jenkinson DS, Jensen LS, Kelly RH, Klein-Gunnwiek H, Komarov AS, Li C, Molina JAE, Meuller T, Parton WJ, Thornley JHM and Whitmore AP, 1997 A comparison of the performance of nine soil organic matter models using datasets from seven long term experiments. *Geoderma*. 81: 153-225.

3. Project Purpose

In the context of concerns of declining productivity outlined above, the development opportunity that this project addressed was the need for basic understanding of the processes involved in turnover of soil organic matter under flood-induced anoxia in order to understand how changes in management affect nutrient supply.

At the time this project was written the NRSP programme output that it sought to address was "Strategies to halt and reverse long-term yield decline in irrigated systems developed and promoted". This was taken as the project's purpose. We proposed to create and testing a model of SOM turnover and N availability, as affected by flooding-induced anoxia, that could be used to identify sustainable and acceptable SOM-management options.

DFID's current RNR strategy and NRSP programme log-frames reflects the emphasis of the current Government on the elimination of poverty. The challenge remains to improve livelihoods of poor people through sustainably enhanced production and productivity of RNR systems. The models developed by this project provide a means to test the sustainability of changes in management.

4. Research Activities

The project was implemented at IRRI by post doctoral scientist Dr Haishun Yang recruited by IACR. A research assistant Ms Maribeth Zarate and technician Mr Andrew Revilleza were recruited as IRRI staff. Dr John Gaunt, IACR and Dr Jon Arah, ITE were appointed by IRRI as internationally recruited staff on secondment from their respective organisations. During the project Dr Arah left ITE to set up AAT Consultants. The sub-contract between IACR and ITE was terminated and a contract with AAT consultants established. The project team interacted with other scientists at IRRI through involvement in IRRI's research programme activities. IRRI provided extensive support through use of its facilities (laboratory and fields) as well as contributing to the costs of the project. IACR provided further technical support in design and construction of the controlled incubation systems (section 4.2) and chemical and mass spectrometric analysis of samples.

As outlined in section 2 we proposed to create an improved SOM transformation model (we call it SOMO) in which:

i) rates and pathways of SOM decomposition should depend explicitly on O_2 concentration;

ii) the model should feature measurable SOM fractions (defined in terms of a specific extraction procedure) rather than hypothetical (un-measurable) SOM pools (defined in terms of first-order decay constants).

Model feature (ii) entails variable SOM fraction reactivities, so the SOMO model must contain a mechanism for allowing that.

We further proposed to embed SOMO as a sub model within a structured field-scale model representing the reaction and transport of O_2. The field-scale model we had in mind was that (Arah & Kirk, 1996) employed in an earlier DFID project (EP R5305) to simulate CH_4 emissions from flooded soil. Finally, by performing a sensitivity analysis of the resulting compound model, we proposed to identify field-scale management variables most likely to affect SOM cycling, and their likely effects.

However, the link between the controlling parameters (depth-profiles of various reaction potentials and transmissivities) of the R5305 CH_4/O_2-distribution model and such management variables as flooding period and residue incorporation proved somewhat tenuous. In an attempt to render our field-scale model more immediately relevant we decided to employ instead an alternative dual-compartment O_2-distribution model (Arah, 1999) developed for the EU Riceotopes project. This model is simpler than R5305, and more suitable for extrapolation to field scale. We call the compound SOMO/Riceotopes model SUMO.

In order to parameterise our O_2-dependent SOM transformation submodel (SOMO), we proposed to design and construct a system that enabled us to conduct various soil incubations with added ^{13}C and ^{15}N isotope tracers under controlled redox (E_h) conditions and to follow the isotopes as they moved from fraction to fraction over the course of the incubation. This entailed the development and construction of the necessary controlled redox incubation system, and the adaptation of an existing SOM fractionation procedure (Sohi *et al*) for use with our soils.

Tracking 4 isotopes (^{12}C, ^{13}C, ^{14}N, ^{15}N) between 5 SOM fractions opens up the possibility of determining up to 20 independent unknowns. If inter-fraction N fluxes can be related to inter-fraction C fluxes (as, *eg*, ^{13}C fluxes are related to ^{12}C fluxes) then the 5-fraction system may be completely determined by 20 such unknowns. Were this to be the case, it would be possible to *measure* inter-fraction fluxes, allowing SOM fraction reactivity to be determined directly, SOM transformation models (including SOMO) to be tested directly, and SOM fraction assays to be used predictively. The result is an analytical program we call SOMA. This was undertaken in addition to contracted activities.

We also measured E_h in the field, to ascertain the effects of management (in particular the intensity of irrigated rice cultivation), and to back up these measurements with sampling and analysis of the SOM fractions – and their chemical properties as indicated by NMR – isolated by our fractionation procedure.

The following section describes the experimental activities, the results and models are described further in section 5. To assist the reader table 4.1 relates the sections of this report to the numbered output and activities of the project logframe (appendix 3).

Table 4.1 Guide to relate Activities and Outputs of our final log-frame to report sections

Report Section	reports on	Log-frame Activity / Output
4.1 Design and construction of incubation system		Activity 1.2.ii Output 1.2.ii
4.2 SOM fractionation procedure		Activity 1.2.i Output 1.2.i
4.3 Controlled incubations		Activity 1.2.iii
4.4 Field measurements		Activity 1.2.iv
5.1 Incubation data		Output 1.2.iii
5.2 Analysis of dual-labelled controlled incubation data (SOMA)		
5.3 Oxygen-dependent SOM transformation submodel (SOMO)		Activity 1.1.i Output 1.1.i
5.4 Field-scale model (SUMO)		Activity 1.1.ii Output 1.1.ii
5.5 SOMA analysis		
5.6 Preliminary optimisation of SOMO parameters		Activity 1.3 Output 1.3
5.7 Sensitivity analysis of SUMO model		Activity 2.1, 2.2 Output 2.1, 2.2
5.8 Field data		Activity 1.4 Output 1.2.iv, 1.4

Log-frame Activity 2.3 and Output 2.3 (management strategies for reversing yield decline/better management of SOM cycling identified) are not reported on since we have as yet been unable satisfactorily to parameterise SOMO. Therefore deriving strategies would be inappropriate.

Report Sections 5.2 and 5.5 (SOMA) report the additional work we did on the direct measurement of SOM inter-fraction fluxes using dual isotope tracing. As explained, this would allow for the development of predictive soil tests for future C and N flow and give a precise meaning to the term “quality” as applied to SOM.

4.1 Design and construction of incubation system

The incubation setup consists of a computer interfaced datalogging and control system (Appendix A4.1) and incubation vessels placed on a shaker (Fig.4.1.1). The datalogging and controlling system performs two functions. First, it monitors and records the data of E_h, pH and temperature of the soil slurry in individual incubation vessels. Second, it controls the E_h of the vessels at target levels which are set in advance. E_h control is achieved by activating the air pump connected to a vessel – introducing O_2 – when the E_h inside the vessel drops below the target value, and then switching it off once the E_h rises above the target value.

The system – hardware and software – was designed, assembled and programmed by Richard Le Fevre of the Bioinformatics Department, IACR Rothamsted. It has 32 voltage-based input channels for either Eh or pH or combined, 16 temperature input channels, and 48 output channels for controlling devices such as air pumps. It monitors the input signals such as E_h, pH and temperature in a continuous manner, and records the data into a logger at a preset interval. Data monitored can be displayed on a computer monitor, and the logged data can be downloaded to the computer. The individual input channels can be set to a threshold with a dead band as a buffer. When the threshold is reached (from above or below, depending on setting), a corresponding output channel is switched on to activate a device such as an air pump. The output channel is switched off when the input signal reaches the level of threshold + buffer. For details of the system refer to Appendix A4.1.

Flasks of 2 L in volume were used to conduct the incubation. They are sealed with rubber stoppers except during soil sampling. E_h and pH electrodes, and air inflow and outflow tubes are inserted through stoppers. Pre-test showed that a soil slurry in the ratio of 3 water : 1 soil was needed in order to achieve a reasonably homogeneous soil environment for the incubation. Flasks were placed on a shaker which runs through the entire incubation. To avoid possible influence of light on microbial activities, the bottles were covered by black cloth.

The whole setup, in particular the datalogging and controlling system, was tested and modified several times before starting the incubations required by the project.

Control of Eh

Target E_h values were given to the controller as thresholds, below which air pumps would be activated to bring in O_2 to raise the E_h up to the threshold values. The underlying assumption was that soil E_h would drop upon addition of fresh C (such as straw) when the supply of O_2 – the major electron acceptor – is limited, as in flooded conditions. The system cannot drive down soil E_h once it is above the threshold, unless this occurs naturally, because no provision was made for addition of reductants (which would be objectionable since they do not commonly occur in nature). Although the flasks were flushed with N_2 during sampling, O_2 unavoidably introduced during the process can cause irreversible oxidation (increase in E_h), especially after the period (normally the first month) of intensive microbial activity.

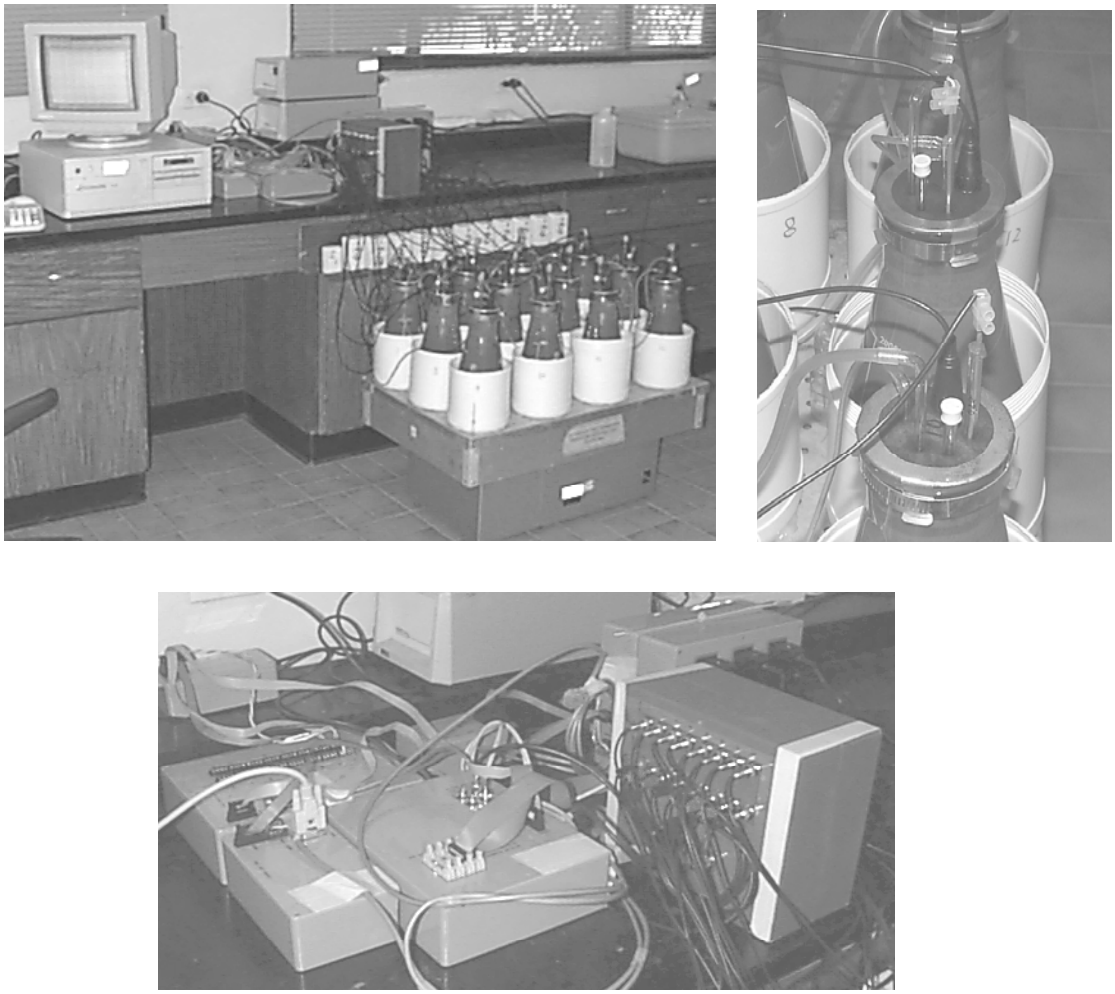

Fig.4.1.1 Incubation system. Top left: general view. Top right: flasks sealed and equipped with electrodes inflow tubes. Bottom: computer interfaced datalogging and E_h control system.

4.2 SOM fractionation procedure

Fractionation of soil organic matter (SOM) is the key to tracing C and N transformations for both incubation experiments and field trials. A fractionation protocol (Fig.4.2.1) developed at IACR Rothamsted (Sohi et al. *submitted*), developed for upland (drained) soils, was adopted and tested for our rice soils. It proved to be applicable with the following minor modifications:

- As soil taken directly from a paddy field or incubation is over-saturated, centrifugation becomes necessary to get rid of the extra water in order to avoid significant dilution of separation medium (NaI solution). Decanted supernatant and the separated floating materials are combined into the soluble fraction and free light fraction (LF_1), respectively (see Table 4.2.1).

- The solution at the end of the fractionation procedure is kept as the soluble fraction (SOM 2). Its C and N contents are analysed. Because sodium iodide NaI in the solution interferes with the oxidation reaction in the C analysis by dichromate oxidation, silver nitrate $AgNO_3$ was used to first precipitate iodide I^{-1}.

The fractions which we report elsewhere as SOM fractions 1-5 correspond on this scheme to SOM fractions as follows (Table 4.2.1):

Table 4.2.1 SOM fractions

Sohi/Gaunt fraction	R6750 fraction
Gaseous	1
Soluble (retained – LF_1 – LF_2 – HF)	2
LF_1	3
LF_2	4
HF	5

Testing the fractionation procedure for suitability involved two aspects. First we wanted to be sure that the procedure does indeed extract SOM fractions which are chemically distinct. We fractionated a triple rice soil from IRRI's long-term field experiment (see Section 4.4) and submitted the LF_1 and LF_2 fractions to NMR (nuclear magnetic resonance) analysis for functional groups. Results are illustrated in Fig.4.2.2.

SOM Fractionation Procedure

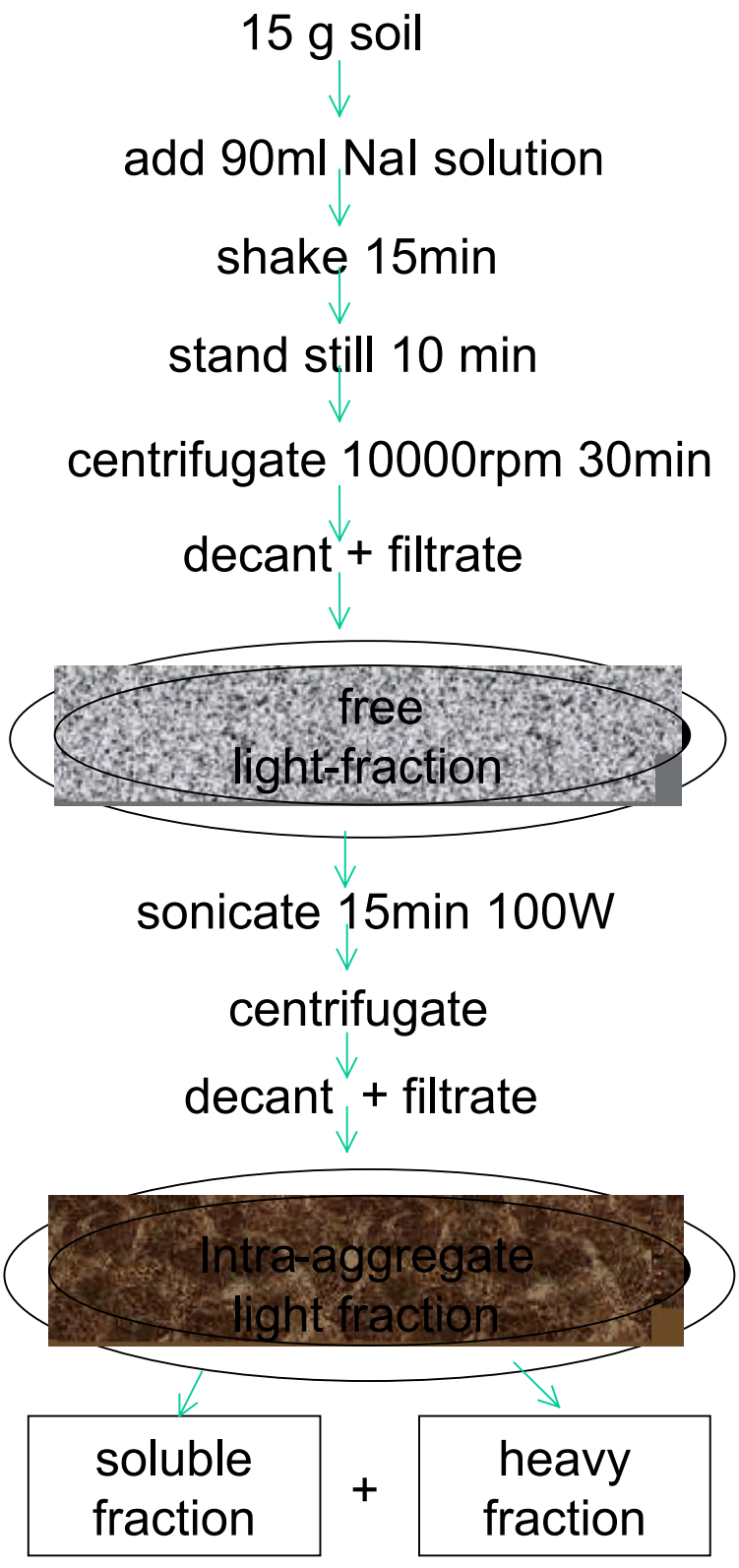

Fig.4.2.1. SOM fractionation procedure

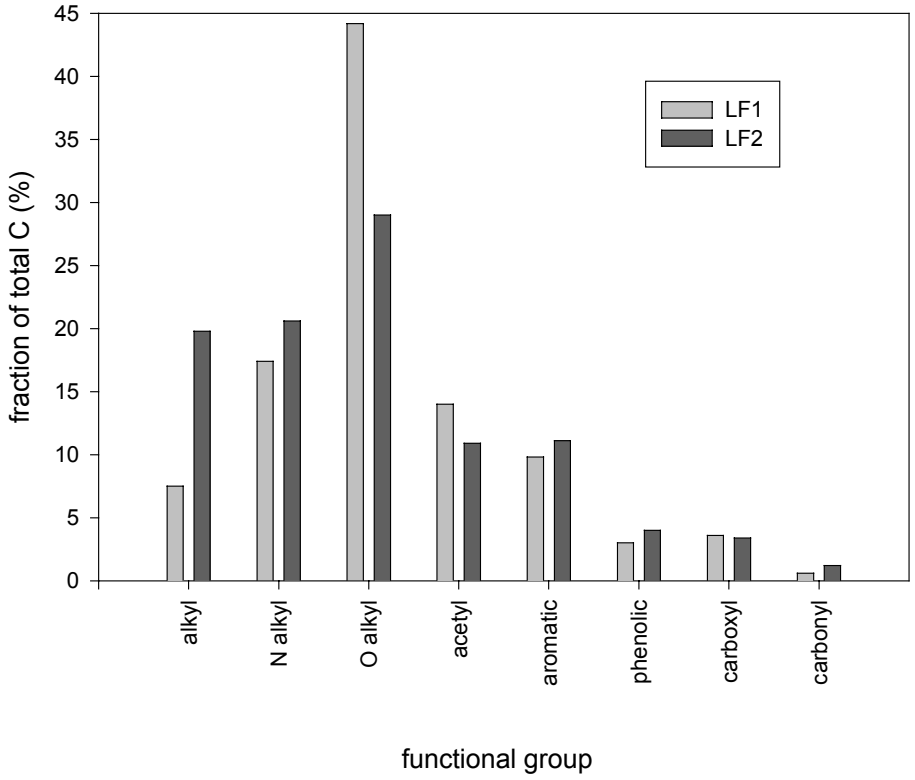

Fig.4.2.2. Functional groups revealed by NMR analysis of SOM fractions LF_1 and LF_2 from a triple rice soil.

Alkyl C and O-alkyl C – important indicators of organic matter state – differ, and in different ways, between the 2 fractions. Specifically, the content of alkyl C in the intra-aggregate light fraction LF_2 is significantly higher than that in the free light fraction LF_1, where the opposite is true for O-alkyl C. This suggests that the former fraction is more humified than the latter, and demonstrates the suitability of the fractionation protocol.

Secondly, we wanted to ascertain the effects of sample pre-treatments on the results of fractionation. This is important because the protocol (Fig.4.2.1) calls for field fresh samples, but sometimes only air dried or freeze dried samples are available. We compared 5 commonly used methods of soil pre-treatment, as detailed in Table 4.2.2.

Table 4.2.2 Soil pre-treatments examined

pre-treatment code	pre-treatment
1	field fresh sample with only hand mixing
2	air dried in blocks and rewetted by capillarity in 2 days
3	air dried, ground to pass 2 mm sieve, rewetted by adding water
4	freeze dried in blocks and rewetted by capillarity in 2 days
5	freeze dried, ground to pass 2 mm sieve, and rewetted by adding water

The 2 soils used for the tests were the IRRI LTE double rice soil triple rice soil, chosen because they are the soils we used in our incubation experiments. Fig.4.2.3 shows the effect of sample pre-treatment on C fractionation; Fig.4.2.4 the equivalent for N.

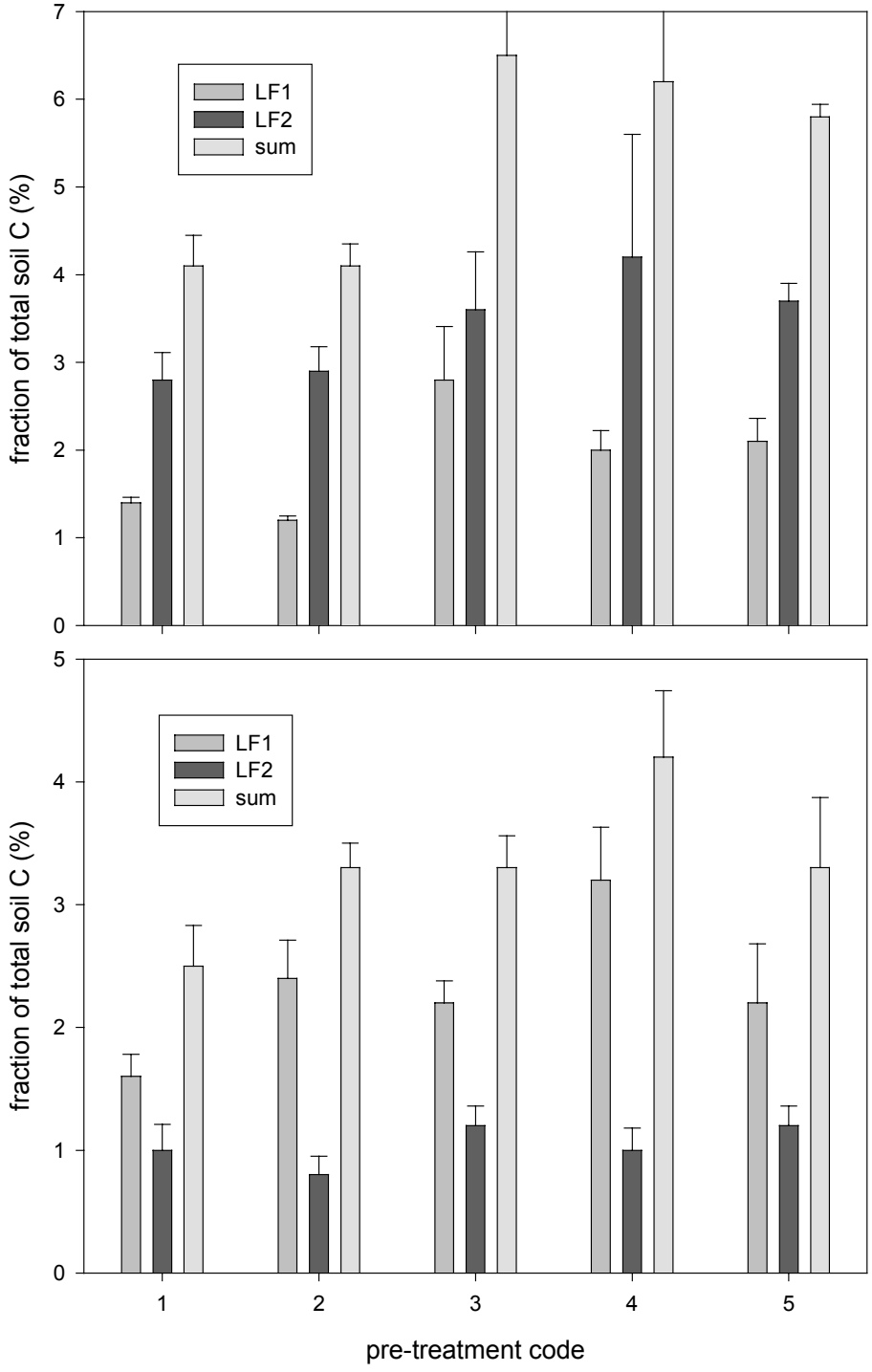

Fig.4.2.3. Effect of soil sample pre-treatment on C fractionation; top : triple rice soil; bottom : double rice soil.

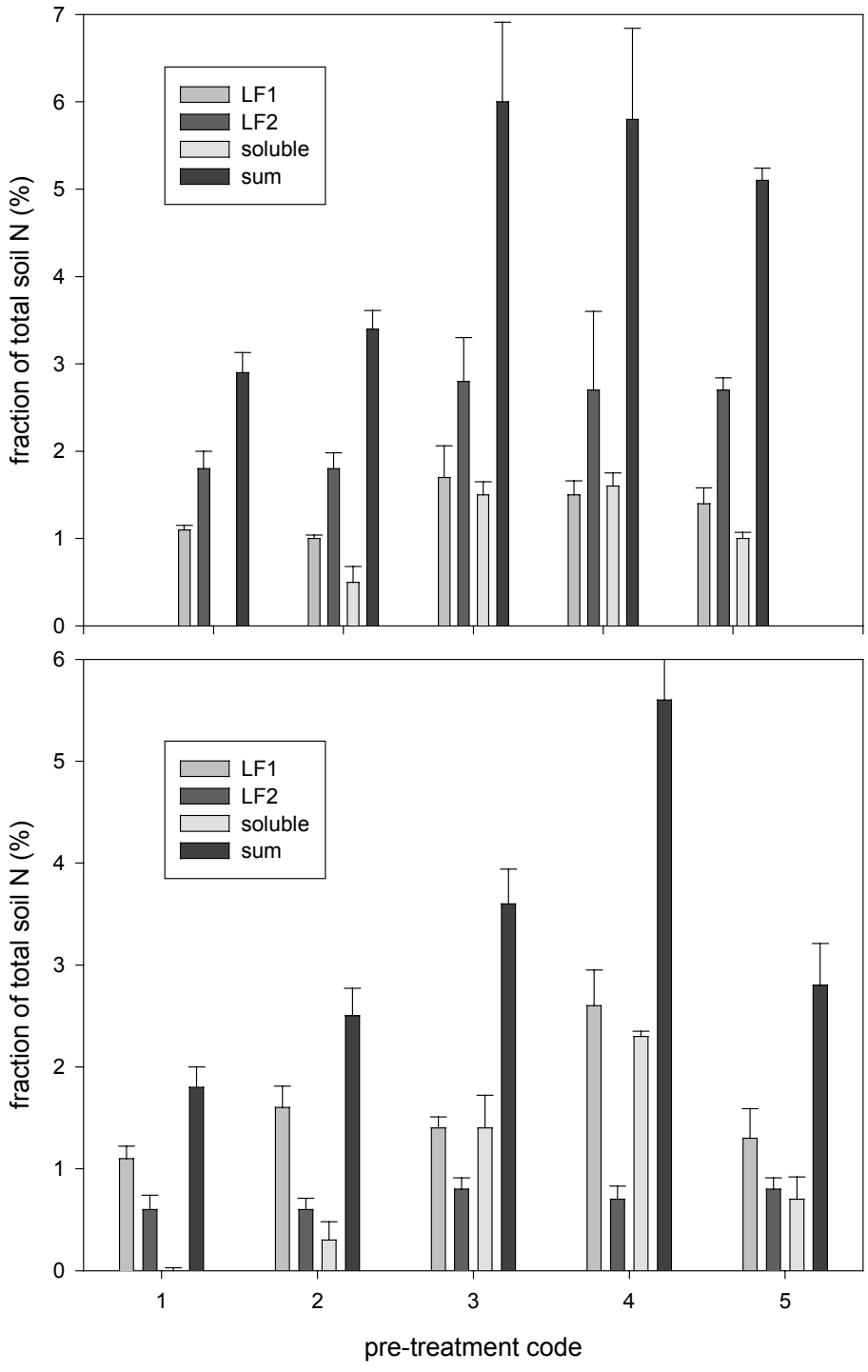

Fig.4.2.4. Effect of soil sample pre-treatment on N fractionation; top : triple rice soil; bottom : double rice soil.

In general, treatments 3 (air-drying + grinding + rewetting) and 4 (freeze-drying + capillary rewetting) resulted in the biggest perturbations to the control (field-fresh) distribution, while treatment 2 (air-drying + capillary rewetting) caused the least. It appears that the bigger the disturbance to soil micro structure, the bigger the influence. For instance, it is very likely that freeze drying or grinding causes more breakdown of soil micro aggregates than air-drying and capillary rewetting. Further, impacts of pre-treatment seem to be greater on the free light fraction LF_1 than on the intra-aggregate light fraction LF_2, probably because the latter is to some extent stabilised by physicochemical fixation and occlusion.

For N (Fig.4.2.4), a significant amount of soluble N was found when the soil was first dried and then rewetted, as in treatments 2 to 5. This is likely due to the strong N mineralization after rewetting of dried soil reported in many previous studies.

Based on these results, we decided to use only fresh soil samples in order to avoid possible side effects by pre-treatment, in particular for soluble N which is important for tracing N transformation.

Reference

Sohi S, Mahieu N, Arah J, Gaunt J. A procedure for isolating soil organic matter fractions suitable for modelling. *Soil Science Society of America Journal* (submitted).

4.3 Controlled incubations

Four consecutive incubation runs were conducted with identical treatments but using 2 different soils from the IRRI research farm. Each run lasted 100 days and comprised 2 replicates. The first 2 runs used the double-rice soil from Field L6/L7 of the IRRI farm, the last 2 the triple-rice soil from the Long Term Continuous Cropping Experiment (LTCCE). The double-rice soil receives a dry fallow of 2 or 3 months each year, while the triple-rice soil is flooded all year around. ^{15}N labelled maize straw (itself differentially ^{13}C-labelled with respect to rice residues) was used to permit the tracing of both C and N without confounding with other sources. The incubations were conducted in the laboratory at constant temperature of 25°C.

Treatments

We were interested in the effects on SOM cycling of O_2 availability and – secondarily – of N addition, and we took the redox potential E_h to be a (ball-park) indicator of O_2 availability. E_h level and N input were therefore the two factors forming the treatments. We targeted 3 levels of soil E_h and 2 levels of N input as indicated in Table 4.3.1:

Table 4.3.1 Incubation E_h and N treatment codes.

N level	E_h level		
	low	medium	high
N_0	1	2	3
N_{150}	4	5	6

Here N_0 denotes no N addition, N_{150} an addition equivalent to 150 kg NO_3-N ha^{-1}, low E_h a target value of –200 mV, medium E_h –100 mV and high E_h 0 mV.

The three E_h levels were selected because aerated soil has E_h above 0 mV, and typical flooded soil shows E_h around -200mV; -100mV was thus considered as a suitable intermediate value. The N input rate of 150 kg N ha^{-1} represents a typical high input in practice at present. N_0 is a control.

All incubations were conducted in quadruplicate for each soil, in a sequence of 4 runs designed to eliminate – or at least to minimise – sequential position as a possible factor.

Soil and gas samplings

Soil of about 50 g dry weight was taken from each flask 8 times in each run, at day 0 (just prior to adding straw and N fertilizer), day 1, day 3, day 7, day 15, day 40, day 70, and day 100. The headspace gas was also sampled at each time of sampling. Soil samples were fractionated using the procedure described above, followed by chemical analysis of all fractions for total C and N, ^{15}N and ^{13}C. Gas samples were analysed for CO_2 and CH_4.

4.4 Field measurements

Two field trials were conducted, each lasting 1 cropping season. The first was in the 1999 dry season (DS: Jan-Apr 1999), the second in the following wet season (WS: Jul-Oct 1999) after a 2 month fallow. They were conducted within an on-going long-term experiment (LTE) which investigates the effects of different schemes of fertilizer, water and straw management on soil nutrient characteristics and rice yield. The relevant factors in the treatments of this on-going host experiment include:

2 schemes of straw management: removal (S_0), incorporation (S_1)
2 rates of fertilizer: low (F_0), high (F_1)
2 schemes of water management: dry fallow (W_0), flood fallow with mid-season drying (W_2)

Our first field trial aimed to look at the effect on SOM transformations of fertilizer N in soil under contrasting schemes of straw and water management. We examined the following 4 treatments:

Table 4.4.1. Treatments examined in field experiment 1.

treatment	water management (W)	straw management (S)
1	0	0
2	0	1
3	2	0
4	2	1

In each case the N input rate was 150 kg N ha^{-1}, applied in 1 basal (30 kg N ha^{-1}) and 3 equal top-dressings. In order to avoid confounding with top-dressed N, only the basal dose received ^{15}N labelled $(NH_4)_2SO_4$. The soil was sampled five times throughout the season, *ie* prior to transplanting, 1, 3 and 6 weeks after transplanting, and at harvest. Soil E_h at 3, 7, 15 cm below the soil surface, and soil pH and temperature of each plot were measured 2 to 3 times per week.

The second field trial was designed to look at the effect of mineral N input rate and water management on transformations of C and N from incorporated straw. Four treatments, as in Table 4.4.2, were examined.

Table 4.4.2. Treatments examined in field experiment 2.

treatment	water management (W)	fertilizer addition (F)
1	0	0
2	0	1
3	2	0
4	2	1

^{15}N labelled rice straw was incorporated in all treatments at the rate of 8 t ha^{-1}. For N fertilizer, non-labelled $(NH_4)_2SO_4$ was used in order to avoid confounding with N from the straw. The soil was sampled 7 times throughout the season, *ie* prior to transplanting, 3, 7, 15, 40 and 70 days after transplanting and at harvest. Soil E_h was measured in the same way as in the first trial.

Field setup

Since the 2 field trials, hosted in an on-going experiment, involved additions of ^{15}N tracer, the area involved had to be much smaller than that of the host plot, and isolated to avoid loss of the tracer. Moreover, the use of ^{15}N as a tracer requires destructive sampling, which is also objectionable in a long-term experiment. We therefore used bottomless PVC pots 20 cm in diameter and 30 cm in height, inserted down to the subsoil in the host plots. For the first field trial 4 pots were installed in each host plot to enable 4 separate destructive soil samplings. For the second field trial, 6 pots were installed in each host plot to enable 6 destructive soil samplings. Each pot received 1 rice seedling.

In order to measure soil E_h at fixed locations throughout the season, we mounted onto steel frames 3 E_h electrodes with tips at 3 different depths, and installed 4 such frames in each plot (Fig.4.4.1).

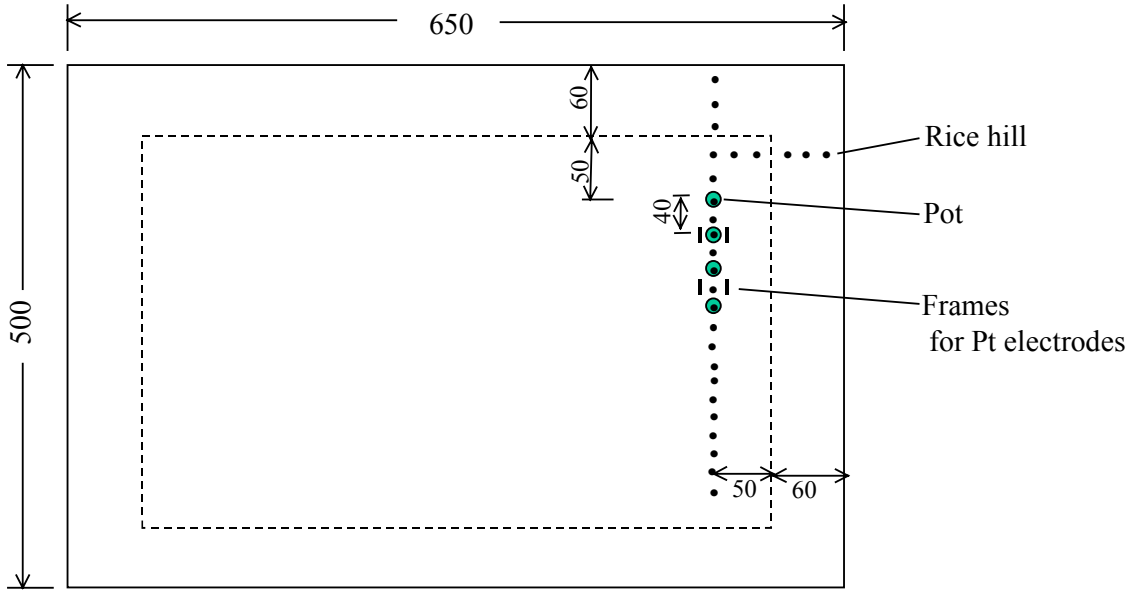

pot size: 20 cm in dia, 30 cm high
plot area: 5 x 6.5 m
width of protection belt: 3 rows (or 60 cm)
distance between hills: 20 cm

Fig.4.4.1 Layout of field experiments. All units are cm except otherwise indicated.

5. Outputs

This project linked experimental and modelling activities and the outputs of the project were specified as process based models of soil C and N transformations with the necessary data for parameterisation and testing.

As described above (section 4) the modelling framework developed by this project consists of three models; a SOM transformation model SOMO based on measurable SOM fractions, where rates and pathways of SOM decomposition should depend explicitly on O_2 concentration; SOMU a structured field-scale model representing the reaction; and SOMA an analytical program, allowing SOM fraction reactivity to be determined, SOM transformation models (including SOMO) to be tested directly, and SOM fraction assays to be used predictively.

By performing a sensitivity analysis of the resulting compound model, we examined field-scale management variables most likely to affect SOM cycling, and their likely effects.

These outputs are described in more detail below.

5.1 Incubation data

Soil redox potential E_h

The E_h records of the four incubation runs are shown in Fig.5.1.1. The treatments led to significant differences between the 3 target E_h settings, though the absolute E_h levels could not be maintained at the targets set in advance, especially after the first month. This is probably largely due to the excess O_2 inevitably introduced during soil sampling, exacerbated by the fact that mineralisation generally declines over time. As discussed above (section 4.1), our incubation system allowed for the introduction of O_2 to drive E_h up, but not for the addition of alternative reductants to drive it down.

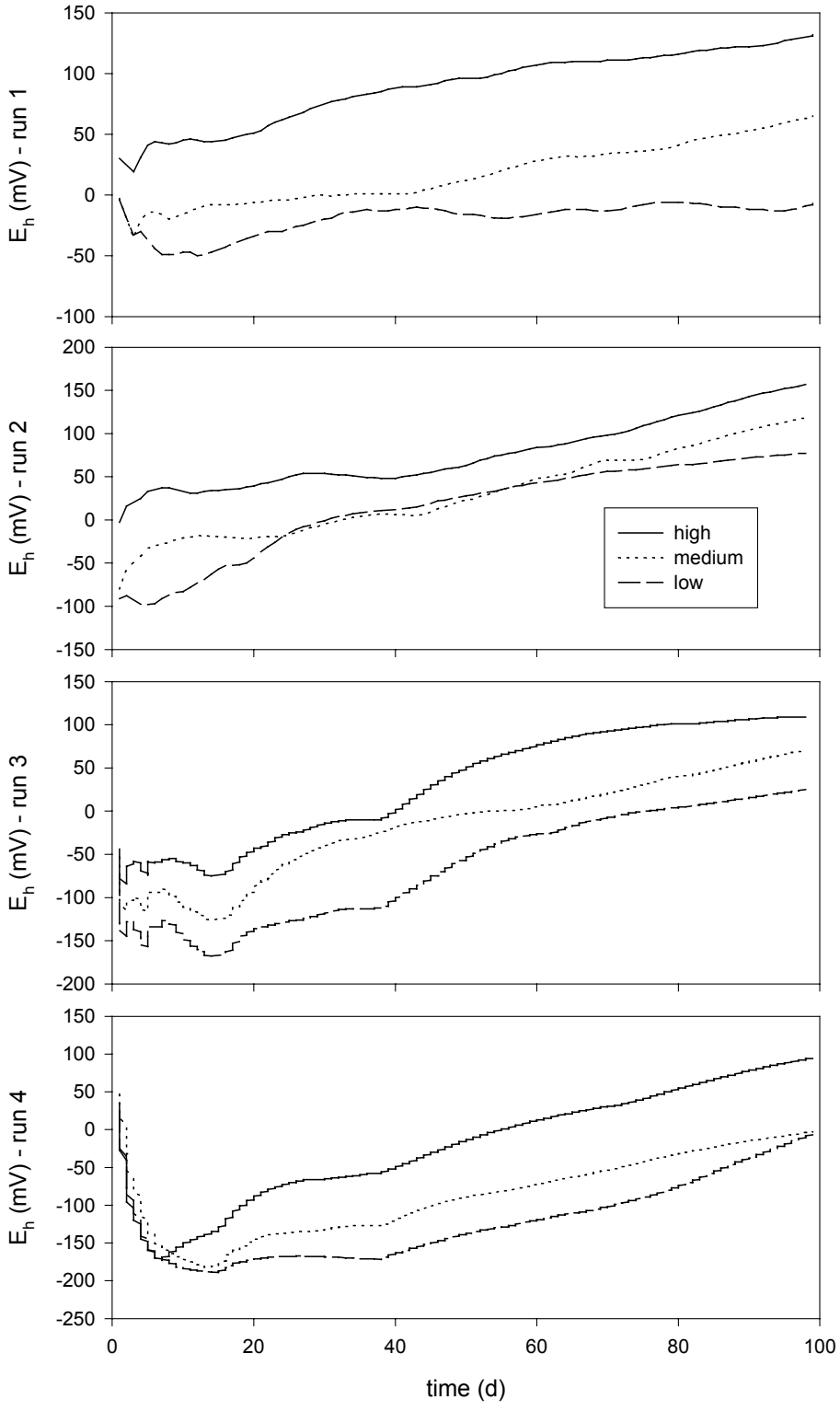

Fig.5.1.1 System E_h against time: 4 incubation runs.

Soil pH

A typical pH record is shown in Fig.5.1.2. As expected, the soil pH under flooded conditions tends to stabilize around 6.5.

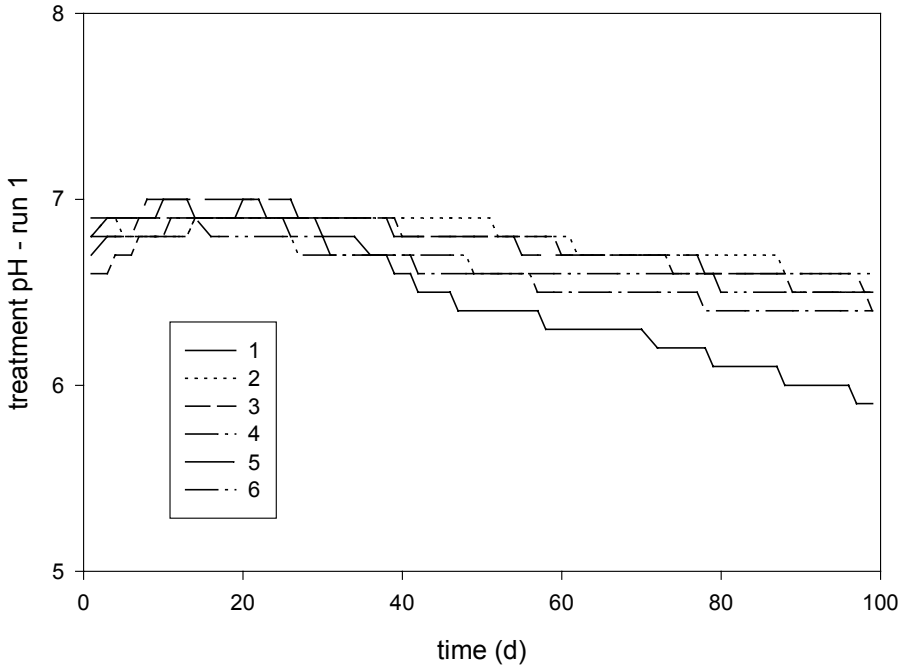

Fig.5.1.2 System pH against time: incubation run 1.

SOM fraction concentrations

Temporal trajectories of measured SOM fraction concentrations (Y_i) are illustrated in Appendix 5.1.1; normalised rates of change ($\Delta Y_i/\Delta t$) in Appendix 5.1.2. In all cases, concentrations Y_1 (gas fraction) and Y_5 (heavy fraction) are derived from measurements of Y_2 (soluble fraction), Y_3 (light fraction 1), Y_4 (dispersible light fraction 2) and total (retained) concentration Y_T as follows:

$$Y_5 = Y_T - Y_2 - Y_3 - Y_4 \quad [1]$$

$$Y_1 \text{ (time } t) = Y_0 + Y_T \text{ (time 0)} - Y_T \text{ (time } t) \quad [2]$$

where Y_0 is an (arbitrary) quantity representing the initial concentration in the headspace (the value of Y_0 is immaterial since in the analysis presented below we assume no C or N fixation). Error bars represent standard deviations calculated from the 4 replicates of each E_h treatment and the 6 of each N treatment.

Concentration units in Appendices A5.1.1 and A5.1.2 are μmol g^{-1} (mol m^{-3} assuming a density of ~1 g cm^{-3}) as required for modelling. In the rest of this section, we summarise our data in the more familiar units of mg g^{-1} (for concentrations), parts per mil (for ^{13}C atom excess) and % (for ^{15}N atom excess):

$$^{13}\text{C atom excess (per mil)} = 1000\ (\gamma - \gamma^o) \quad [3]$$

$$^{15}\text{N atom excess (\%)} = 100\ (\alpha - \alpha^o) \quad [4]$$

where γ (γ^o) is the (background) ^{13}C atom fraction and α (α^o) the (background) ^{15}N atom fraction.

Effect of E_h

Low soil E_h tends to slow down the decomposition of newly added straw (Fig.5.1.3). At the end of 100 days, the soil incubated at the low E_h setting had ^{13}C concentration significantly higher than those of the medium and high E_h settings, indicating slower break down of C from maize straw under low E_h. This trend cannot be seen from the total C concentrations, clearly demonstrating the usefulness of the ^{13}C tracer in such studies. For N, both total N and ^{15}N results showed similar trends.

As the free light fraction (LF_1; SOM fraction 3) was composed largely of semi-decomposed organic matter, the higher ^{15}N concentration in this fraction at low soil E_h setting (Fig.5.1.4) further confirms the slower decomposition of recently added organic material at low soil E_h. But the effect on intra-aggregate (LF_2; SOM fraction 4) C and N is not clear from the data available so far. Low E_h also seems to conserve soluble N (Fig.5.1.5).

The slower decomposition of organic C and N at low soil E_h was probably attributable to depressed microbial activity at limited availability of O_2, the major electron acceptor. Moreover, the limited O_2 supply may have also resulted in the conservation of soluble N – presumably mainly in mineral form. This is because NH_4^+ released during anoxic straw decomposition would not be oxidized to NO_3^- which is prone to loss by denitrification. Such a conservation effect in low soil E_h would imply that more N would be potentially available, as NH_4^+, for the crop.

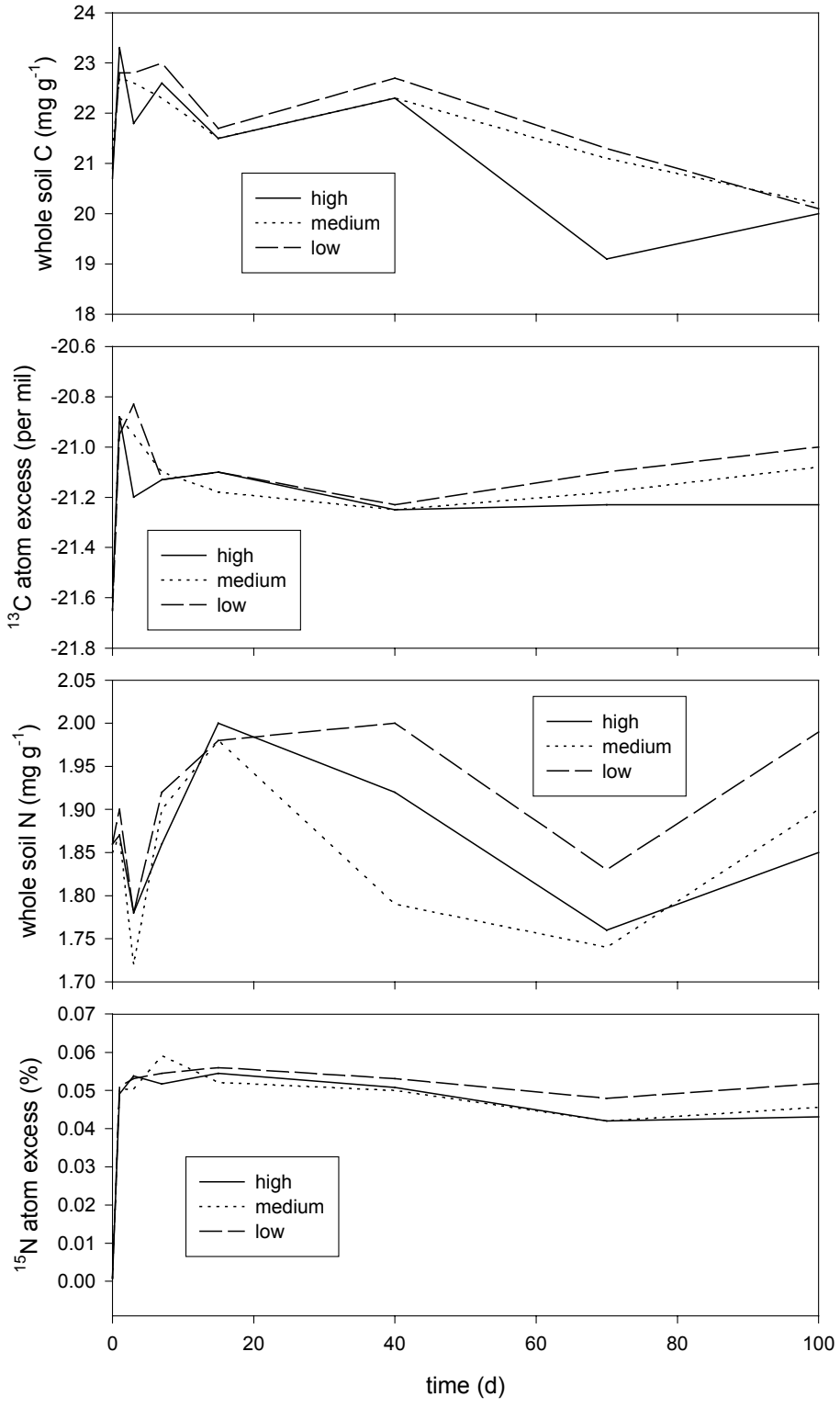

Fig.5.1.3 Whole soil C, ^{13}C, N and ^{15}N concentrations and atom excesses as affected by E_h setting: run 1.

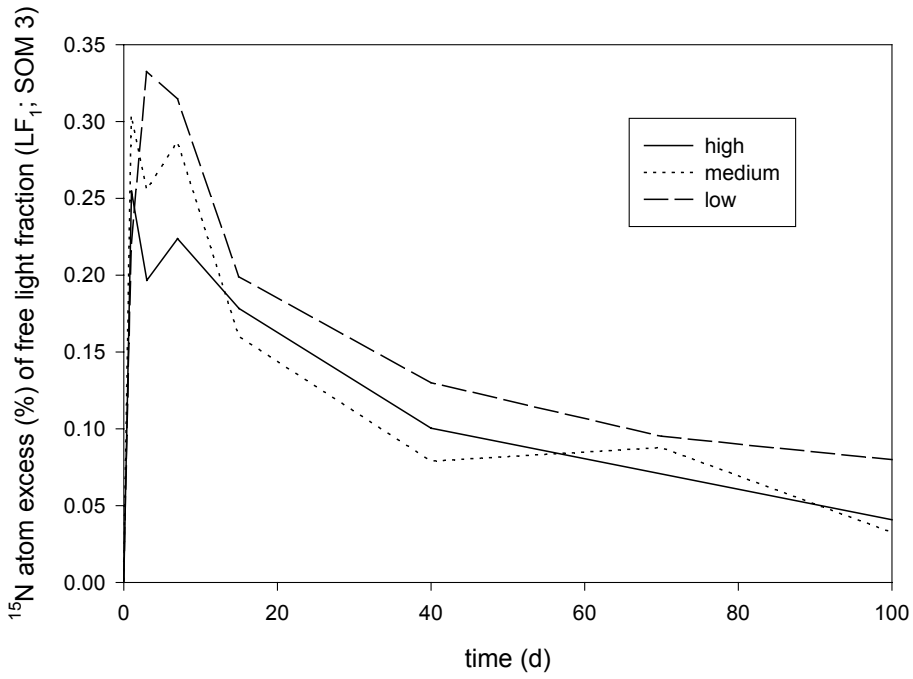

Fig.5.1.4 SOM fraction 3 (LF_1) ^{15}N atom excess as affected by E_h setting: run 1.

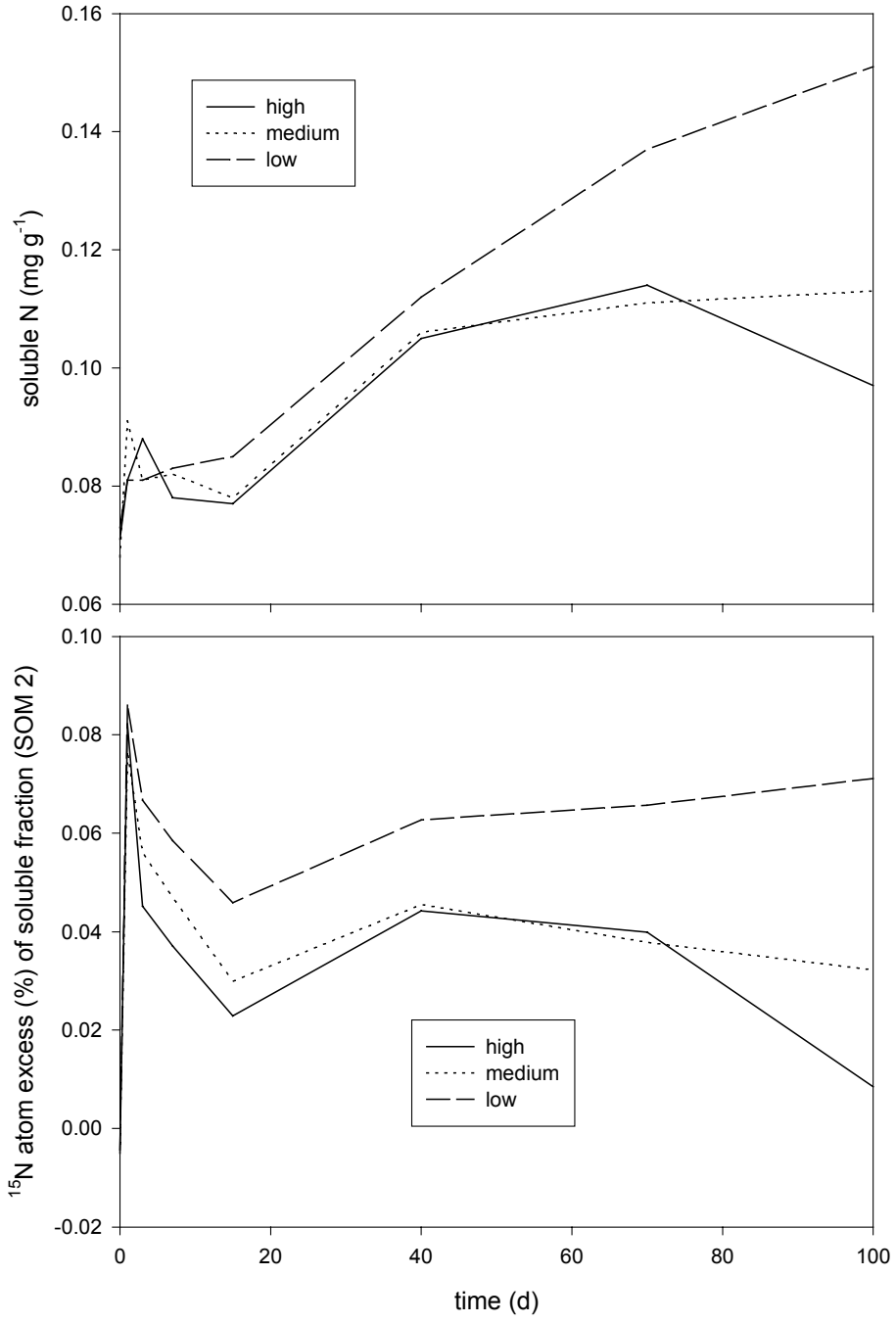

Fig.5.1.5 SOM fraction 2 (soluble) N concentration and ^{15}N atom excess as affected by E_h setting: run 1.

Effect of mineral N

Whole soil sample data (Fig.5.1.6) show that with addition of 150 kg N ha^{-1} more straw was decomposed, indicating an enhancement effect of mineral N on straw mineralization. The effect can also be seen from the ^{13}C concentration of the free light fraction (LF_1; SOM 3; Fig.5.1.7) and the intra-aggregate light fraction (LF2; SOM 4; Fig.5.1.8), though it is not obvious from the ^{15}N data. Such an enhancement of decomposition with added N has been seen in many previous studies, and is due to increased microbial activity where N is freely available.

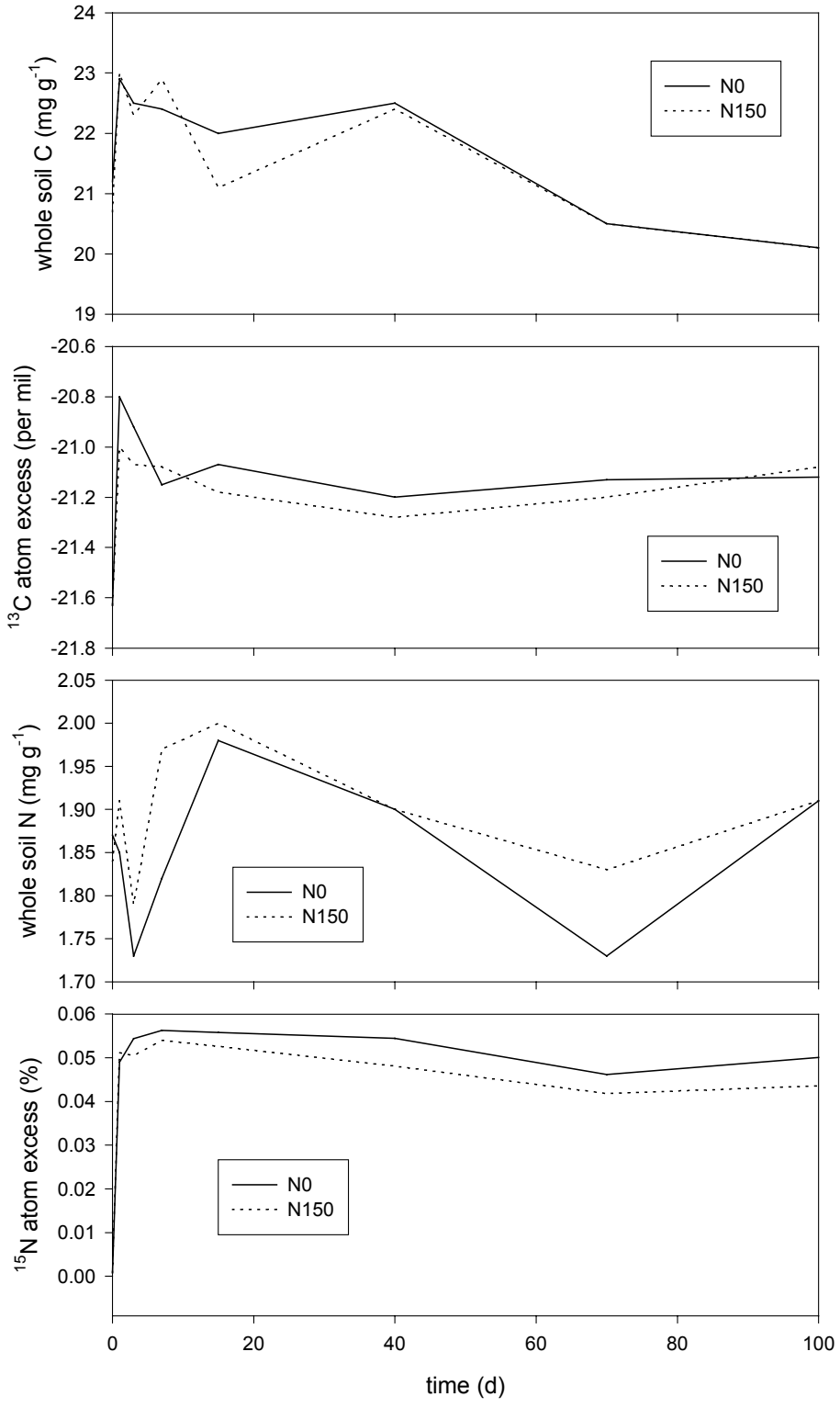

Fig.5.1.6 Whole soil C, ^{13}C, N and ^{15}N concentrations and atom excesses as affected by mineral N addition: run 1.

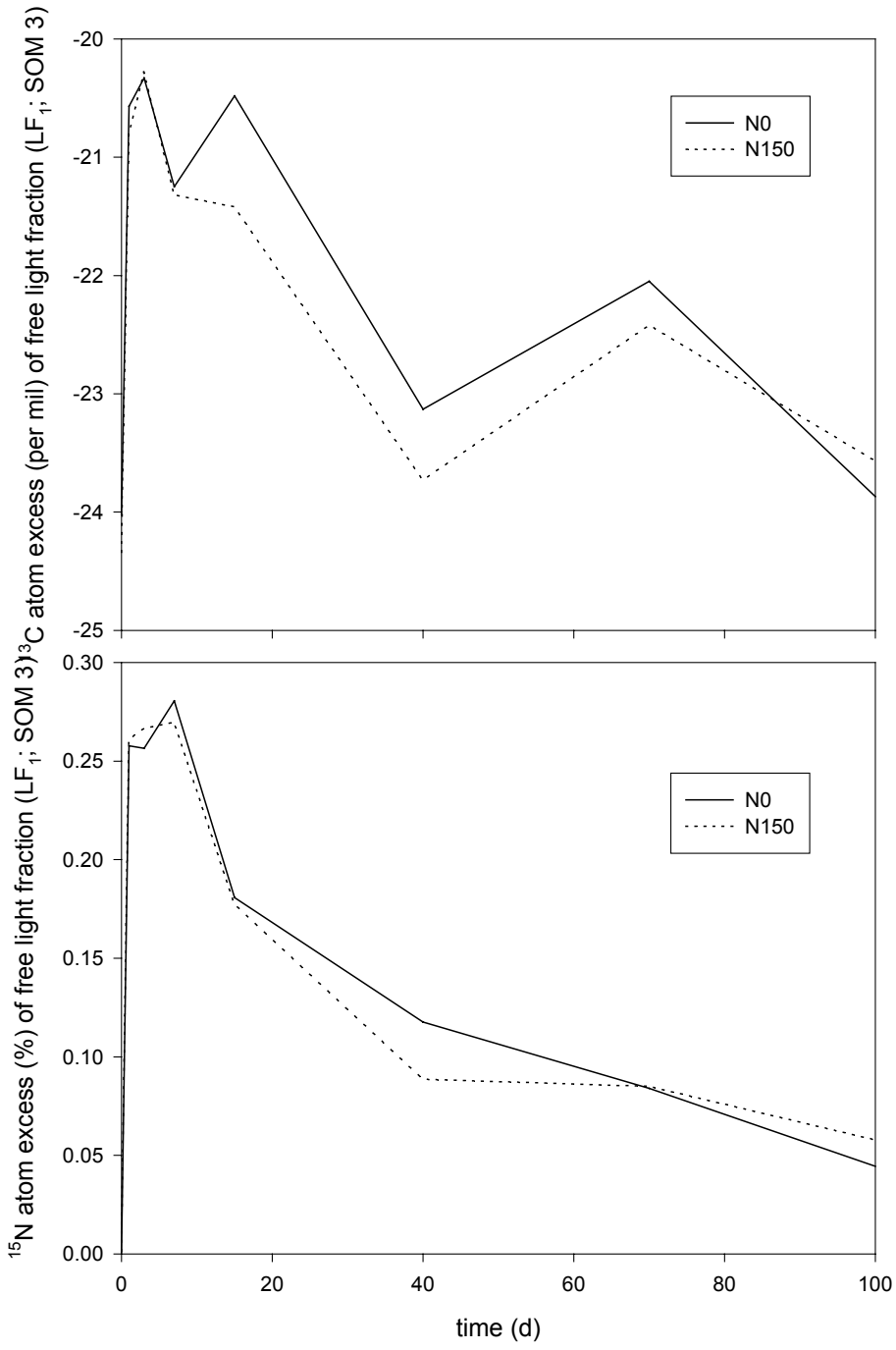

Fig.5.1.7 SOM fraction 3 (LF_1) ^{13}C and ^{15}N atom excesses as affected by mineral N addition: run 1.

5.2 Analysis of dual-labelled controlled incubation data (SOMA)

We follow here the notation of Arah (2000). There are five mutually exclusive and exhaustive SOM fractions, denoted by subscript *i*. Fraction 1 is gaseous, fraction 2 soluble. The $^{(13)}$C flux from fraction *i* to fraction *j* is $^{(13)}J_{ij}$; the corresponding $^{(15)}$N flux $^{(15)}F_{ij}$. Then, by definition:

$$\frac{\Delta C_i}{\Delta t} = \sum_{j \neq i}^{5} J_{ji} - \sum_{j \neq i}^{5} J_{ij} \qquad (1 \le i \le 5) \qquad [1]$$

$$\frac{\Delta N_i}{\Delta t} = \sum_{j \neq i}^{5} F_{ji} - \sum_{j \neq i}^{5} F_{ij} \qquad (1 \le i \le 5) \qquad [2]$$

and, assuming negligible discrimination between stable isotopes:

$$\frac{\Delta {}^{13}C_i}{\Delta t} = \sum_{j \neq i}^{5} \gamma_j J_{ji} - \gamma_i \sum_{j \neq i}^{5} J_{ij} \qquad (1 \le i \le 5) \qquad [3]$$

$$\frac{\Delta {}^{15}N_i}{\Delta t} = \sum_{j \neq i}^{5} \alpha_j F_{ji} - \alpha_i \sum_{j \neq i}^{5} F_{ij} \qquad (1 \le i \le 5) \qquad [4]$$

where γ_i is the ^{13}N atom fraction and α_i the ^{15}N atom fraction of SOM fraction *i*.

While we cannot take N to be a conserved tracer for C, we can reasonably assume that decomposition of SOM fractions other than the soluble releases N *pro rata*:

$$\sum_{j \neq i}^{5} F_{ij} = \rho_i \sum_{j \neq i}^{5} J_{ij} \qquad (3 \le i \le 5) \qquad [5]$$

where ρ_i is the N:C ratio of source SOM fraction *i*.

Equations [1]-[5] provide 23 constraints on the 40 unknown fluxes J_{ij} and F_{ij}. We provide further constraints by assuming, for a predominantly anoxic incubation, that there is no C fixation (photosynthesis) or N fixation:

$$J_{1j} = 0 \qquad (1 \le j \le 5) \qquad [6]$$

$$F_{1j} = 0 \qquad (1 \le j \le 5) \qquad [7]$$

and that N loss occurs only from the soluble pool:

$$F_{i1} = 0 \qquad (i \neq 2) \qquad [8]$$

This leaves 29 unknown fluxes, too many to be fixed unambiguously by the 23 constraints. We need to find – or to postulate – some relationships between the remaining J_{ij} and F_{ij}. We do this, somewhat counter-intuitively, by resolving them into two components, roughly speaking a biological (*type I*) and a physical (*type II*) flux. Biological (type I) fluxes work to preserve the N:C ratio ρ_j of the destination SOM fraction *j*; physical (type II) fluxes conserve the N:C ratio ρ_i of the source SOM fraction *i*. In particular, as Table 5.2.1 indicates:

$$F_{ij}^{II} = \rho_i J_{ij}^{II} \qquad (i, j \neq 1) \qquad [9]$$

where the superscript *II* denotes a type II flux component.

Table 5.2.1 Type I and type II flux components.

flux	type I component		Type II component	
source/destination	C flux J^I_{ij}	N flux F^I_{ij}	C flux J^{II}_{ij}	N flux F^{II}_{ij}
21	J^I_{21}	F^I_{21}		
23	J^I_{23}	F^I_{23}	J^{II}_{23}	$\rho_2 J^{II}_{23}$
24	J^I_{24}	F^I_{24}	J^{II}_{24}	$\rho_2 J^{II}_{24}$
25	J^I_{25}	F^I_{25}	J^{II}_{25}	$\rho_2 J^{II}_{25}$
31	J^I_{31}			
32	J^I_{32}	F^I_{32}	J^{II}_{32}	$\rho_3 J^{II}_{32}$
34	J^I_{34}	F^I_{34}	J^{II}_{34}	$\rho_3 J^{II}_{34}$
35	J^I_{35}	F^I_{35}	J^{II}_{35}	$\rho_3 J^{II}_{35}$
41	J^I_{41}			
42	J^I_{42}	F^I_{42}	J^{II}_{42}	$\rho_4 J^{II}_{42}$
43	J^I_{43}	F^I_{43}	J^{II}_{43}	$\rho_4 J^{II}_{43}$
45	J^I_{45}	F^I_{45}	J^{II}_{45}	$\rho_4 J^{II}_{45}$
51	J^I_{51}			
52	J^I_{52}	F^I_{52}	J^{II}_{52}	$\rho_5 J^{II}_{52}$
53	J^I_{53}	F^I_{53}	J^{II}_{53}	$\rho_5 J^{II}_{53}$
54	J^I_{54}	F^I_{54}	J^{II}_{54}	$\rho_5 J^{II}_{54}$

This seems to leave us even worse off than before. We now have (Table 5.2.1) 16 unknown type I C fluxes (J^I_{ij}), 13 unknown type I N fluxes (F^I_{ij}) and 12 unknown type II C fluxes (J^{II}_{ij}), for a total of 41 unknowns. However, the following additional constraints on biological (type I) fluxes:

$$\sum_{j\neq i}^{5} F^I_{ji} = \rho_i \sum_{j\neq i}^{5} J^I_{ji} \qquad (3 \le i \le 5) \qquad [10]$$

raise the total number of constraints to 32, and we can legitimately assume several of the physical (type II) fluxes to be negligible. Arah (2000) takes all but J^{II}_{34}, J^{II}_{35} and J^{II}_{45} to be zero, thereby reducing the number of unknowns to the number of constraints, and demonstrates the ability of singular value decomposition (SVD) to recover (most of) the individual fluxes used in a simulation of the 5-fraction incubation. Even in this situation, however, the set of constraints does not uniquely determine the set of unknowns (though it does determine most of their interesting sums). The analytical technique (SVD) is sufficiently robust to handle a degree of under-determination, simply attributing greater uncertainty to its calculated values when these are not uniquely specified.

Recognising this, and after a number of exploratory analyses not presented here, we here assume that the six type II fluxes J^{II}_{32}, J^{II}_{42}, J^{II}_{43}, J^{II}_{52}, J^{II}_{53} and J^{II}_{54} are zero, and employ an under-determined (m = 32; n = 36) SVD with a (normalised) tolerance of 0.001 to calculate best-fit values for the remaining inter-fraction fluxes.

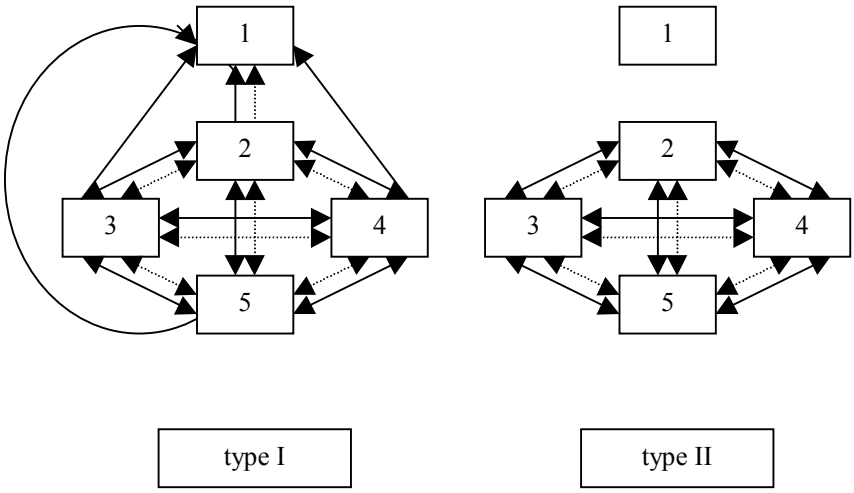

Fig.5.2.1 Model system : solid lines represent C fluxes, dotted lines N fluxes.

References

Arah JRM (2000) Isotope tracing of C and N fluxes between measurable SOM fractions. *European Journal of Soil Science* (submitted).

5.3 Oxygen-dependent SOM transformation submodel (SOMO)

Model description

Assume for the moment a homogeneous soil (effectively a well-stirred chemical reactor). Consider the species given in Table 5.3.1 and the biochemical reactions in Table 5.3.2. There are 5 SOM fractions with subscripts 1-5; as above, subscript 1 denotes the gaseous fraction, subscript 2 the (non-volatile) soluble fraction, subscript 3 the free light fraction (LF_1), subscript 4 the additional light fraction released on sonication (LF_2), and subscript 5 the residue (HF). C and N (and their isotopes) are tracked, in addition to oxygen (O), oxidized redox buffer (B), reduced redox buffer (R), carbon dioxide (G) and methane (M). Solution-phase concentrations of all species are denoted by upper-case italics; gas-phase concentrations by lower-case italics.

Table 5.3.1. Species and concentrations.

symbol	species	Unit
$^{(13)}C_{1\text{-}5}$	SOM fraction carbon (carbon 13)	mol m^{-3}
$^{(15)}N_{1\text{-}5}$	SOM fraction nitrogen (nitrogen 15)	mol m^{-3}
O	oxygen	mol C eq m^{-3}
B	oxidised buffer	mol C eq m^{-3}
R	reduced buffer	mol C eq m^{-3}
G	carbon dioxide	mol m^{-3}
M	methane	mol m^{-3}

Oxidised buffer B (Table 5.3.1) represents an activity-weighted average of all the potential conserved oxidants (Fe^{3+}, Mn^{4+}, SO_4^{2-}) present in the system; reduced buffer R represents the corresponding reduced forms (Fe^{2+}, Mn^{2+}, S^{2-}). This minimal model is not concerned with the nature of the conserved redox buffer, merely with its function (which is to inhibit SOM C-disproportionation - methanogenesis - while oxidised, and to consume O_2 by reoxidation when reduced). Concentrations *B* and *R* are expressed in terms of C equivalents. Oxidation of one molecule of SOM C ($CH_2O \rightarrow CO_2$) releases 4 electrons, so the notional oxidation state of R is equal to that of B minus 4. Thus one mole of B may represent four moles of Fe^{3+}, two of Mn^{2+}, half a mole of SO_4^{2-}, or any combination thereof. Nitrate (NO_3^-) is not subsumed in B since its reduced forms are gaseous and thus not conserved.

Gaseous carbon dioxide (CO_2) and methane (CH_4) are both parts of C_1. They are included here – as model components G and M – because of the wider importance of CH_4 emissions, the fact that CH_4 flux data is relatively accessible, and because CH_4 oxidation can play a major role in determining system oxia/anoxia.

Table 5.3.2. Biochemical reaction kinetics.

reaction	partial stoichiometry	Kinetics
v_{Oi}	$C_i + O \rightarrow G$	$k_i C_i O / (K_O + O)$
v_{Bi}	$C_i + B \rightarrow R + G$	$k_i C_i B / [(K_B + B)(1 + \eta_O O)]$
v_{Ci}	$2\ C_i \rightarrow M + G$	$k_i C_i / [(1 + \eta_O O)(1 + \eta_B B)]$
v_R	$O + R \rightarrow B$	$k_R O R / (K_R + R)$
v_M	$2\ O + M \rightarrow G$	$k_M O M / (K_M + M)$

The solution-phase concentration *X* of (volatile) substance X is proportional to the gas-phase concentration *x*:

$$x = \alpha X \qquad [1]$$

where the solubility constant α is assumed for simplicity to be the same for all volatiles (O, G, M).

Reactions are represented by single-substrate Michaelis-Menten kinetics, with reduction of redox buffer B (concentration B) inhibited by O (concentration O) where present, and methanogenesis inhibited by both O and B. The efficiency of the former inhibition is represented by the coefficient η_O, and of the latter by η_B.

Reaction constants k_i (one for each SOM fraction other than the gaseous) are assumed to be equal for oxic, suboxic and anoxic reactions, the actual rates being modulated by other terms. This is a (potentially gross) simplification, which might be altered in future versions of the model. We return to consider those factors which control k_i at the end of this section.

The formulae in Table 5.3.2 provide SOMO with the first feature we identified as essential for an adequate treatment of SOM cycling in periodically flooded soil – sensitivity to oxygen. They also introduce the non-specific intermediate redox buffer B (reduced form R), because work on CH_4 emissions indicates the important role played in some soils by Fe^{3+}, Mn^{4+} and SO_4^{2-}. In this respect, and in the differentiation of SOM fraction 1 into its components CO_2 and CH_4, SOMO thus exceeds its minimum design specifications. This makes it more complicated, but more realistic and more flexible.

Carbon fluxes J_{ij} are split between the various SOM fractions according to partition coefficients η_{ij}, where i is the source fraction and j the target. By definition:

$$\sum_{j \neq i} \phi_{ij} = 1 \qquad [2]$$

and, following the SOMA treatment above:

$$J_{1j} = 0 \qquad [3]$$

The partition coefficients in Table 5.3.3 are required by the model.

Table 5.3.3. Carbon flux partition coefficients.

source fraction	target fraction				
	1	2	3	4	5
2	$1 - (\phi_{23} + \phi_{24} + \phi_{25})$	0	ϕ_{23}	ϕ_{24}	ϕ_{25}
3	$1 - (\phi_{32} + \phi_{34} + \phi_{35})$	ϕ_{32}	0	ϕ_{34}	ϕ_{35}
4	$1 - (\phi_{42} + \phi_{43} + \phi_{45})$	ϕ_{42}	ϕ_{43}	0	ϕ_{45}
5	$1 - (\phi_{52} + \phi_{53} + \phi_{54})$	ϕ_{52}	ϕ_{53}	ϕ_{54}	0

We assume, for simplicity, that these partition coefficients apply equally to the oxic reactions (ν_{Oi}), the suboxic reactions (ν_{Bi}) and the anoxic reactions (ν_{Ci}) of Table 5.3.2. This is actually unlikely to be the case – oxic and anoxic metabolisms follow different pathways, as well as proceeding at different rates – but we opt for simplicity here in the hope of being able to parameterise our model using real data.

Nitrogen fluxes F_{ij} are related to C fluxes J_{ij} as follows:

$$F_{i1} = 0 \qquad i \neq 2 \qquad [4]$$

$$F_{i2} = \rho_i \left(J_{i1} + J_{i2} \right) \qquad i > 2 \qquad [5]$$

$$F_{ij} = \rho_j J_{ij} \qquad j > 2 \qquad [6]$$

where ρ_i is the N:C ratio of SOM fraction i. The N flux F_{21} from the soluble to the gaseous fraction encompasses denitrification and volatilisation of ammonia. We represent it as a simple first-order loss process, with rate constant k_N:

$$F_{21} = k_N N_2 \qquad [7]$$

According to equation [6], biochemical transformations tend to preserve the N:C ratio of the target (*ie* product) SOM fraction. Physical transformations (which we denote by the lower case symbols j_{ij} for C flux and f_{ij} for N flux), by contrast, preserve the N:C ratio of the source fraction:

$$f_{ij} = \rho_i j_{ij} \qquad [8]$$

Again following the SOMA scheme outlined above, we assume that physical transformations occur predominantly from the lighter to the heavier SOM fractions, *ie*:

$$j_{ij} = 0 \qquad j \le i \qquad [9]$$

Physical transformations are first-order reactions:

$$j_{ij} = k_{ij} C_i \qquad [10]$$

requiring the (physical) reaction constants given in Table 5.3.4.

Table 5.3.4. Physical transformation reaction constants.

source fraction	target fraction		
	3	4	5
2	k_{23}	k_{24}	k_{25}
3	0	k_{34}	k_{35}
4	0	0	k_{45}

The stable isotopes ^{13}C and ^{15}N are treated as true tracers within the model. That is, for all *i* and *j*:

$$^{13}J_{ij} = \gamma_i J_{ij} \qquad [11]$$

$$^{13}j_{ij} = \gamma_i j_{ij} \qquad [12]$$

$$^{15}F_{ij} = \alpha_i F_{ij} \qquad [13]$$

$$^{15}f_{ij} = \alpha_i f_{ij} \qquad [14]$$

where superscript 13 or 15 denotes the relevant isotopic flux, γ_i is the ^{13}C atom fraction of SOM fraction *i* and α_i its ^{15}N atom fraction.

Finally, as mentioned above, the model requires a means to allow SOM fraction reactivity k_i to vary over time. This is essential if the model pools C_i and N_i are to correspond to measurable SOM fractions. Current SOM transformation models overwhelmingly assume constant k_i, thereby precluding their application to measurable SOM fractions. Agren and Bosatta (1987) take k_i to decline with the age of what they term each SOM cohort (addition of fresh organic matter to the system), and track each cohort over time. However, what actually determines SOM fraction reactivity is not its age but its chemical composition and physical state, both of which vary not so much with time as with the progress of decomposition itself, as – in essence – the bugs eat the best bits first.

What we want is some intrinsic measure of how much decomposition a given SOM fraction has undergone. One possibility is the C:N ratio, another – which we use here for the first time – is the redox charge density *E*, which we define as follows:

$$E_i = \frac{Z_i}{C_i} \qquad [15]$$

where Z_i is the redox charge of SOM fraction i and C_i its C concentration. Reactions ν_{Oi}, ν_{Bi} and ν_{Ci} result in the changes ΔZ_i and ΔC_i indicated in Table 5.3.5.

Table 5.3.5. Redox charge density and reaction.

reaction	ΔC_i	ΔZ_i
ν_{Oi}	-1	4
ν_{Bi}	-1	4
ν_{Ci}	-2	0

By keeping track of the changes ΔC_i and ΔZ_i associated with each simulated reaction, we can follow the redox charge density E_i. All reactions increase E_i; additions of new C_i, either from outside the SOM system (root exudation, residue incorporation) or from within it (by cycling), reduce E_i by diluting the existing charge Z_i. This gives us a natural index of the "degree of reactedness" of SOM fraction i. We use it to modulate the fraction reactivity k_i as follows:

$$k_i = k_i^o \exp\left(-k_E E_i\right) \qquad [16]$$

where k^o_i is the standard state (unmodified) reactivity of SOM fraction i. Again, for simplicity, we use the same redox modifier coefficient k_E for all fractions – again, this is a simplification which it might be necessary to abandon in future.

Model parameters

The SOMO model requires the parameters of Table 5.3.6 and the initial values of Table 5.3.7. Default values listed in both Tables should be replaced by measured and/or optimised values wherever possible.

The initial state variables reported in Table 5.3.7 are all in principle measurable, though the measurement of SOM fraction redox charge density has not so far – to our knowledge – been attempted. Recognising this, it might be more appropriate to represent E^o_i as optimisable parameters rather than measurable initial state variables. In this case, the model requires a total of 36 parameters. This is a large number to be optimised. Nevertheless, since the model simulates (predicts) the C, ^{13}C, N and ^{15}N concentrations of each of 5 measurable SOM fractions at every sampling or timestep – that is, 20 values per timestep – and since each incubation is sampled as many as 7 times, there are grounds for hoping that optimisation might not prove impossible.

Model output

As mentioned above, the SOMO model produces as primary output the values of C_i, $^{13}C_i$, N_i and $^{15}N_i$ as functions of time. These values can be combined in various ways – to give the ^{13}C and ^{15}N atom fractions γ_i and α_i, for example – which might better reveal what is actually going on in the simulated system. Among the compound values of potential interest are:

$$E' = -\frac{R_U T}{4F} \ln\left(\frac{R}{B}\right) \qquad [17]$$

where R_U is the universal gas constant (0.082 L atm/(K mol)), F Faraday's constant (96500 C) and T the absolute temperature (K; default value 298). E' is a measure of the departure from its standard value – call it E'^o – of the redox potential of a pure B/R solution. Given the non-specific nature of the modelled entities B and R we cannot expect to attach a definite value to E'^o, but we can nevertheless hope that there will be a domain within which changes in E' will equate – albeit roughly – with changes in the measurable soil redox potential E_h.

Table 5.3.6. SOMO model parameters.

meaning	symbol	default value*	Unit
solubility constant	α	0.1	m^3 water m^{-3} air
(standard state) biochemical transformation rate constants	k^o_2	0.01	d^{-1}
	k^o_3	0.005	d^{-1}
	k^o_4	0.001	d^{-1}
	k^o_5	0.0001	d^{-1}
	k_R	0.01	d^{-1}
	k_M	0.01	d^{-1}
	k_N	0.01	d^{-1}
redox charge modifier	k_E	5	mol C mol^{-1} *e*
Michaelis-Menten constants	K_O	0.1	m^3 mol^{-1}
	K_B	0.1	m^3 mol^{-1}
	K_R	0.1	m^3 mol^{-1}
	K_M	0.1	m^3 mol^{-1}
inhibition coefficients	η_O	10	m^3 mol^{-1}
	η_B	1	m^3 mol^{-1}
partition coefficients	ϕ_{23}	0.2	-
	ϕ_{24}	0.2	-
	ϕ_{25}	0.2	-
	ϕ_{32}	0.2	-
	ϕ_{34}	0.2	-
	ϕ_{35}	0.2	-
	ϕ_{42}	0.2	-
	ϕ_{43}	0.2	-
	ϕ_{45}	0.2	-
	ϕ_{52}	0.2	-
	ϕ_{53}	0.2	-
	ϕ_{54}	0.2	-
physical transformation rate constants	k_{23}	0.01	d^{-1}
	k_{24}	0.01	d^{-1}
	k_{25}	0.01	d^{-1}
	k_{34}	0.001	d^{-1}
	k_{35}	0.001	d^{-1}
	k_{45}	0.0001	d^{-1}
			3

* to be replaced where possible by values optimised by fitting against measured data.

Table 5.3.7. SOMO model initial state variables.

meaning	symbol	default value*	Unit
initial SOM fraction C	C_1^o	10	mol m^{-3}
	C_2^o	20	mol m^{-3}
	C_3^o	50	mol m^{-3}
	C_4^o	100	mol m^{-3}
	C_5^o	1000	mol m^{-3}
initial SOM fraction ^{13}C	$^{13}C_1^o$	1	mol m^{-3}
	$^{13}C_2^o$	2	mol m^{-3}
	$^{13}C_3^o$	4	mol m^{-3}
	$^{13}C_4^o$	10	mol m^{-3}
	$^{13}C_5^o$	100	mol m^{-3}
initial SOM fraction N	N_1^o	1	mol m^{-3}
	N_2^o	2	mol m^{-3}
	N_3^o	5	mol m^{-3}
	N_4^o	8	mol m^{-3}
	N_5^o	75	mol m^{-3}
initial SOM fraction ^{15}N	$^{15}N_1^o$	0.004	mol m^{-3}
	$^{15}N_2^o$	0.010	mol m^{-3}
	$^{15}N_3^o$	0.020	mol m^{-3}
	$^{15}N_4^o$	0.032	mol m^{-3}
	$^{15}N_5^o$	0.300	mol m^{-3}
initial SOM fraction redox charge density	E_2^o	0.1	mol *e* mol^{-1} C
	E_3^o	0.1	mol *e* mol^{-1} C
	E_4^o	0.1	mol *e* mol^{-1} C
	E_5^o	0.1	mol *e* mol^{-1} C
initial gaseous CO_2 concentration	g^o	0	mol m^{-3}
initial gaseous CH_4 concentration	m^o	0	mol m^{-3}
initial gaseous O_2 concentration	o^o	0	mol m^{-3}
initial B concentration in solution	B^o	5	mol m^{-3}
initial R concentration in solution	R^o	0	mol m^{-3}

* to be replaced where possible by measured values.

SOMO also produces as output (predicts) the rate P_M of CH_4 production:

$$P_M = \sum_i (1 - \sum_j \phi_{ij}) \nu_{Ci} \qquad [18]$$

as well as the oxidation rate ν_M and thus, for a well-stirred system, the CH_4 emission rate J_M:

$$J_M = P_M - \nu_M \qquad [19]$$

Finally, SOMO simulates the redox charge density E_i of the various SOM fractions. This property can be measured, albeit destructively and with difficulty.

Specimen results

The next few pages illustrate the capacity of SOMO to simulate (sensibly) the major features of SOM cycling in soil. Figures 5.3.1-5.3.5 illustrate the output of the model under the default conditions outlined above (Tables 5.3.6 and 5.3.7).

The initial state variables of Table 5.3.7 represent an idealised anoxic incubation in which all fractions start with N:C ratios ρ equal to 0.1, ^{13}C atom fractions γ equal to 0.1 and ^{15}N atom fractions α equal to 0.004 except that: (i) SOM fraction 4 has ρ equal to 0.08 and SOM fraction 5 has ρ equal to 0.075 – *ie* both are depleted in N; (ii) SOM fraction 3 has γ equal to 0.08 – it is depleted in ^{13}C; and (iii) SOM fraction 2 has α equal to 0.005 – it is enriched in ^{15}N.

Simulated SOM fraction concentrations (C_i, $^{13}C_i$, N_i and $^{15}N_i$) are illustrated in Fig.5.3.1. SOM fraction 5 is not included since it is so much larger than the other fractions that to include it would mask all the other data. Further, it changes relatively little.

Figure 5.3.2 illustrates the changing composition of all 5 SOM fractions.

Figure 5.3.3 shows the rates of gross mineralisation (*ie* efflux from each fraction) simulated by the model.

Figure 5.3.4 shows SOM fraction biochemical reactivity constants k_i.

Figure 5.3.5 shows how O_2 (O), oxidised redox buffer (B), reduced redox buffer (R), CO_2 (G) and CH_4 (M) concentrations vary over the course of the simulation. In this case – an anoxic incubation – O is zero throughout.

The figures in Appendix A5.3.1 illustrate the equivalent simulated output for an oxic incubation, in which O is maintained at 1 mol m^{-3} throughout. Those in Appendix A5.3.2 illustrate output for a closed incubation in which O starts at 1 mol m^{-3} and is depleted by reaction.

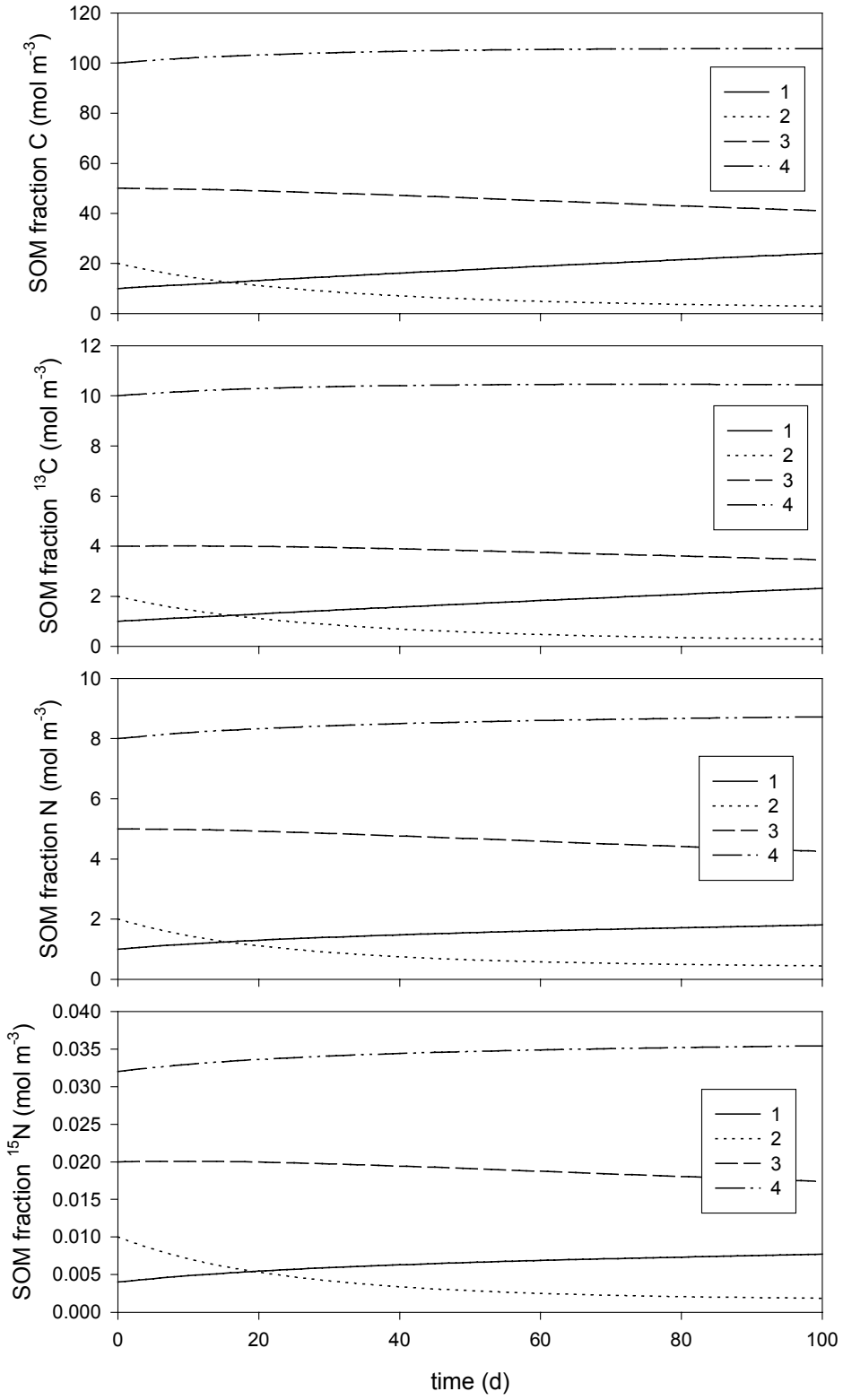

Fig.5.3.1 Output of SOMO model: default parameter values and initial state. SOM fraction concentrations.

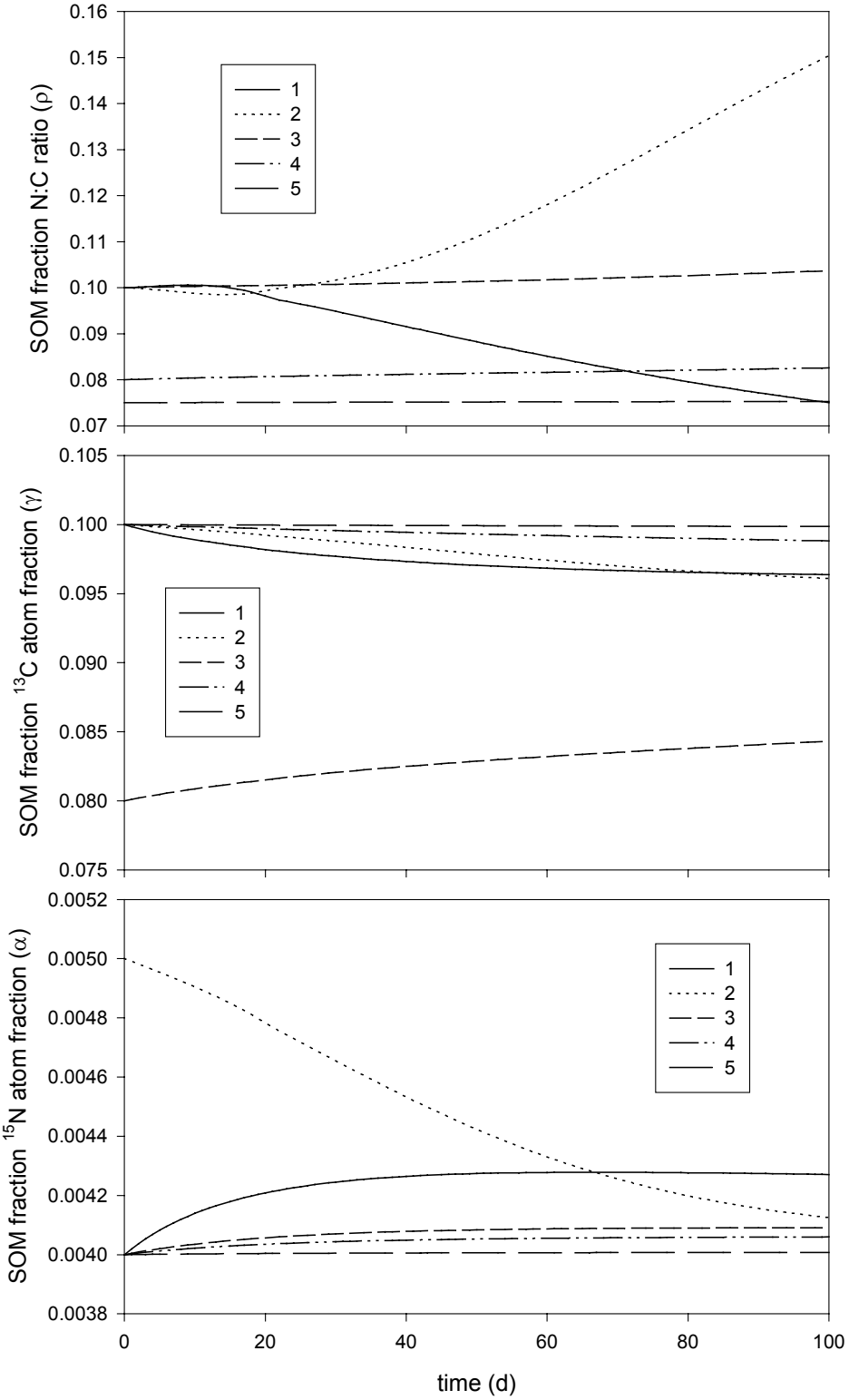

Fig.5.3.2 Output of SOMO model: default parameter values and initial state. SOM fraction properties.

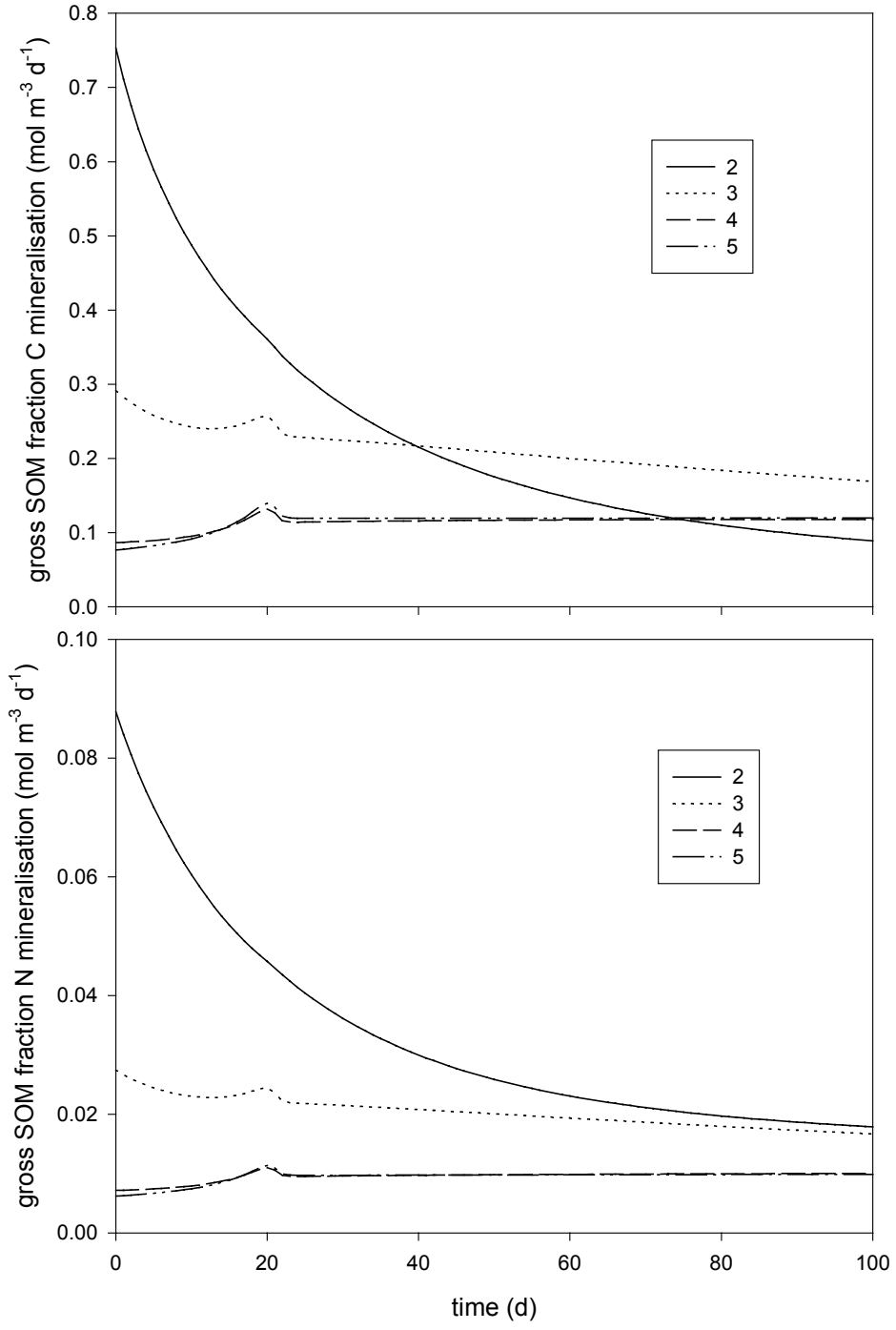

Fig.5.3.3 Output of SOMO model: default parameter values and initial state. Gross SOM fraction mineralisation rates.

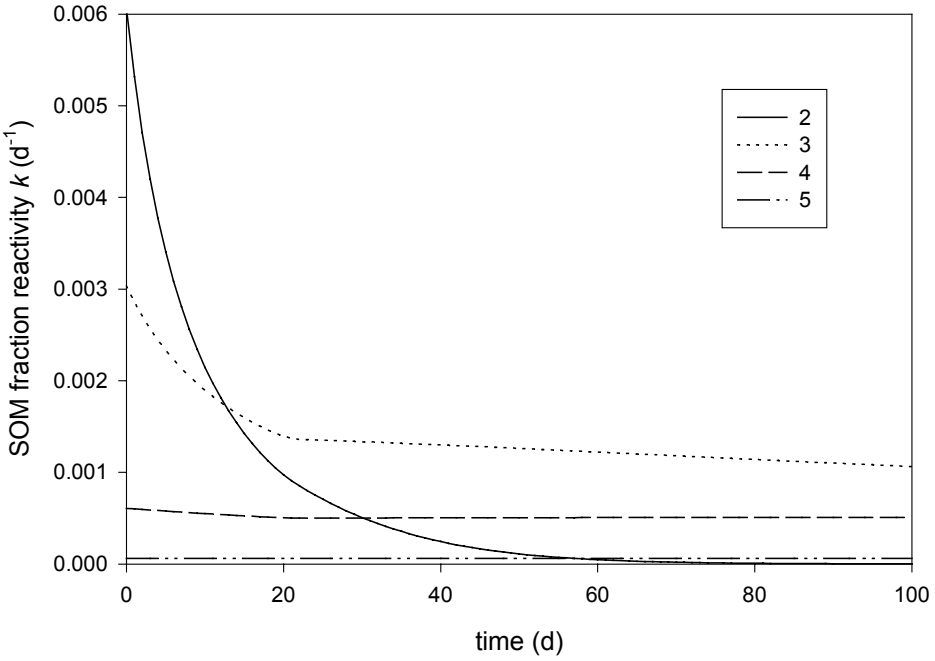

Fig.5.3.4 Output of SOMO model: default parameter values and initial state. SOM fraction reactivities.

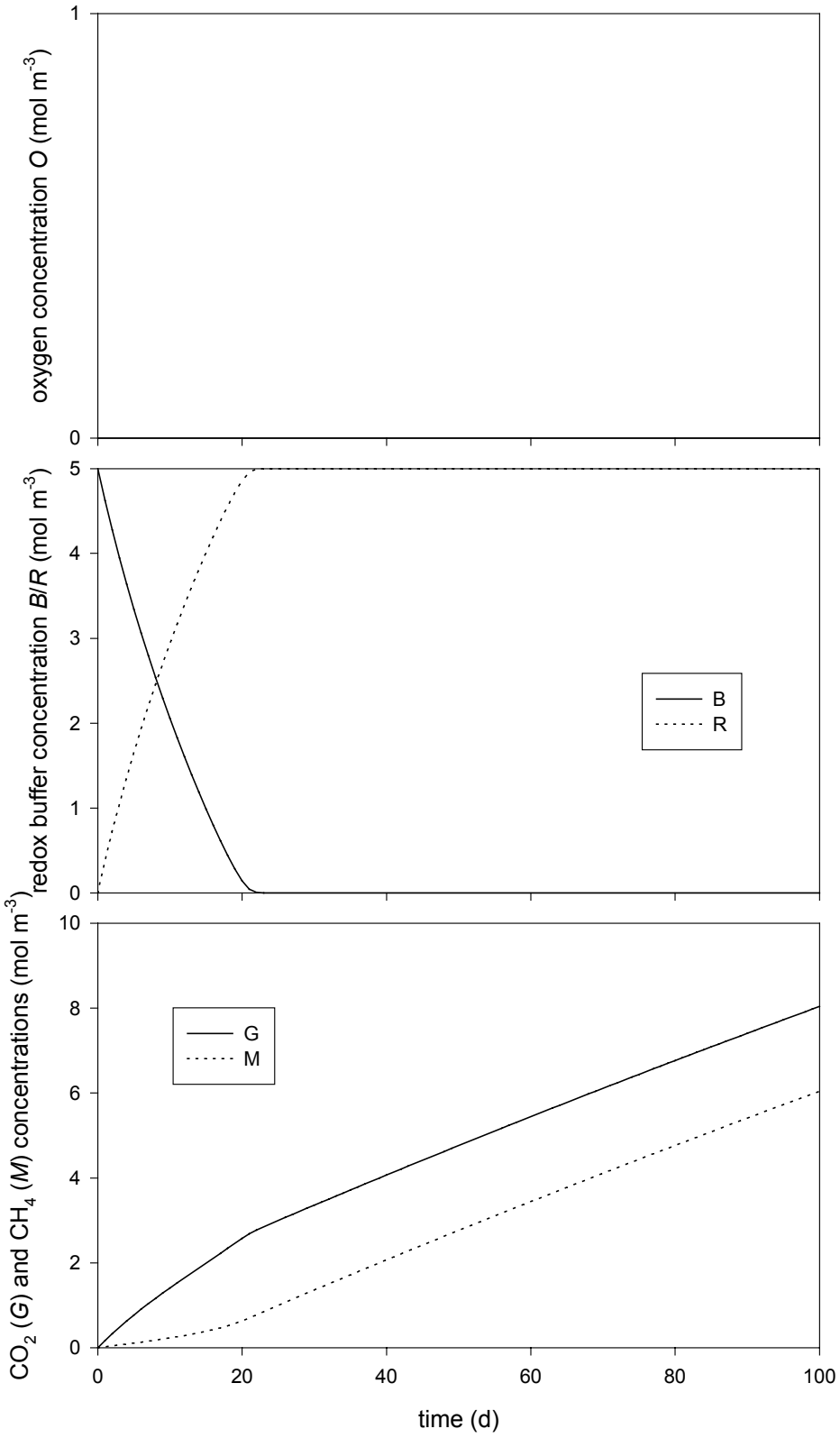

Fig.5.3.5 Output of SOMO model: default parameter values and initial state. Concentrations.

5.4 Field-scale model (SUMO)

The reactions and processes represented by SOMO take place in the field in a soil which is far from the idealised well-stirred reactor of the submodel. The controlling variable O (O_2 concentration) varies greatly from place to place (spatial variability) and from time to time (temporal variability). We have attempted in the past (Arah and Kirk, 1996, 2000; EP 5305) to represent this variability as a function of depth z and time t, and this approach has been adopted with some success (Matthews *et al*, 2000). Here, for simplicity – and because the alternative approach has also proved successful in other contexts (Arah 1999, EU Riceotopes program) – we adopt a dual-compartment (rhizosphere-bulk) treatment as detailed below.

Figure 5.4.1 illustrates the general idea. Soil in the immediate vicinity of plant roots is treated as a relatively homogeneous rhizosphere; more remote soil is simply regarded as bulk. SOMO reactions obey the same kinetics (as above, section 5.3) in each zone, but the rhizosphere is distinguished by (i) direct inputs of SOM C and N due to root exudation and death; (ii) root uptake of mineral N; and (iii) aerenchyma-mediated contact with the atmosphere. In the case of irrigated (flooded) rice cultivation, property (iii) controls soil-atmosphere exchange of the trace gases CO_2 and CH_4, and O_2 ingress and therefore the oxidation status of the entire system.

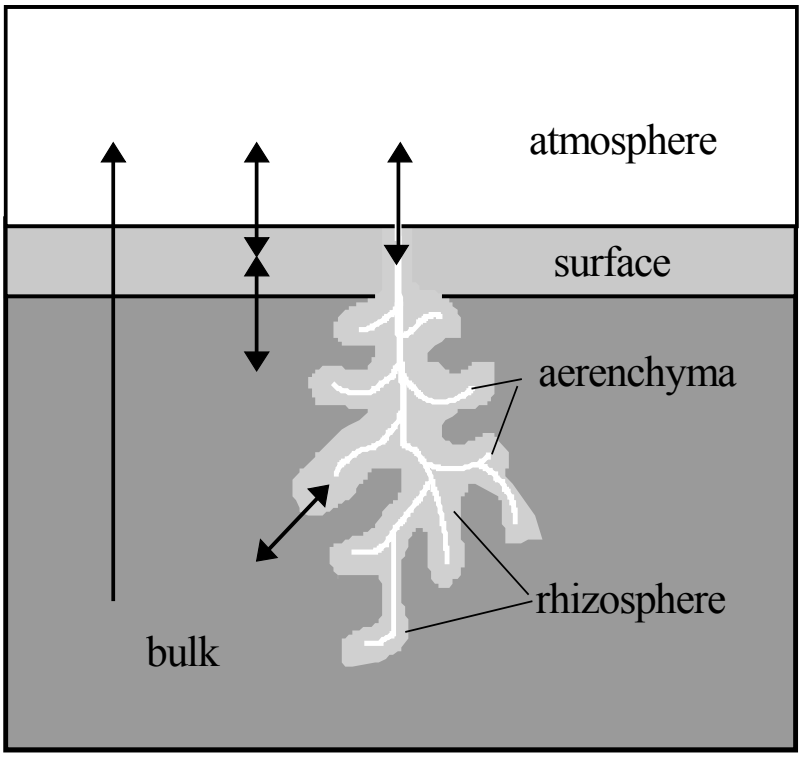

Fig.5.4.1 Partitioned (compartmentalised) model of SOM cycling in flooded soil. Shading denotes zones, arrows fluxes.

Figure 5.4.1 shows surface soil as a discrete zone. That zone is effectively merged with the rhizosphere in what follows. Model analysis (not shown) indicates that tri-partition is unnecessary, that the most important features of the system are captured by representing it in two parts.

Inter-compartment fluxes

First consider a static compartmentalised system of total volume V. Denote compartment properties (volume, concentrations, rates) by subscripts a, b and r as indicated in Table 5.4.1.

Table 5.4.1. SUMO model compartments.

compartment	subscript
atmosphere	*a*
bulk	*b*
rhizosphere	*r*

Fluxes between compartments follow the general formula:

$$J_{ij} = \kappa_{ij} Y_i \quad [1]$$

where Y_i is the relevant concentration in compartment *i* and the transfer coefficients κ_{ij} are as follows:

Table 5.4.2. Inter-compartmental transfer coefficients κ_{ij}.

source compartment *i*	target compartment *j*	transfer coefficient κ_{ij} (d^{-1})
volatiles		
a	*b*	λD_V
a	*r*	νA_r
b	*a*	λD_V
b	*r*	$\lambda D_V A_r$
r	*a*	νA_r
r	*b*	$\lambda D_V A_r$
non-volatiles		
a	*b*	0
a	*r*	0
b	*a*	0
b	*r*	$\lambda D_N A_r$
r	*a*	0
r	*b*	$\lambda D_N A_r$

where:

$$D_N = \theta D \quad [2]$$

$$D_V = D \frac{\left(10^4 \varepsilon + \alpha\theta\right)}{\left(\varepsilon + \alpha\theta\right)} \quad [3]$$

D ($m^2\ d^{-1}$) is some sort of average diffusion constant for all species in solution (subsuming any effects of tortuosity), ε is the air-filled porosity (m^3 air m^{-3} soil) and θ the volumetric moisture content (m^3 water m^{-3} soil). Volatiles are C_1, N_1, G and M; all other species are non-volatile. Equivalent bulk-phase concentrations Y_a for the atmosphere are calculated from:

$$Y_a = y_a\left(\varepsilon + \alpha\theta\right) \quad [4]$$

According to Table 5.4.2, transfers between the subsurface compartments (*b* and *r*) depend on their interfacial surface area A_r, the appropriate diffusion constant D_N or D_V, and an interface-specific resistivity coefficient λ; transfers between the bulk soil (*b*) and the atmosphere (*a*) depend on D_N (D_V) and

λ, the interfacial surface area being taken to be equal to unity; and rhizosphere-atmosphere ($r - a$) transfers depend on A_r and another resistivity coefficient ν.

In the dynamic situation brought about by crop growth, the rhizosphere volume V_r changes over time, causing corresponding changes in: (i) the bulk soil volume V_b; (ii) the rhizosphere-bulk (and rhizosphere-atmosphere) interfacial surface area A_r; (iii) the concentrations Y_i of all species within each zone; and (iv) intercompartmental fluxes J_{ij}. We take:

$$V_b = V - V_r \qquad [5]$$

$$\frac{\partial \mathrm{Y}_i}{\partial t} = -\frac{\partial \mathrm{Y}_j}{\partial t} = -Y_i\left(\frac{\partial V_j}{\partial t}\right) \qquad \frac{\partial V_j}{\partial t} > 0 \qquad [6]$$

Equation [6] represents the effects of the encroachment of compartment j (concentration Y_j equal to content Y_j divided by volume V_j) on compartment i – and *vice versa*; according to equation [5] compartments b and r are mutually exclusive. Where, as in the case of SOM fraction C, a redox charge is associated with each component content Y_i, this is transferred *pro rata*. It may be worth pointing out that in these equations the subscripts i and j refer to system compartments, not SOM fractions.

Diffusion-mediated transfers J_{ij} between compartments are governed by equation [1], whatever the changes in compartment volume.

Rhizosphere processes

The growing plant does not just occupy a changing volume V_r of the below-ground system. It also: (i) returns organic matter to the system by root exudation and root death; (ii) takes up nutrients – mainly N – and water in order to grow; and (iii) in the case of an aerenchymatous plant such as rice, provides a privileged route for gaseous soil-atmosphere exchange.

Here we represent these processes as simply as possible – as mere proportionalities – while flagging-up the potential for linking our model to a more detailed physiological treatment of crop development. We assume:

$$V_r = \sigma_V C_R \qquad [7]$$

$$A_r = \sigma_A C_R \qquad [8]$$

$$J_r = \sigma_J C_R \qquad [9]$$

where V_r is rhizosphere volume, A_r is r-b interfacial area, J_r is C input to the rhizosphere, C_R is root C and the various σs are proportionality constants.

Rhizosphere C input is partitioned between SOM compartments 2 (soluble) and 3 (LF_1) according to Table 5.4.3, and rhizosphere N inputs F_r follow C inputs, with N:C ratio ρ_P equal to that of the simulated plant (see below).

Table 5.4.3 Partitioning of rhizosphere C input J_r.

destination (target) fraction j	partition coefficient ϕ_J
2	ϕ_J
3	$1 - \phi_J$

Rhizosphere (*ie* plant) N uptake U depends on supply N_{2r} (soluble N in the rhizosphere) and demand Q:

$$U = \min\left(N_{2r}, Q\right) \qquad [10]$$

where min(x,y) denotes the minimum of x and y.

Plant growth

We need an algorithm relating N uptake to root growth. A crop growth model such as CERES (Carberry *et al*, 1989) might provide such an algorithm, and interfacing our model with one or both of these is clearly a priority for the future. R6750 does not provide for such an interface, however: we are forced to adopt something simpler.

We take N to be the major factor limiting growth and the unconstrained below-ground growth pattern to be a Gaussian as follows:

$$C_R^{pot} = C_R^{\max} \exp\left[-0.5 \left(\frac{t - t_{\max}}{\sigma_t} \right)^2 \right] \qquad [11]$$

where C_R^{pot} is the potential root C content, $C_R^{\max}$ the potential maximum root C content, $t_{\max}$ the time at which that maximum root mass (density) occurs and σ_t a measure of the spread. In effect, equation [11] expresses what a well-fed plant tries to do.

Differentiating equation [11] gives an expression for potential root growth in terms of potential root C:

$$\frac{\partial C_R^{pot}}{\partial t} = C_R^{\max} \left(\frac{t_{\max} - t}{\sigma_t^2} \right) \exp\left[-0.5 \left(\frac{t - t_{\max}}{\sigma_t} \right)^2 \right] = \left(\frac{t_{\max} - t}{\sigma_t^2} \right) C_R^{pot} \qquad [12]$$

Substituting the actual root C content C_R for the potential C_R^{pot} at any given time, and assuming (i) a constant plant N:C ratio of ρ_P and (ii) a constant root:plant fraction of φ_R, we obtain the following expression for the N demand for growth Q_g:

$$Q_g = \left(\frac{\rho_P}{\varphi_R} \right) \left(\frac{t_{\max} - t}{\sigma_t^2} \right) C_R \qquad [13]$$

In addition to this, there is a maintenance N demand Q_m required to offset the effects of root exudation and death. According to equation [9], this is:

$$Q_m = \rho_P J_r = \rho_P \sigma_J C_R \qquad [14]$$

Equations [11]-[13] apply during the period of plant (specifically root) growth ($0 < t < t_{\max}$); equations [10] and [14] apply throughout. Thus:

$$Q = Q_m + Q_g \qquad 0 < t < t_{\max} \qquad [15]$$

$$Q = Q_m \qquad t > t_{\max} \qquad [16]$$

and:

$$\frac{\partial C_R}{\partial t} = \min\left(\frac{N_{2r}}{Q}, 1 \right) \left(\frac{t_{\max} - t}{\sigma_t^2} \right) C_R \qquad 0 < t < t_{\max} \qquad [17]$$

$$\frac{\partial C_R}{\partial t} = -\sigma_J C_R \qquad t > t_{\max} \qquad [18]$$

Equations [17] and [18] allow root C content (and hence all other plant properties, according to our simplistic picture in which plant N:C is constant at ρ_P and the root:plant ratio is constant at φ_R) to be simulated as functions of rhizosphere mineral N.

Table 5.4.3 indicates the parameters required by SUMO in addition to those (Table 5.3.6) required by the submodel SOMO. Table 5.4.4 indicates SUMO's additional state variables.

Table 5.4.3 Parameters required by SUMO.

meaning	symbol	default value	Unit
diffusion constant in solution	D	10^{-4}	$m^2\ d^{-1}$
transfer coefficient	λ	20	m^{-1}
	ν	1	m^{-2}
efflux partition coefficient	ϕ_J	0.5	-
root property	σ_A	10	$m^2\ mol^{-1}\ C_R$
	σ_V	0.01	$m^3\ mol^{-1}\ C_R$
	σ_J	0.01	$mol\ C\ d^{-1}\ mol^{-1}\ C_R$
root growth parameter	C_R^{max}	8	$mol\ C_R\ m^{-3}$
	t_{max}	75	D
	σ_t	25	D
root:plant fraction	φ_R	0.5	-
plant N:C ratio	ρ_P	0.1	$mol\ N\ mol^{-1}\ C$

Table 5.4.4 State variables required by SUMO.

meaning	symbol	default value	unit
system volume	V	0.5	m^3
air-filled porosity	ε	0	$m^3\ m^{-3}$
volumetric moisture content	θ	0.75	$m^3\ m^{-3}$

Figures 5.4.2-5.4.7 illustrate the development of the system during a period (100 d) of crop growth. The soil is flooded throughout ($\varepsilon = 0$), and there are no N additions. All parameters and initial state variables are as in Tables 5.3.6, 5.3.7, 5.4.3 and 5.4.4, with the exception that the initial gas and solution phase concentrations C_1^o, C_2^o, G^o, M^o, N_1^o, and N_2^o are calculated using standard atmospheric concentrations and equation [4] – *ie* assuming an equilibrium between gas and solution phases.

Figure 5.4.2 shows how bulk (*b*) and rhizosphere (*r*) concentrations of O_2 (*O*), B (*B*) and R (*R*) change over time. Figure 5.4.3 shows the corresponding changes in SOM fraction *i* C concentration C_i in both compartments, and Fig.5.4.4 the changes in SOM fraction *i* N concentration N_i. Figure 5.4.5 shows simulated changes in bulk and rhizosphere SOM fraction reactivity k_i, Fig.5.4.5 simulated system effluxes, and Fig.5.4.7 the system N budget.

These figures represent only a small subset of SUMO's output. Compartment (atmosphere, bulk, plant, rhizosphere, root) concentrations and contents of all species ($C_{1\text{-}5}$, $N_{1\text{-}5}$, G, M, O), intercompartment fluxes, compartment volumes (V_r, V_b) and a wide range of derived variables can be reported. Figures 5.4.2-5.4.7 are merely illustrative.

References

Arah JRM (1999) *Modelling natural isotope fractionation during methane production and oxidation in ricefields*. Final report on EU RICEOTOPES programme.

Arah JRM & Kirk GJD (1996) *Methane generation and consumption in ricefields*. Final report on ODA Environment Programme Project R5305.

Arah JRM & Kirk GJD (2000) Modeling rice-plant-mediated methane emissions. *Nutrient Cycling in Agroecosystems* (in press).

Carberry PS, Muchow RC & McCown RL (1989) Testing the CERES-Maize simulation model in a semi-arid tropical environment. *Field Crops Research*. 20:297-315.

Matthews RB, Wassmann R, Arah JRM & Knox J (2000) Up-scaling of experimental measurements of CH4 emissions from rice fields in South East Asia usinga process-based crop/methane simulation model within a GIS environment. *Nutrient Cycling in Agroecosystems* (in press).

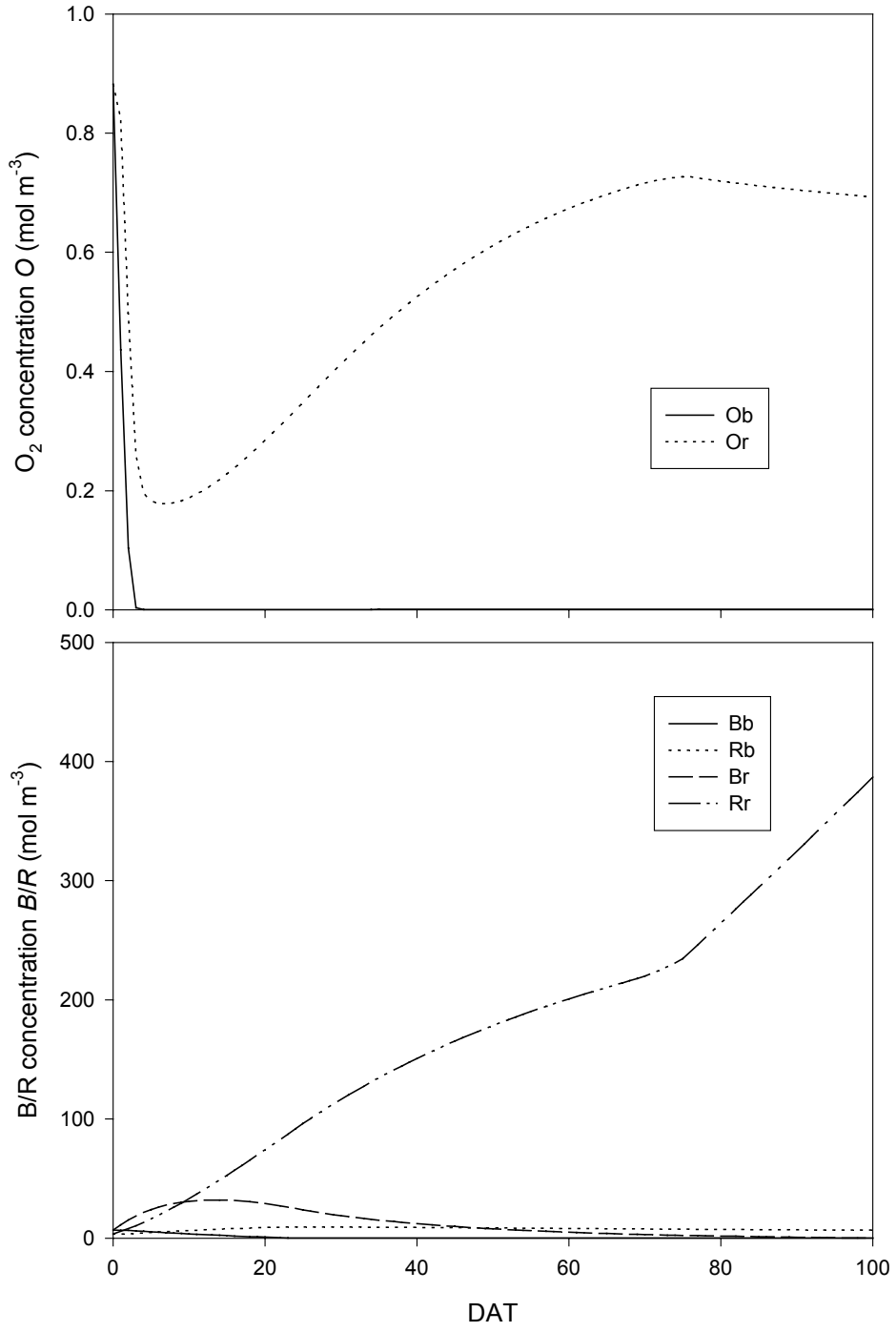

Fig.5.4.2 Simulated concentrations (mol m^{-3}) of O_2 (*O*), oxidised redox buffer (*B*) and reduced redox buffer (*R*) in bulk (*b*) and rhizosphere (*r*) compartments: default parameter values, no N addition.

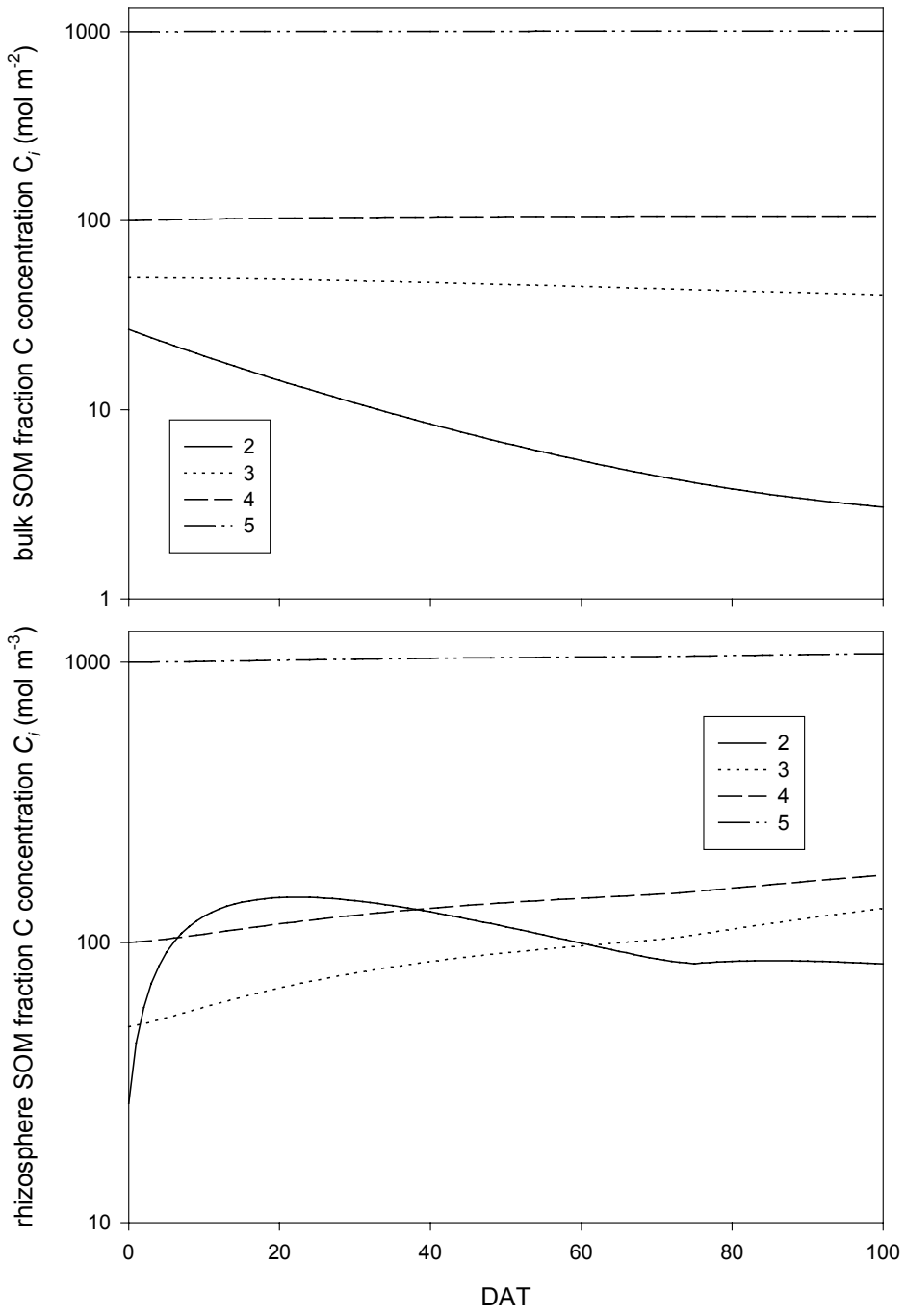

Fig.5.4.3 Simulated C concentrations C_i (mol m^{-3}) of SOM fractions 2-5 in bulk (*b*) and rhizosphere (*r*) compartments: default parameter values, no N addition.

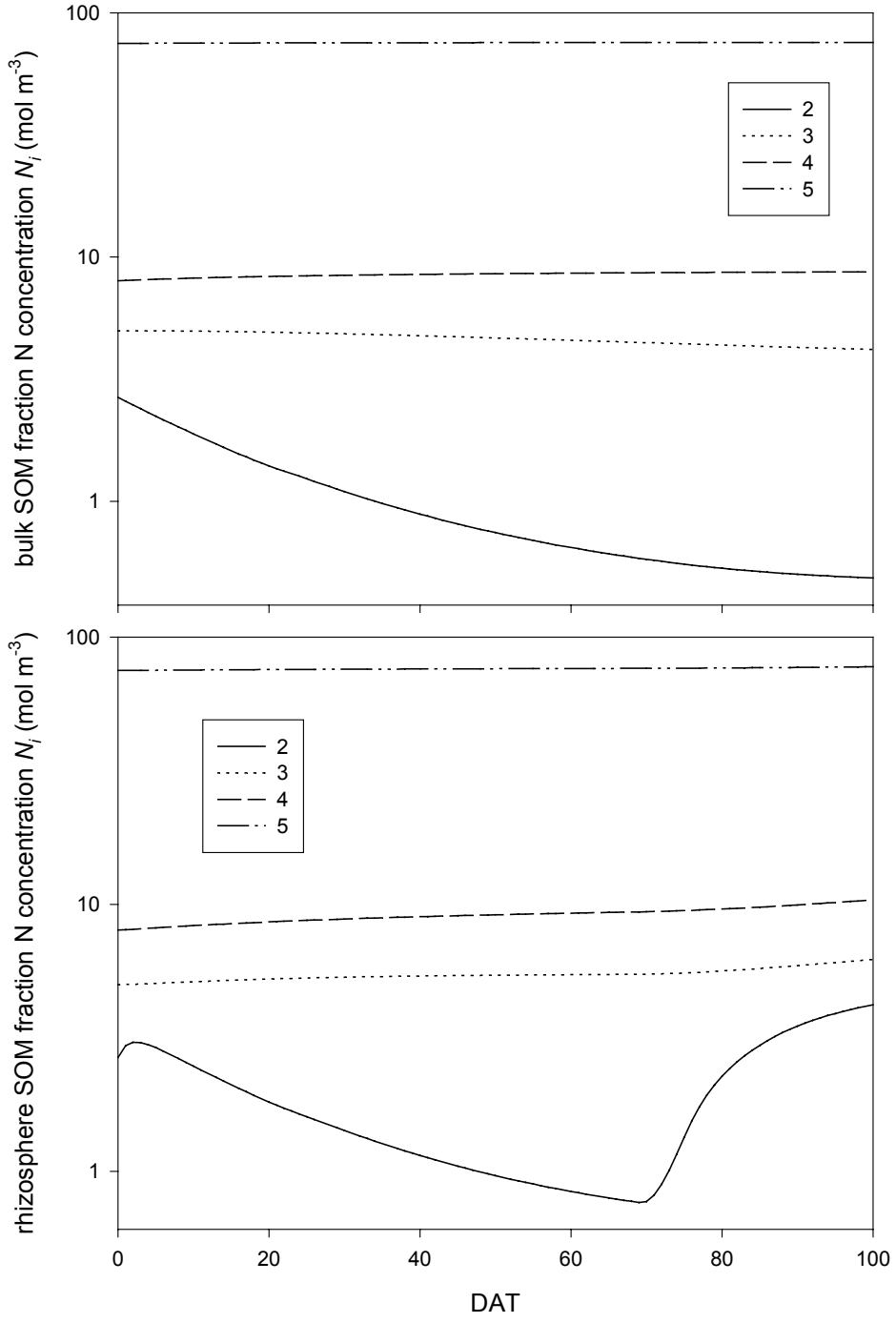

Fig.5.4.4 Simulated N concentrations N_i (mol m^{-3}) of SOM fractions 2-5 in bulk (*b*) and rhizosphere (*r*) compartments: default parameter values, no N addition.

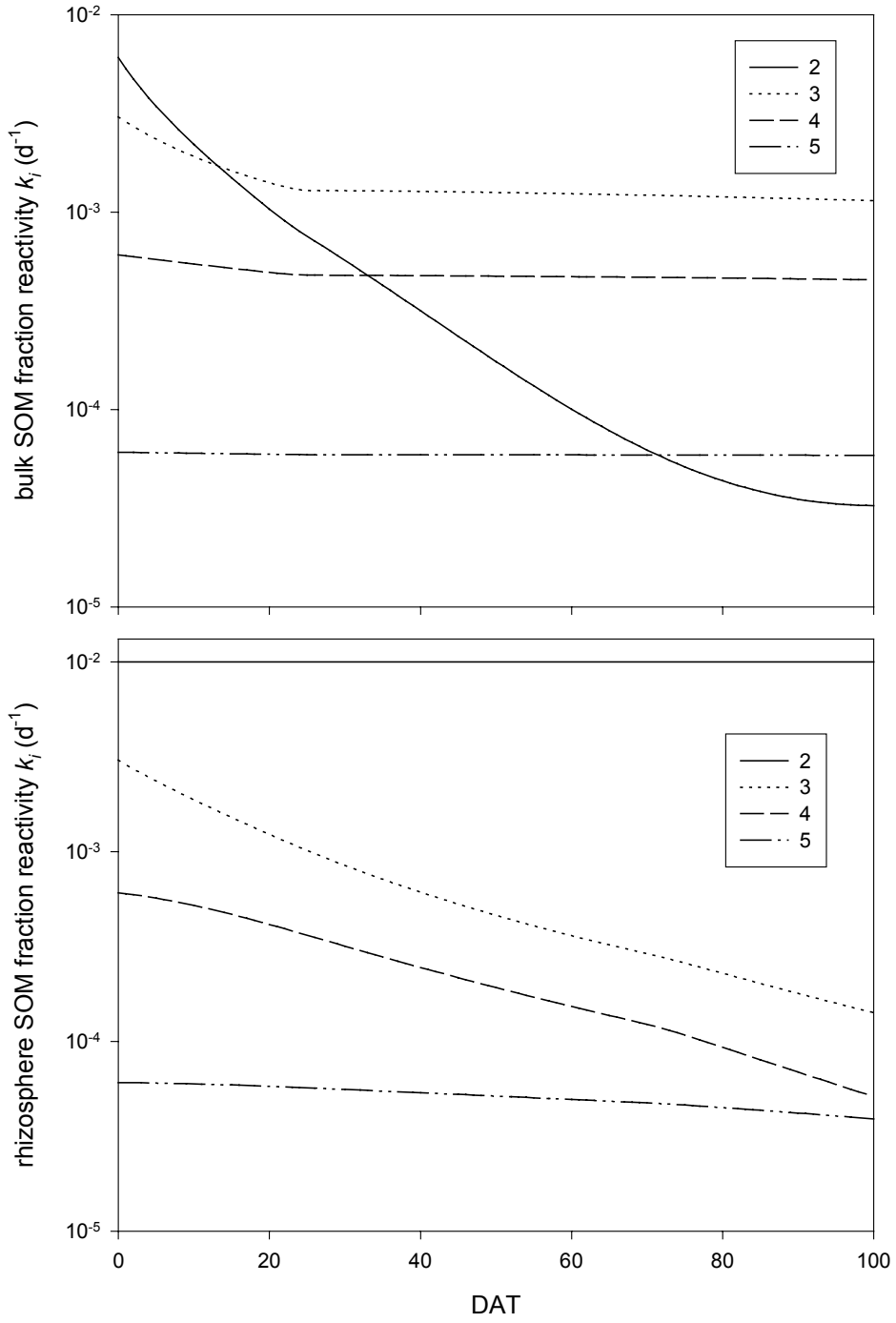

Fig.5.4.5 Simulated SOM fraction reactivity k_i (d^{-1}) of SOM fractions 2-5 in bulk (*b*) and rhizosphere (*r*) compartments: default parameter values, no N addition.

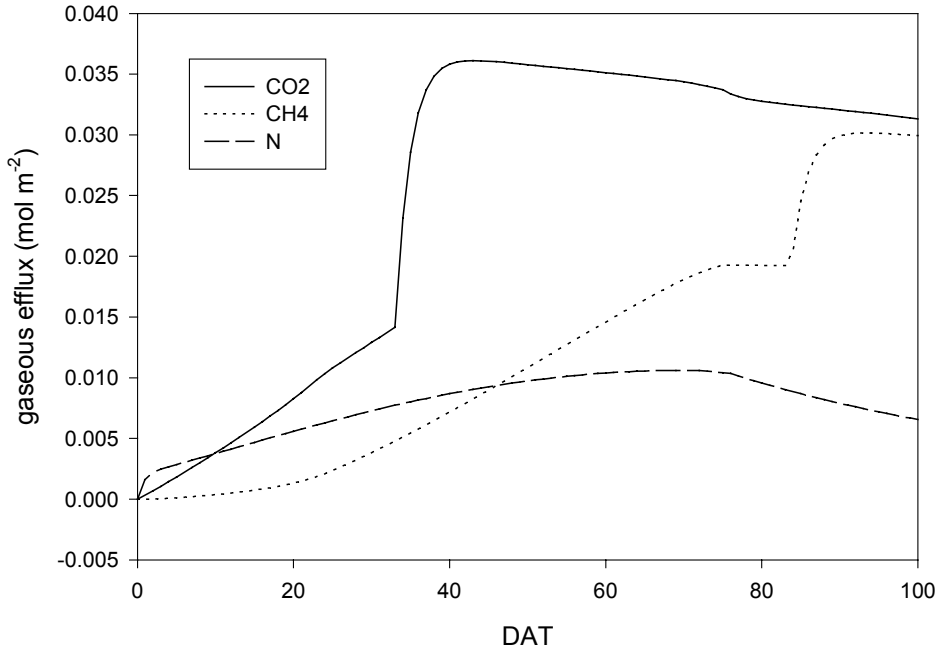

Fig.5.4.6 Simulated rates of N demand and uptake (mol N m^{-3} d^{-1}): default parameter values, no N addition.

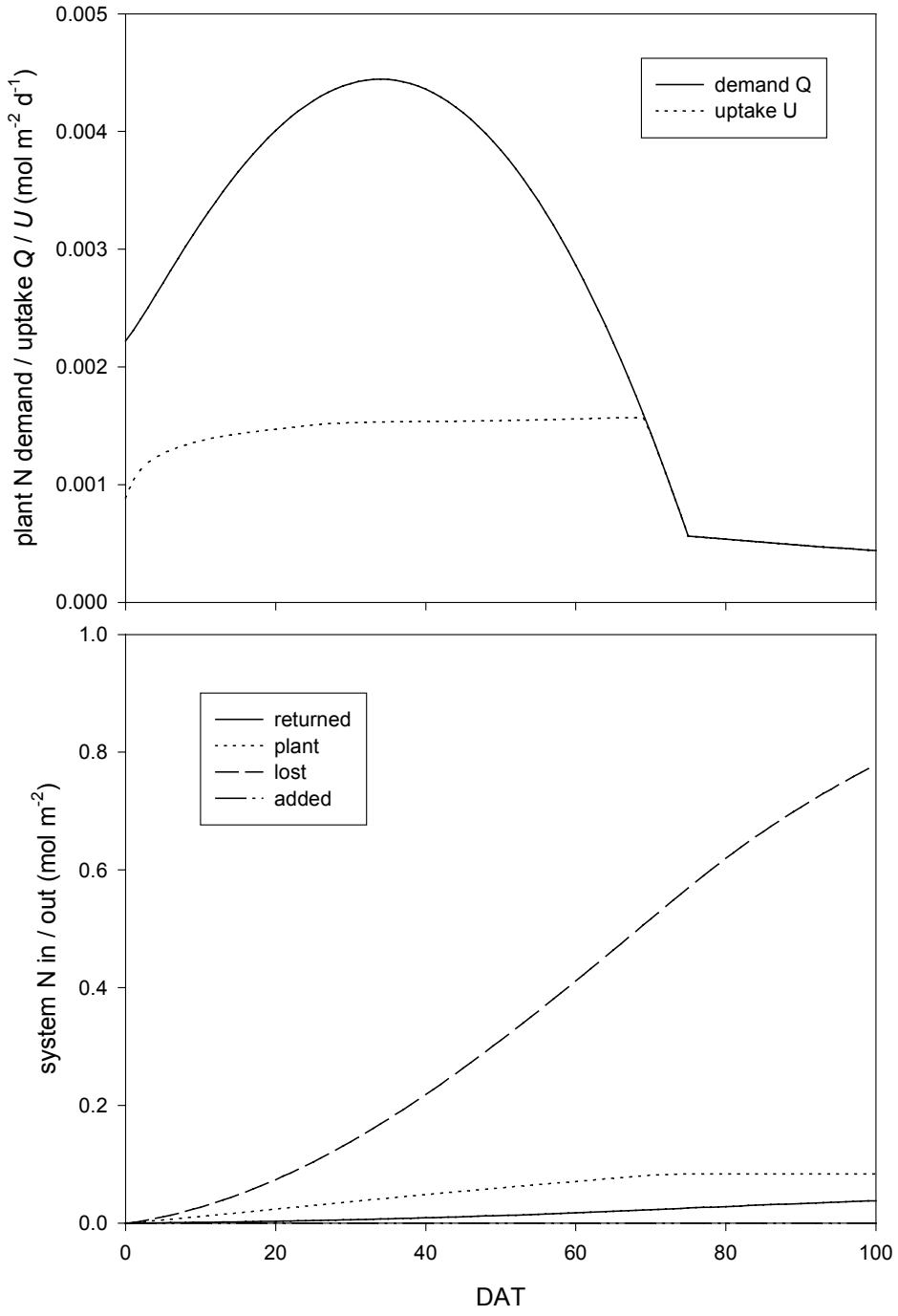

Fig.5.4.7 Simulated system properties (mol m^{-2}): default parameter values, no N addition.

Field-scale

We have in SUMO a model of interactive SOM cycling and plant growth, albeit one in which the treatment of the latter is very simplistic. We now need to relate SUMO's controlling variables and parameters to system-level factors open to management. Anticipating the results of our scenario study (Section 5.7) – in particular, management factor 3 – Table 5.4.5 indicates these relationships.

Table 5.4.5 System-level (management) and SUMO variables.

management option	controls	SUMO variables
flooding/drainage		ε, θ
fertilizer addition		N_{2b}
residue incorporation/removal		$C_{2r/b}$, $C_{3r/b}$, $N_{2r/b}$, $N_{3r/b}$
cultivar selection		φ_J, ν, σ_A, σ_V, σ_J, $t_{\max}$, σ_t, φ_R, ρ_P
cropping density		V
target crop yield		$C_R^{\max}$, N_{2b}

The management-level option of flooding or drainage directly controls the air-filled porosity ε and the volumetric moisture content θ of the system. Fertilizer additions – assumed to be largely into the bulk soil rather than the rhizosphere – directly affect the soluble N concentration N_{2b}. Residue management – assumed to involve homogenisation where straw is incorporated – affects the soluble and LF_1 C and N concentrations of both below-ground compartments. Cultivar selection controls the plant properties φ_R and ρ_P, the plant-growth properties $t_{\max}$ and σ_t, the root properties ν, σ_A, σ_V and σ_J, and the root exudate property φ_R – thankfully, intercultivar differences in these properties are likely to be relatively minor, with the exception of the rhizosphere transmissivity factor ν, which is high for an aerenchymatous crop such as rice but low for most upland crops. Cropping density determines the volume V potentially available to the roots of the growing crop.

Target crop yield is a second-level management variable, encompassing within it various other choices – such as which cultivar to use, what cropping density to employ, and so forth. We assume in what follows that where a specific yield is targeted, fertilizer N additions are tailored to be adequate to meet that target. So responsive a regime for fertilizer N addition is by no means usually the case, but it is the target of at least one major programme at IRRI (Greenland *et al*, 1999), and we adopt it as a potential management option here.

Figures 5.4.8-5.4.13 illustrate the SUMO output equivalent to that in Figs.5.4.2-5.4.7 for the case where nitrogen (N) is added at just the rate necessary to sustain optimal crop growth, *ie*:

$$N_{add} = \left(\frac{V_b + V_r}{V_r}\right)\left(Q - \frac{N_{2r}}{2}\right) \qquad Q > \frac{N_{2r}}{2} \qquad [19]$$

$$N_{add} = 0 \qquad Q \le \frac{N_{2r}}{2} \qquad [20]$$

Fertilizer N is added whenever the mineral N content of the rhizosphere (N_{2r}) falls below 2 times the N demand Q, at precisely the rate needed to bring N_{2r} back up to twice the demand. Fertilizer additions are assumed to be indiscriminate; additions to the rhizosphere and the bulk soil are in proportion to their volumes.

Section 5.7 explores default-SUMO behaviour over a range of situations deemed to be both typical and significant.

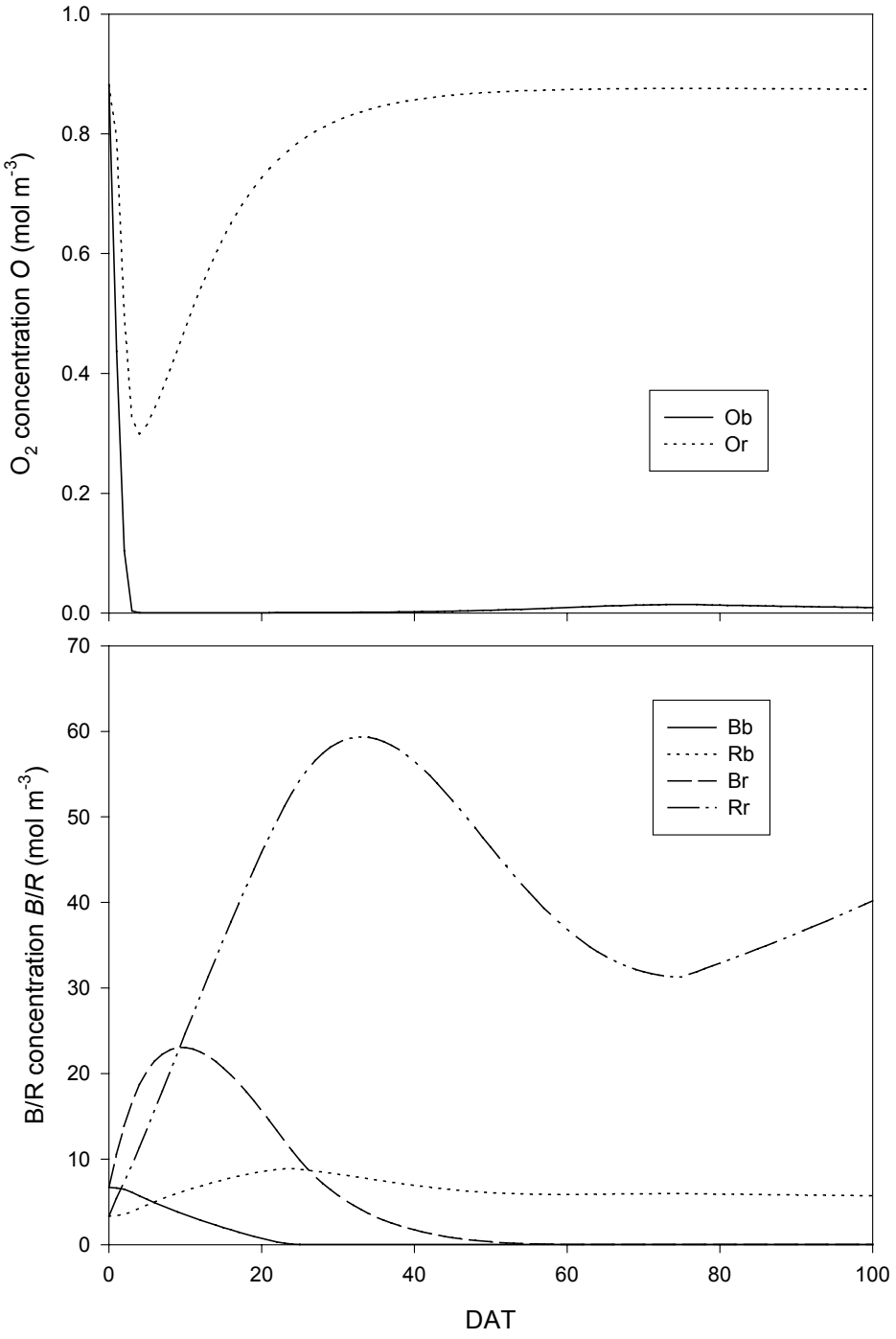

Fig.5.4.8 Simulated concentrations (mol m^{-3}) of O_2 (*O*), oxidised redox buffer (*B*) and reduced redox buffer (*R*) in bulk (*b*) and rhizosphere (*r*) compartments: default parameter values, optimal N addition.

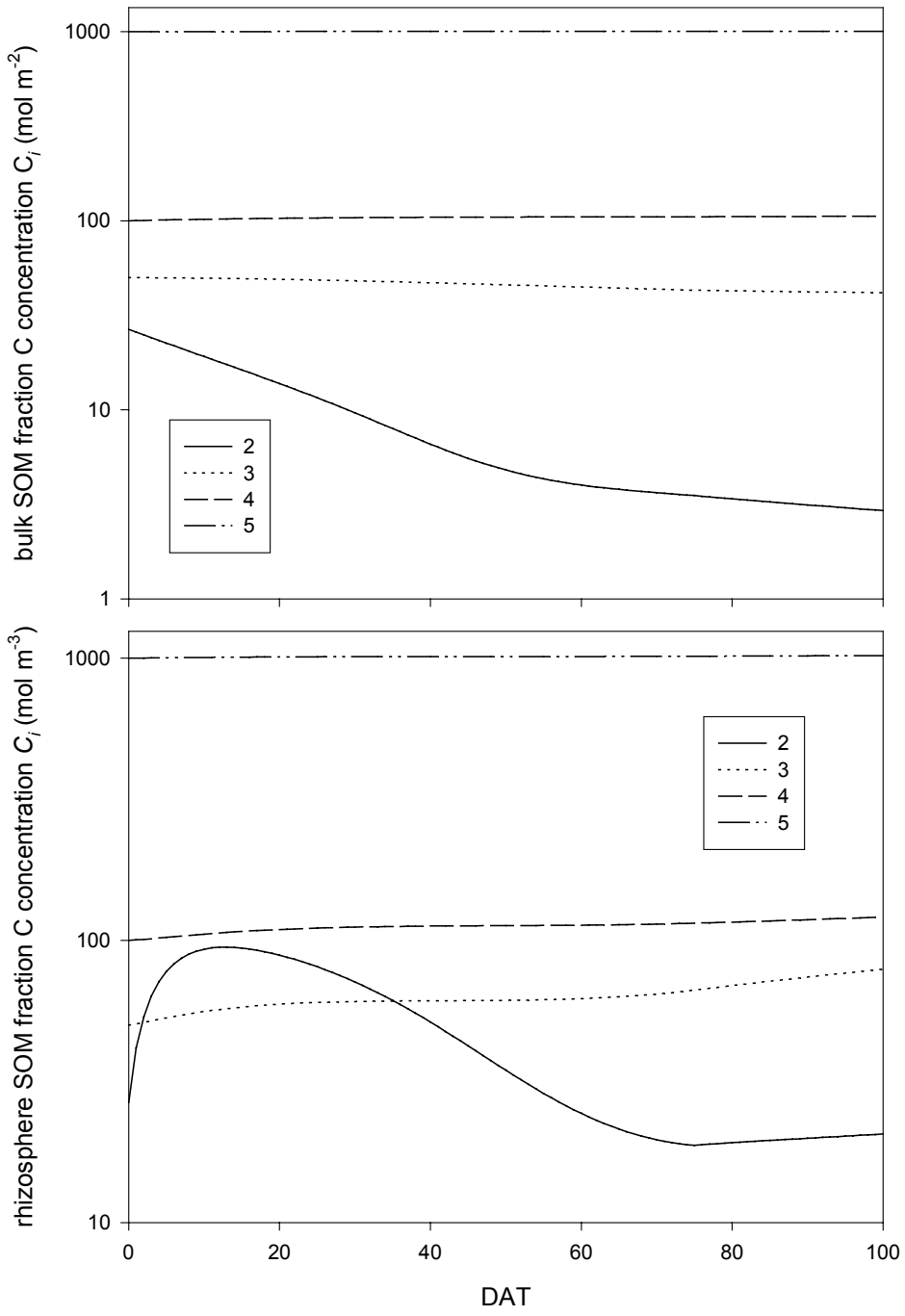

Fig.5.4.9 Simulated C concentrations C_i (mol m^{-3}) of SOM fractions 2-5 in bulk (*b*) and rhizosphere (*r*) compartments: default parameter values, optimal N addition.

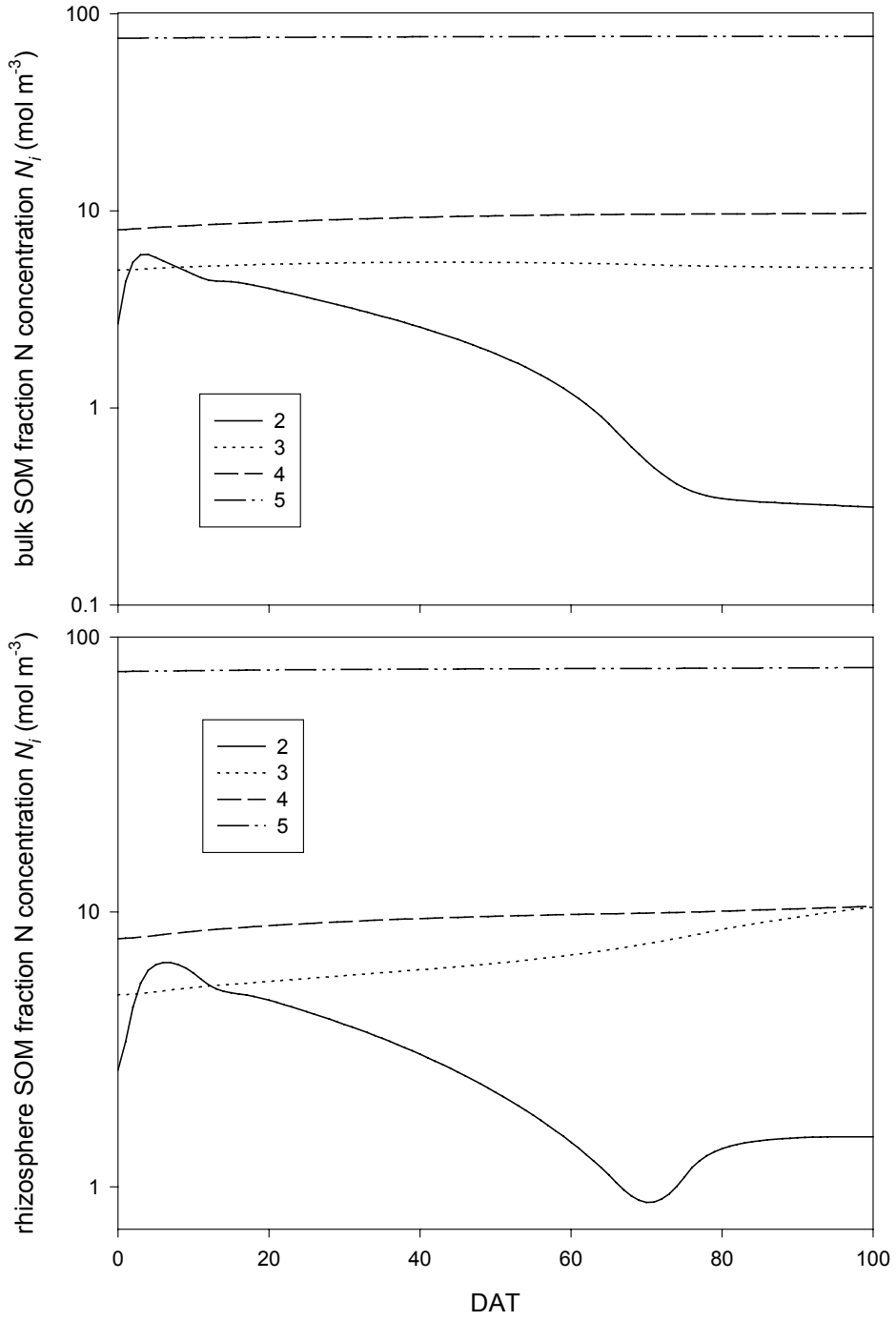

Fig.5.4.10 Simulated N concentrations N_i (mol m^{-3}) of SOM fractions 2-5 in bulk (*b*) and rhizosphere (*r*) compartments: default parameter values, optimal N addition.

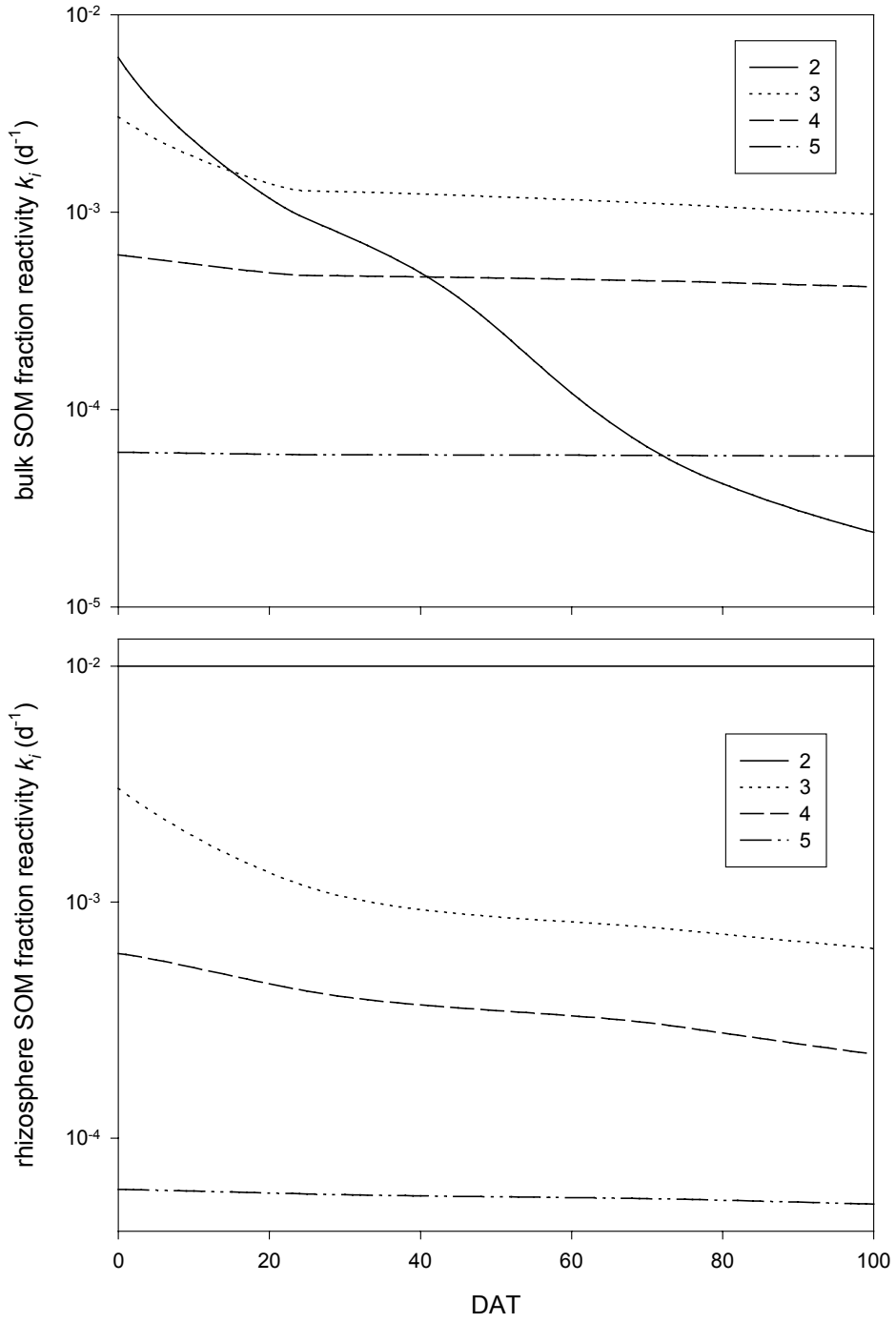

Fig.5.4.11 Simulated SOM fraction reactivity k_i (d^{-1}) of SOM fractions 2-5 in bulk (*b*) and rhizosphere (*r*) compartments: default parameter values, optimal N addition.

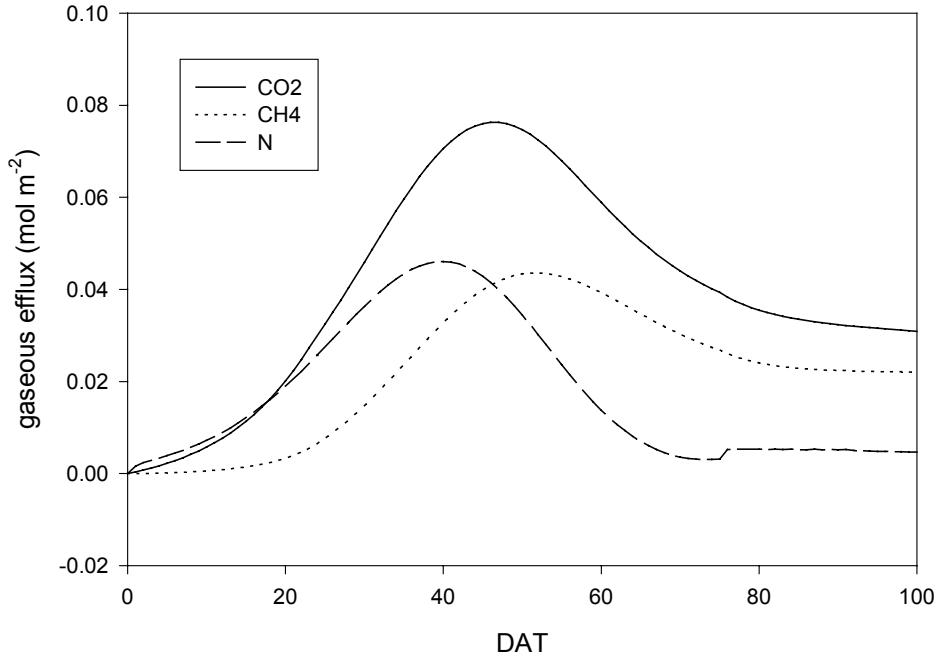

Fig.5.4.12 Simulated rates of N demand and uptake (mol N m^{-3} d^{-1}): default parameter values, optimal N addition.

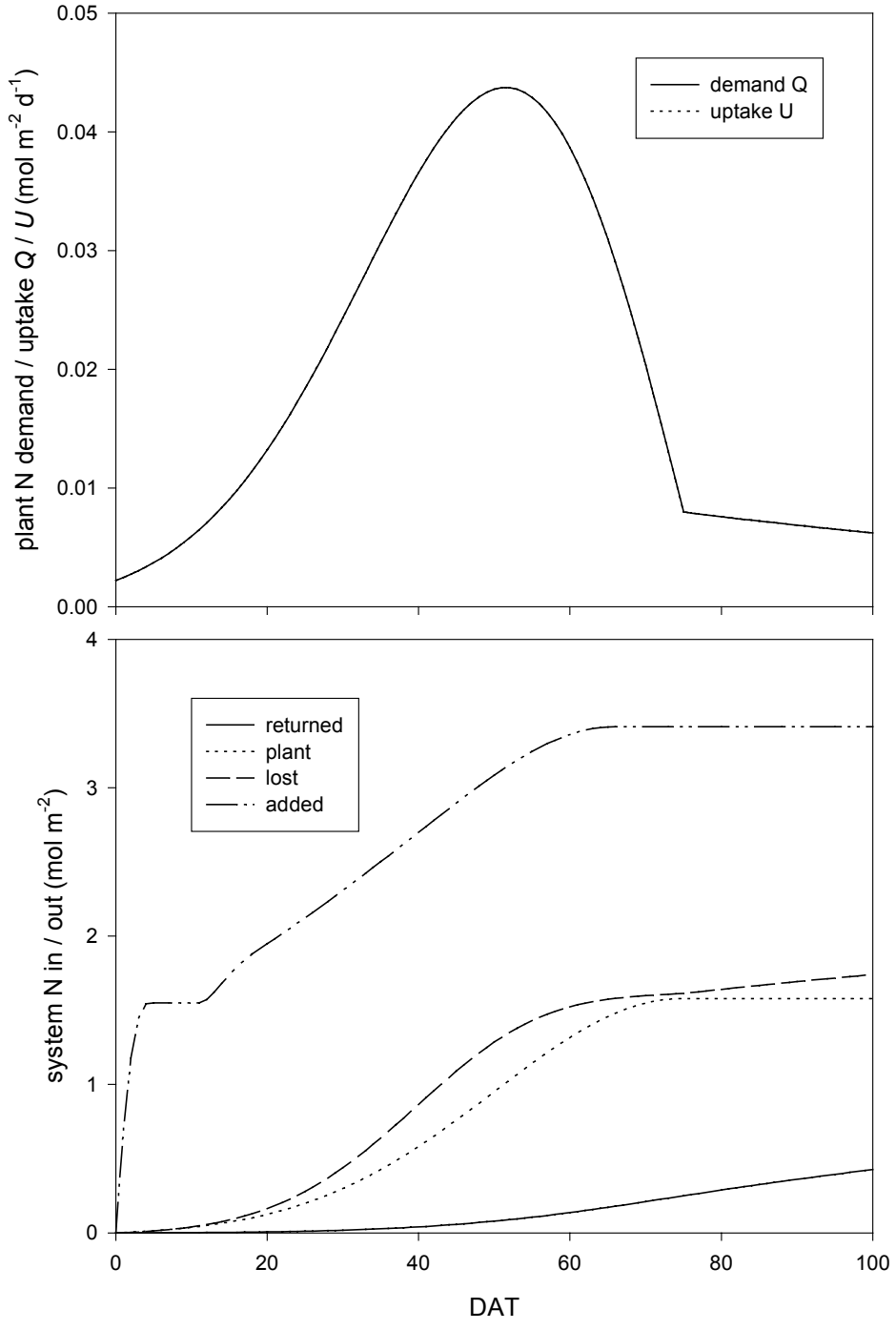

Fig.5.4.13 Simulated system properties (mol m^{-2}): default parameter values, optimal N addition.

References

Greenland D, Plucknett D, Asaduzzaman MD, Swarup A & Dryer H (1999) Report of the external review of the project 'Reversing Trend of Decling Rice Productivity'. International Rice Research Institute, Philippines..

5.5 SOMA analysis

Two things are immediately apparent on inspection of the incubation data presented in Appendices A5.1.1 and A5.1.2. The concentrations (Y_1) of the gaseous fraction appear occasionally to fall as well as to rise, and the error bars on the rates of change ($\Delta Y_i/\Delta t$) are enormous. Our model assumes no fixation, and must therefore fail where Y_1 actually falls. We hope that data from further incubations will eliminate these troublesome values while at the same time reducing the standard deviations we face. One possibility – that of fitting some sort of smoothed curve to the experimental data before attempting analysis by SVD – we reserve for the future.

Calculated fluxes

SVD-calculated inter-fraction type I (biological) C fluxes J^I_{ij} and N fluxes F^I_{ij}, and type II (physical) C fluxes J^{II}_{ij} are illustrated in Appendix A5.5.1 (high E_h treatment: Figures 1-3; medium E_h treatment: Figures 4-6; low E_h treatment: Figures 7-9; N_0 treatment: Figures 10-12; N_{150} treatment: Figures 13-15).

Calculated effluxes (gross mineralisation/immobilisation)

Appendix A5.5.2 illustrates total C and N effluxes from pools 2-5 for the 5 treatments (Figures 1-5).

Calculated effective first-order reactivities

Appendix A5.5.3 (Figures 1-5) illustrates the corresponding effective first-order reactivities kJ_i and kF_i:

$$kJ_i = \sum_{j \neq i}^{5} J_{ij} / C_i \qquad (2 \leq i \leq 5) \qquad [1]$$

$$kF_i = \sum_{j \neq i}^{5} F_{ij} / C_i \qquad (2 \leq i \leq 5) \qquad [2]$$

Many calculated fluxes, effluxes and reactivities are negative. Such values have no meaning. They are caused by (i) the intrinsic inability of the postulated model to deal with declining Y_1 (Y_1 should not decline in an anoxic system); (ii) the large uncertainties associated with each measurement of $\Delta Y_i/\Delta t$; and (iii) the under-determination of the system. We attempt below an alternative approach to fitting this unsatisfactory data, but first simply disregard the meaningless calculated results.

Appendix A5.5.4 illustrates (Figures 1-2) how non-negative kJ_i and kF_i depend on E_h treatment; Figures 3-4 illustrate the same for the N treatment. While there are log-scale differences between the calculated values for the different treatments, it would be premature (in view of the large error-bars not shown and the number of meaningless values discarded) to declare them significant.

Figures 5.5.1 and 5.5.2 illustrate the calculated non-negative C and N reactivities kJ_i and kF_i for all treatments, together with fitted second-order polynomial log-log curves. These curves are not presented as definitive; they merely demonstrate the truth of our primary hypothesis – that the reactivity of measurable SOM fractions must be allowed to change over time.

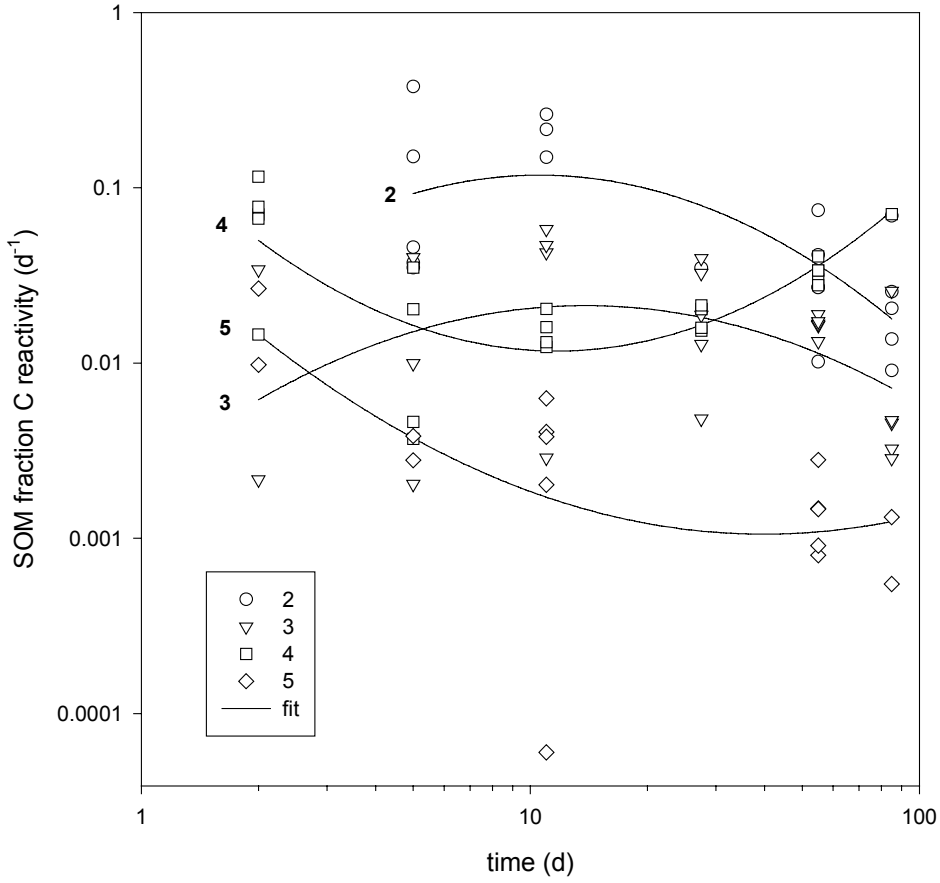

Fig.5.5.1 SOM fraction C reactivity as a function of time: all treatments.

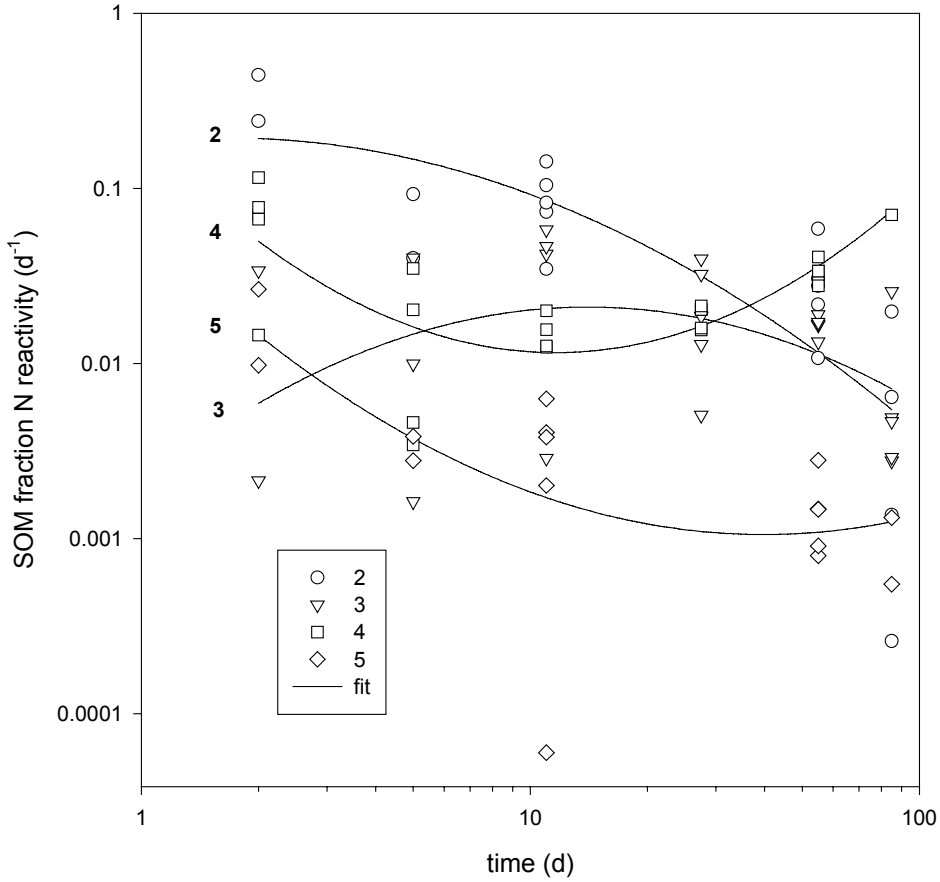

Fig.5.5.2 SOM fraction N reactivity as a function of time : all treatments.

5.6 Preliminary optimisation of SOMO parameters

Our efforts to optimise SOMO's parameters were frustrated by the same variability which confounded our efforts to use SOMA to measure inter-fraction fluxes directly. Rather than recount this frustration in detail, we here indicate only a fraction of our work.

Figures 5.6.1 and 5.6.2 illustrate the performance of SOMO against the measured data from incubation 1 treatment high E_h. Spots denote measurements, lines simulation. Parameters are default (Tables 5.3.6 and 5.3.7) except that initial SOM fraction concentrations are set equal to their measured values.

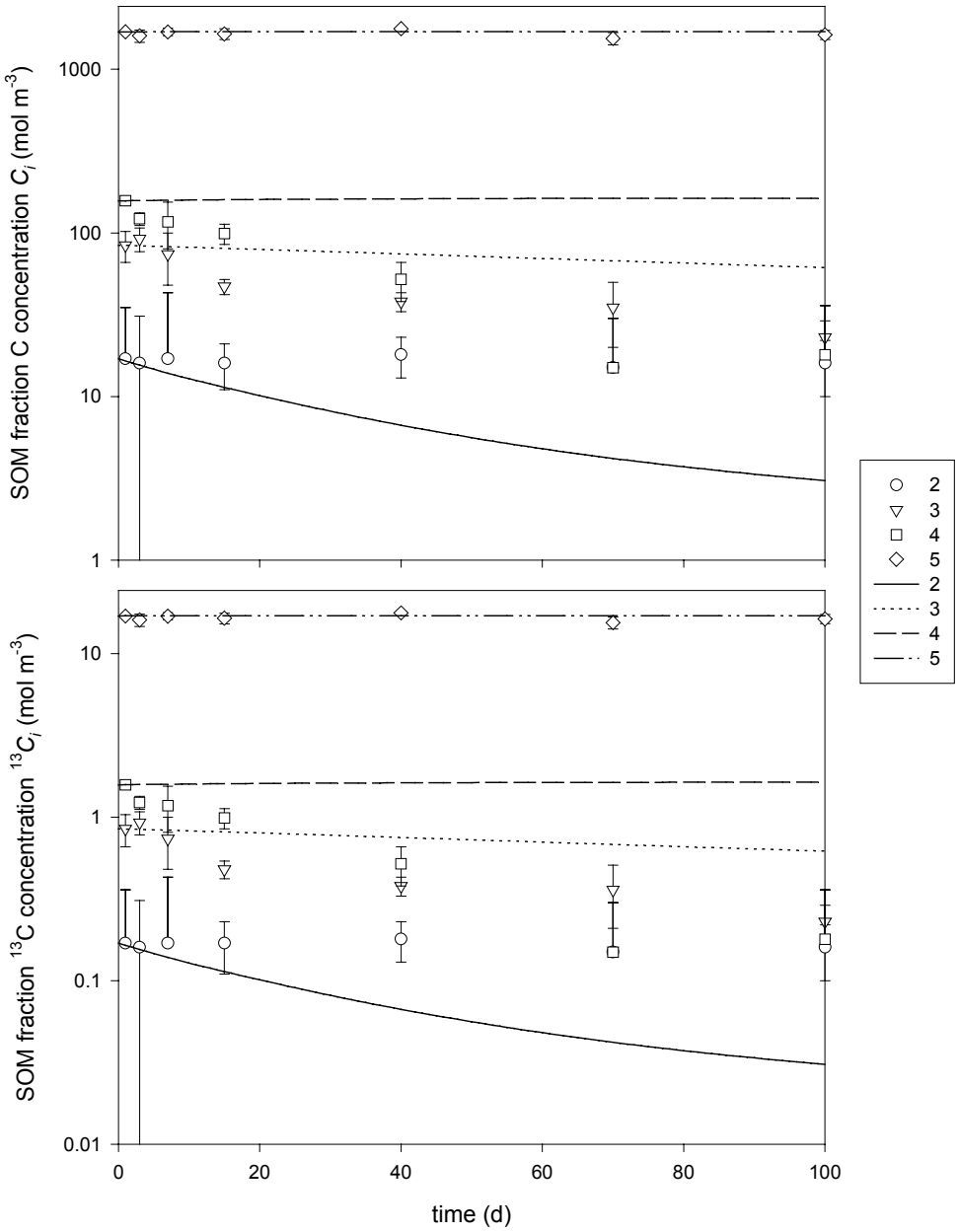

Fig.5.6.1 Measured and simulated SOM C (top) and ^{13}C (bottom) concentrations: un-optimised model.

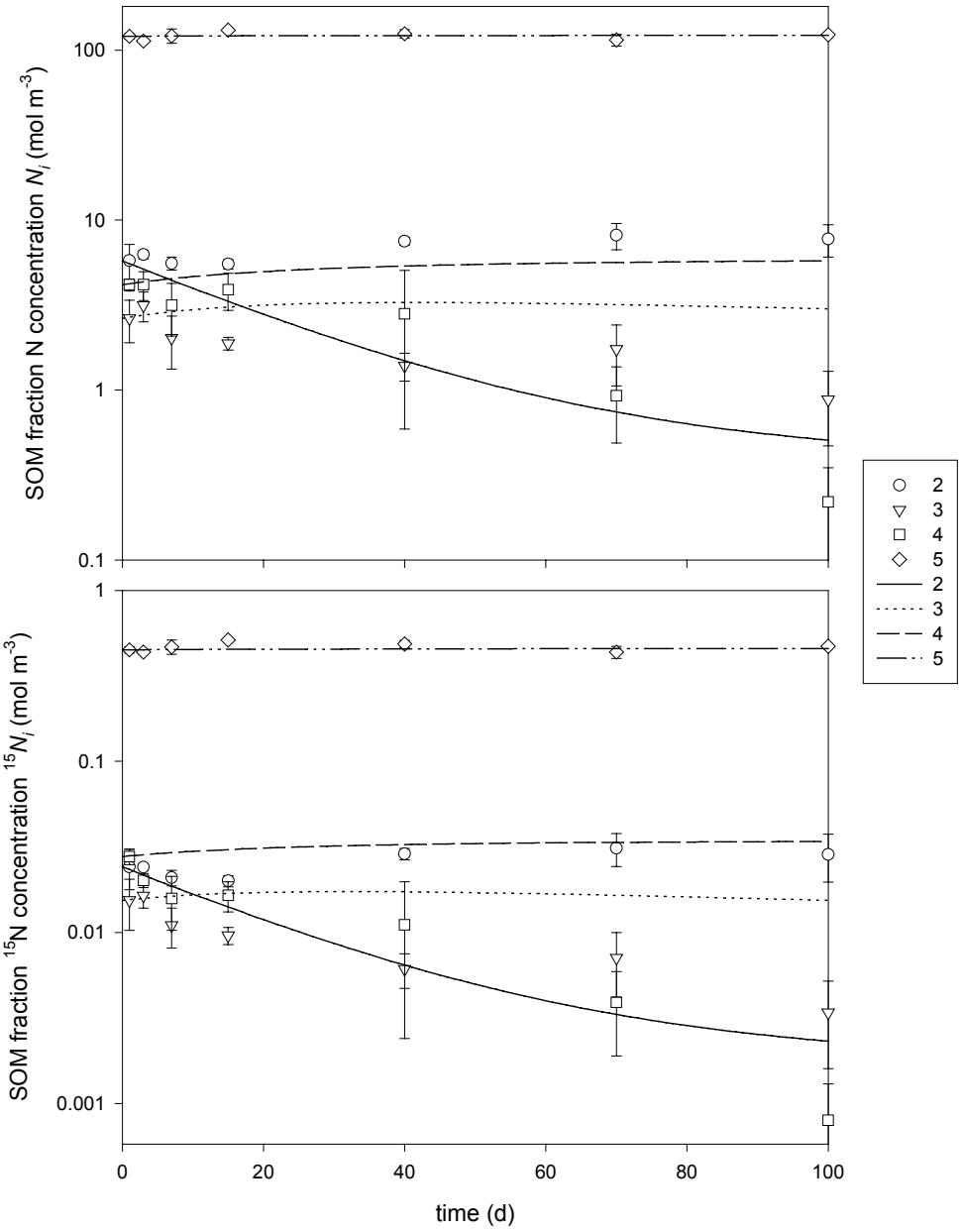

Fig.5.6.2 Measured and simulated SOM N (top) and ^{15}N (bottom) concentrations: un-optimised model.

Figures 5.6.3 and 5.6.4 illustrate the equivalent data following an attempt to optimise the model's standard state rate constants. This attempt was only partially successful, χ^2 being reduced from around 2000 (as for the default parameter values) to around 800.

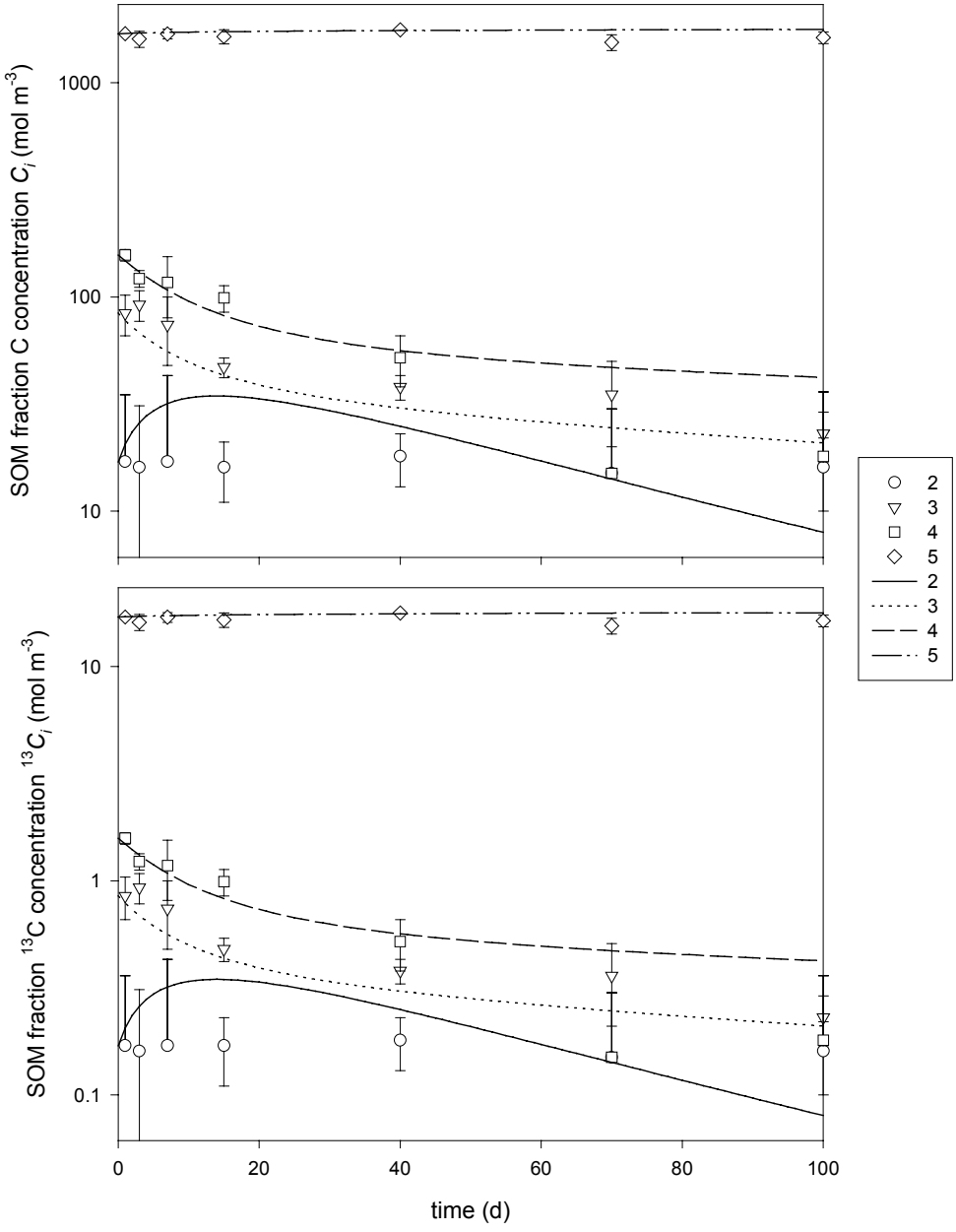

Fig.5.6.3 Measured and simulated SOM C (top) and ^{13}C (bottom) concentrations: partially optimised model.

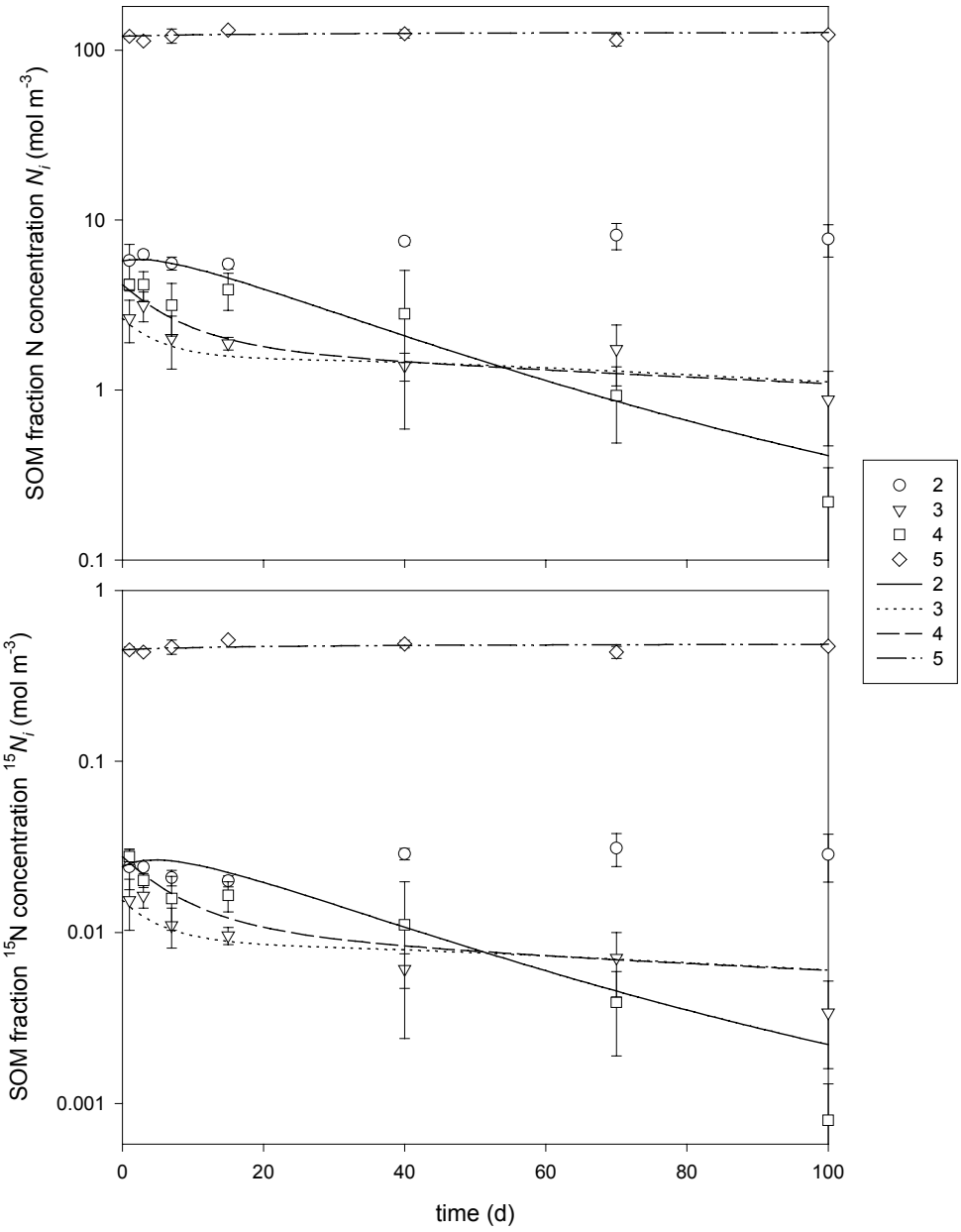

Fig.5.6.4 Measured and simulated SOM N (top) and ^{15}N (bottom) concentrations: partially optimised model.

Optimised parameter values and their uncertainties are given in Table 5.6.1.

Table 5.6.1 Optimised parameter values and uncertainties.

parameter	optimised value	uncertainty
k^o_2	5.7×10^{-9}	1.5×10^{-5}
k^o_3	0.16	0.04
k^o_4	0.09	0.01
k^o_5	10^{-22}	10^{-22}
k_M	0.01	0.01
k_R	7.3×10^{-5}	6.7×10^{-5}

With such a degree of uncertainty attaching to the optimised parameter values – and it is even worse for other treatments – we simply withhold judgement for the moment and proceed with our defaults. We can realistically hope that analysis of incubation runs 2-4 might improve our data and thereby permit better parameter optimisation.

5.7 Sensitivity analysis of SUMO

Although we have so far been unable satisfactorily to parameterise SOMO and hence SUMO, we can still explore the behaviour of SUMO with its default values (Tables 5.3.6-5.3.7 and 5.4.3-5.4.4). To do so, we need to narrow the range of the potential management variables indicated in Table 5.4.5. In order to schematise the enormous range of actual cultivation patterns, we are forced to make several sweeping generalisations and simplifying assumptions. These are not strictly speaking intrinsic to SUMO; given the relevant information (patterns of flooding, plant growth, residue and fertilizer management) any system – no matter how complex – may be modelled. Simplification and generalisation allow the underlying patterns to emerge.

Scenario study

We conducted a literature survey (see References below) to identify the patterns of management options most commonly employed – and most likely to be employed – by rice farmers in Asia. We identified the following 3 major factors, with the following levels:

Factor 1 Rice cropping intensity and/or rotation pattern, which determines both the water and the O_2 regimes of the soil and also the potential level of C input to the soil.

1 triple rice (year-round flooding)
2 double rice + upland crop (2/3 year flooding, 1/3 year dry)
3 double rice + dry fallow (2/3 year flooding, 1/3 year dry)
4 rice + upland crop (1/3 year flooding, 2/3 year dry)

Factor 2 Crop residue management, which determines the level of C input to the soil.

1 100% straw removal
2 50% straw removal
3 no straw removal

Factor 3 Crop yield, which determines – in conjunction with (2) –C and N inputs to the soil.

1 100% potential (8 t ha^{-1} for rice)
2 50% potential
3 25% potential

The levels of factor 1 span the range from the most intense rice production (triple rice) where irrigation water is available all year round, to the most common double rice pattern where less water is available, to the rainfed areas where water is only available for one season of rice. The upland crop mentioned under levels 2 and 4 may generally be taken to be wheat (with potential yield 6 t ha^{-1}). Levels of factor 2 cover the range of possible straw management options. Levels of factor 3 cover the likely range of production system performance.

Combining the identified factors and levels generates 36 possibilities, but some combinations formed by factors 2 and 3 virtually overlap, and the number of effective 2-3 combinations can be reduced to 5, as indicated by the highlighted entries in Table 5.7.1.

Table 5.7.1 Crop residue/crop yield combinations of interest

factor 2 (straw removal)	factor 3 (crop yield)		
	1 (100%)	2 (50%)	3 (25%)
1 (100%)		*x*	*x*
2 (50%)		*x*	
3 (0%)	*x*	*x*	

These 5 combinations cover minimum, medium and maximum levels of C input. They can be combined with the 4 cropping patterns of factor 1 to generate 20 potentially interesting scenarios, as indicated in Table 5.7.2.

Table 5.7.2 Scenarios of interest

scenario	factor 1	factor 2	factor 3
1	1	1	2
2	1	1	3
3	1	2	2
4	1	3	1
5	1	3	2
6	2	1	2
7	2	1	3
8	2	2	2
9	2	3	1
10	2	3	2
11	3	1	2
12	3	1	3
13	3	2	2
14	3	3	1
15	3	3	2
16	4	1	2
17	4	1	3
18	4	2	2
19	4	3	1
20	4	3	2

SUMO input for sensitivity analysis

We assume a 366-day year comprising 3 potential growing seasons each of 100 days separated by 22-day periods of fallow/ground preparation. Growing seasons may be flooded (irrigated rice) or drained (upland crop); fallow periods are assumed to be drained prior to upland cropping, flooded prior to cultivation of irrigated rice. Further, irrigated rice cultivation involves pre-season puddling, which is equivalent to homogenisation of the rhizosphere (*r*) and bulk (*b*) compartments.

The levels of management factor 1 are schematised in SUMO terms by Table 5.7.3, in which the maximum extent of potential root (and hence plant) growth C_R^{max} is represented by the multiple of factor 3 and the maximum potential root mass C_R^{opt} for the relevant crop.

Table 5.7.3 SUMO representation of management factors 1 (column 1) and 3 (f_3).

factor level	SUMO variable	Julian day					
		1-22	22-122	122-124	124-224	224-246	246-346
1	ε	0	0	0	0	0	0
	θ	0.75	0.75	0.75	0.75	0.75	0.75
	C_R^{max}	0	$f_3\ C_R^{opt}{}_{rice}$	0	$f_3\ C_R^{opt}{}_{rice}$	0	$f_3\ C_R^{opt}{}_{rice}$
2	ε	0	0	0	0	0.05	0.05
	θ	0.75	0.75	0.75	0.75	0.7	0.7
	C_R^{max}	0	$f_3\ C_R^{opt}{}_{rice}$	0	$f_3\ C_R^{opt}{}_{rice}$	0	$f_3\ C_R^{opt}{}_{wheat}$
3	ε	0	0	0	0	0.05	0.05
	θ	0.75	0.75	0.75	0.75	0.7	0.7
	C_R^{max}	0	$f_3\ C_R^{opt}{}_{rice}$	0	$f_3\ C_R^{opt}{}_{rice}$	0	0
4	ε	0	0	0.05	0.05	0.05	0.05
	θ	0.75	0.75	0.7	0.7	0.7	0.7
	C_R^{max}	0	1	0	0	0	$f_3\ C_R^{opt}{}_{wheatr}$

where f_3 is 1 for factor 3 level 1, 0.75 for factor 3 level 2 and 0.5 for factor 3 level 3, and fertilizer N is added to the rhizosphere as required to maintain the f_3 production level.

Table 5.7.4 indicates how the levels of management factor 2 (residue management) translate into SUMO terms.

Table 5.7.4 SUMO representation of management factor 2.

factor level	addition on harvest to SOM fraction			
	ΔC_{2b}	ΔC_{3b}	ΔN_{2b}	ΔN_{3b}
1	0	0	0	0
2	$0.5\ \varphi_R\ C_S$	$0.5\ (1\text{-}\varphi_R)\ C_S$	$0.5\ \rho_P\ \varphi_R\ C_S$	$0.5\ \rho_P\ (1\text{-}\varphi_R)\ C_S$
3	$0.75\ \varphi_R\ C_S$	$0.75\ (1\text{-}\varphi_R)\ C_S$	$0.75\ \rho_P\ \varphi_R\ C_S$	$0.75\ \rho_P\ (1\text{-}\varphi_R)\ C_S$

Here we assume that above-ground residues C_S follow the same pattern of partitioning between the soluble and LF_1 fractions as below-ground inputs, and that they possess the same N:C ratio ρ_P. According to our simple picture of plant development, the concentration C_S of the above ground residue (straw) is:

$$C_S = \frac{\varphi_S}{\varphi_R} C_R \qquad [1]$$

where φ_S, the fraction of plant C/N/biomass in the straw, is 0.25. At all levels of factor 2, the total below-ground C content C_R is returned on harvest to the rhizosphere:

$$\Delta C_{2r} = \varphi_J C_R \qquad [2]$$

$$\Delta C_{2r} = (1 - \varphi_J) C_R \qquad [3]$$

Below-ground N $\rho P\ C_R$ is returned *pro rata*.

SUMO output for identified scenarios

Appendix 5.7 illustrates specimen SUMO output from 4-year simulations of the 20 scenarios of Table 5.7.2. We don't have space to include all the simulated variables of potential interest; only the fertilizer N required to maintain the yield level of factor 3, and the gaseous emission fluxes are illustrated.

Figures 5.7.1-5.7.4 below indicate some more of the potential uses of SUMO. The system is that of scenario 1 (triple rice, 100% straw removal, N addition as required to maintain a yield of 50% potential – *ie* 4 t ha^{-1}). The model simulates species concentrations within each of its compartments (Figs.5.7.1-5.7.3), gas fluxes (Fig.5.7.3) and system level properties such as N contents and requirements (Fig.5.7.4). Of course, it also simulates many other properties of interest – inter-compartmental fluxes, SOM fraction reactivities, gross mineralisation rates, fertilizer efficiency and so forth, but we do not wish to labour the point here.

The simulations presented here involve repeated application of the same scenario (*ie* unchanging management). It is equally possible to examine changes in management, and the effects such changes might have on the soil and system properties of interest. We don't go into that here because (i) it would grossly overextend the report, and (ii) since SOMO is not yet properly parameterised we wish to avoid giving the impression that SUMO's simulations are definitive. Suffice to say that work is still in progress.

References

Hossian M (1996) Recent development in the Asian rice economy: Challenges for rice research. In: *Rice Research in Asia: Progress and Priorities* (Evenson RE, Herdt RW & Hossain M, eds). CAB International Wallingford, pp.17-33.

Lawlor DW (1991) Concepts of nutritin in relation to cellular processes and environment. In: *Plant Growth: Interactions with Nutrition and Environment* (Portor JR & Lawlor DW, eds). Society of Experimental Biology Seminar Series, No. 43. Cambridge University Press, Cambridge, pp.4-5.

Pokhrel TP (1997) Cropping patterns and farming systems in rainfed agriculture in selected countries of Asia. In: *Rainfed Agriculture in Asia*. Asian Productivity Organization, Tokyo, pp.51-70.

Ranaweera NFC (1997) Prospects of rainfed agriculture in Asia and Pacific Region. In: *Rainfed Agriculture in Asia*. Asian Productivity Organization, Tokyo, pp.157-166.

Singh, RB & Paroda, RS (1994) Sustainability and productivity of rice-wheat systems in the Asia-Pacific region: Research and technology development needs. In: *Sustainability of Rice-Wheat Production Systems in Asia* (Paroda RS, Woodhead T & Singh RB, eds). Regional Office for Asia and Pacific, FAO, Bangkok, pp.1-35.

Swinnen J (1994) Production and turnover of root-derived organic matter in the rhizosphere of wheat and barley under field conditions. PhD Thesis, Catholic University of Leuven.

Thapa GB & Koirala GP (1997) Current situation of rainfed agriculture in the member countries. In: *Rainfed Agriculture in Asia*. Asian Productivity Organization, Tokyo, pp.31-50.

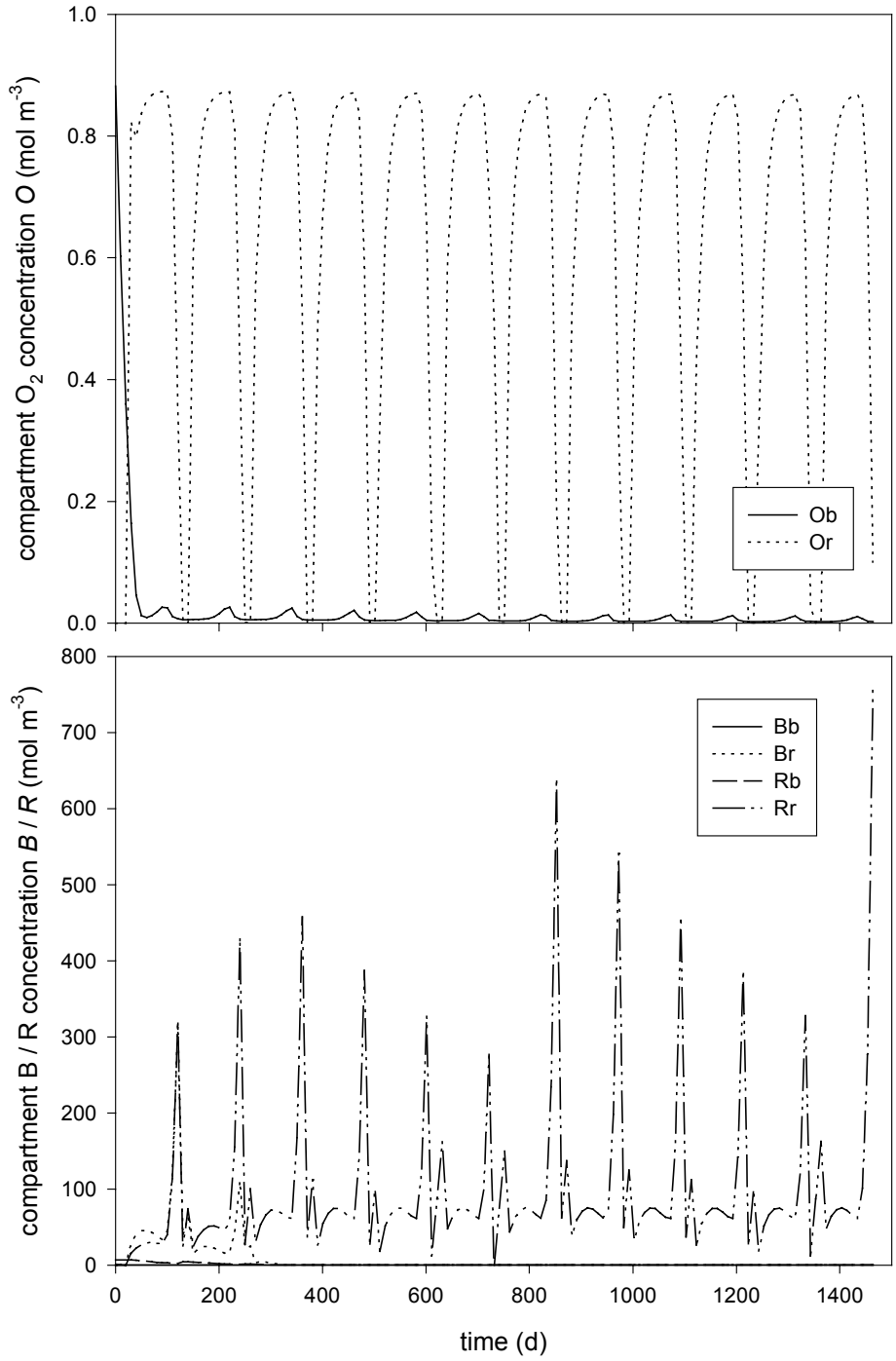

Fig.5.7.1 Simulated compartment concentrations *O* (top) and *B* / *R* (bottom) : 4-year run of scenario 1 (triple rice, 100% straw removal, fertilizer addition for 50% potential yield).

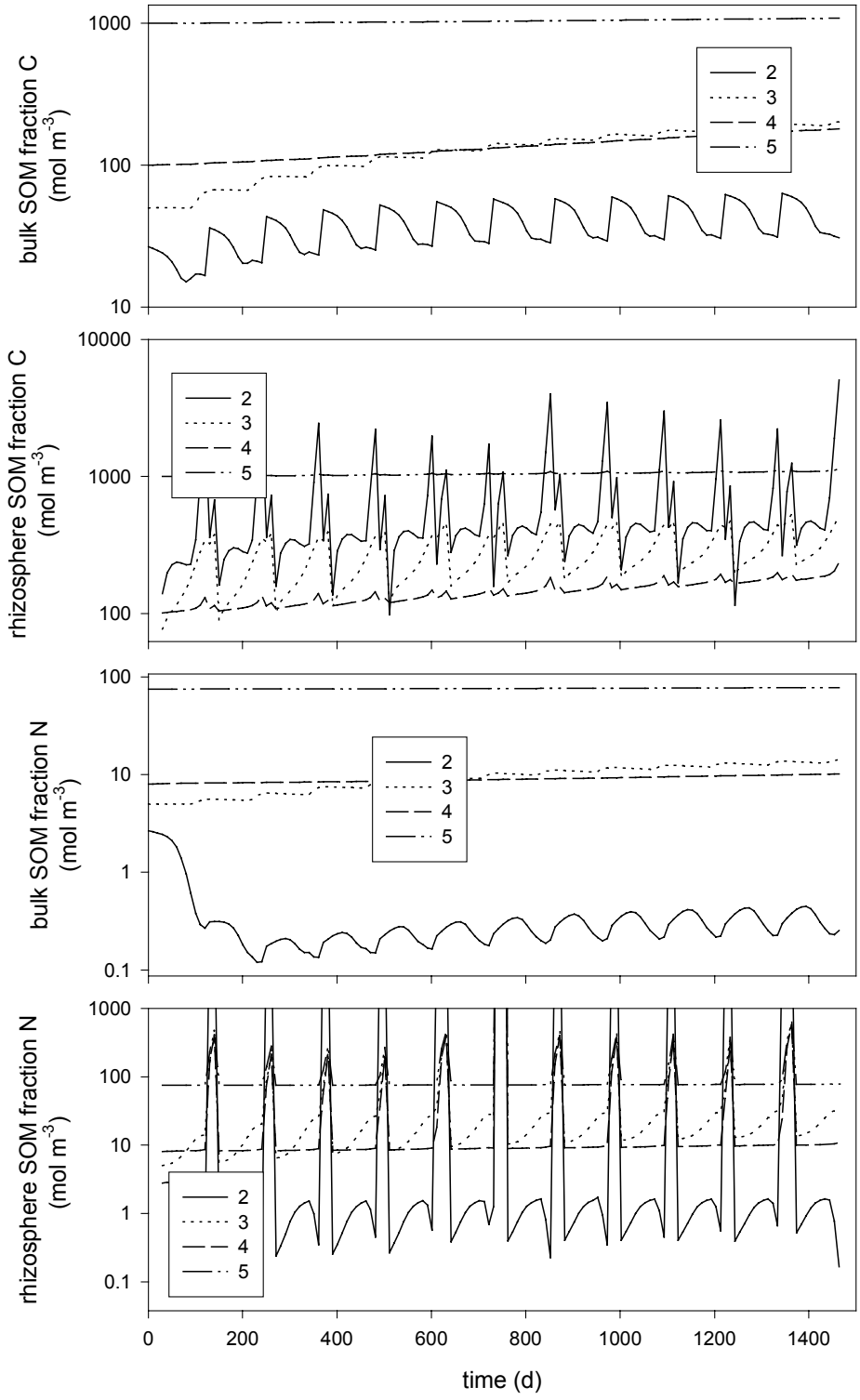

Fig.5.7.2 Simulated SOM fraction concentrations *C* (upper) and *N* (lower) in the bulk and rhizosphere compartments: 4-year run of scenario 1 (triple rice, 100% straw removal, fertilizer addition for 50% potential yield).

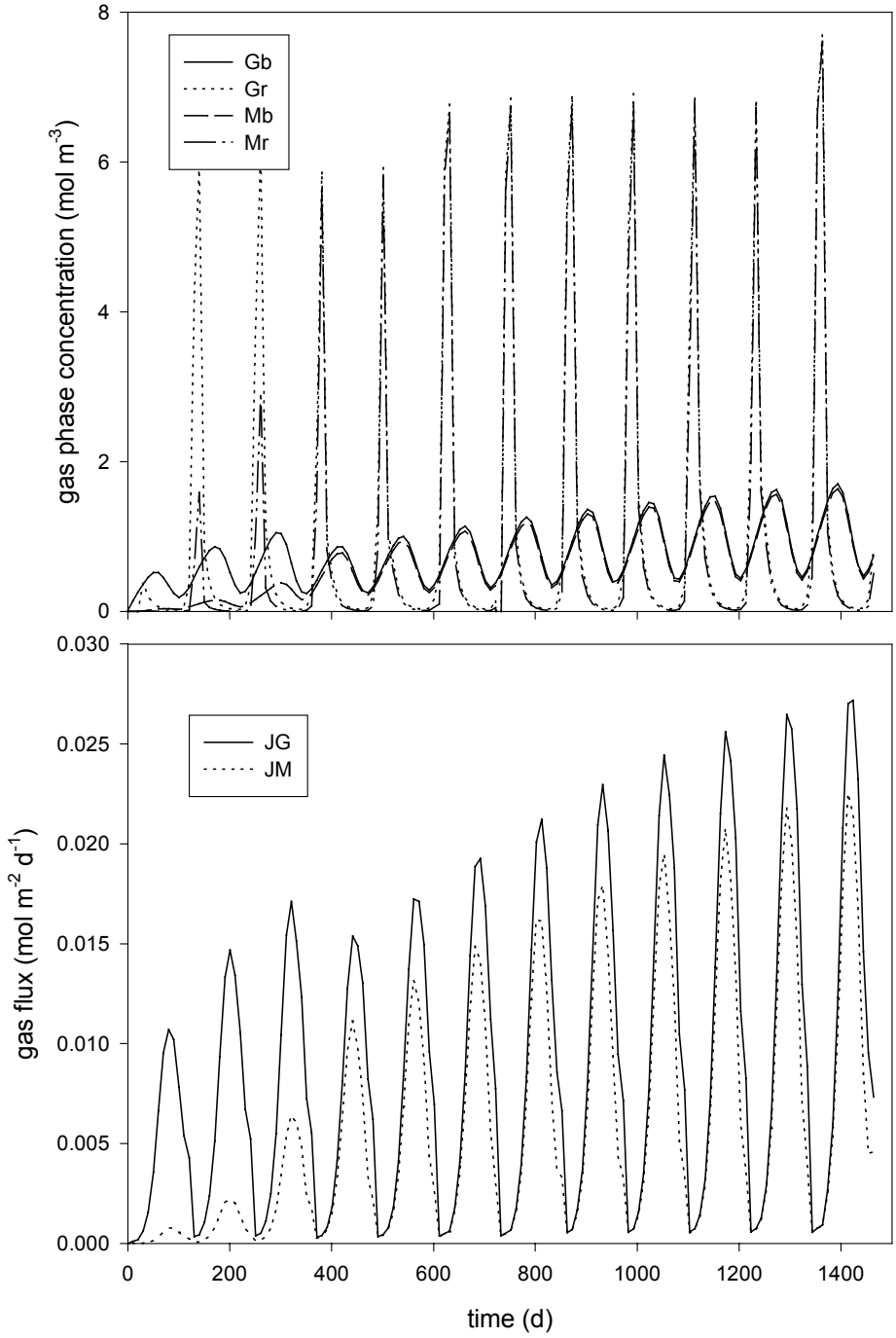

Fig.5.7.3 Simulated compartment concentrations G (CO_2) and M (CH_4) (top) and emission fluxes J_G and J_M (bottom) : 4-year run of scenario 1 (triple rice, 100% straw removal, fertilizer addition for 50% potential yield).

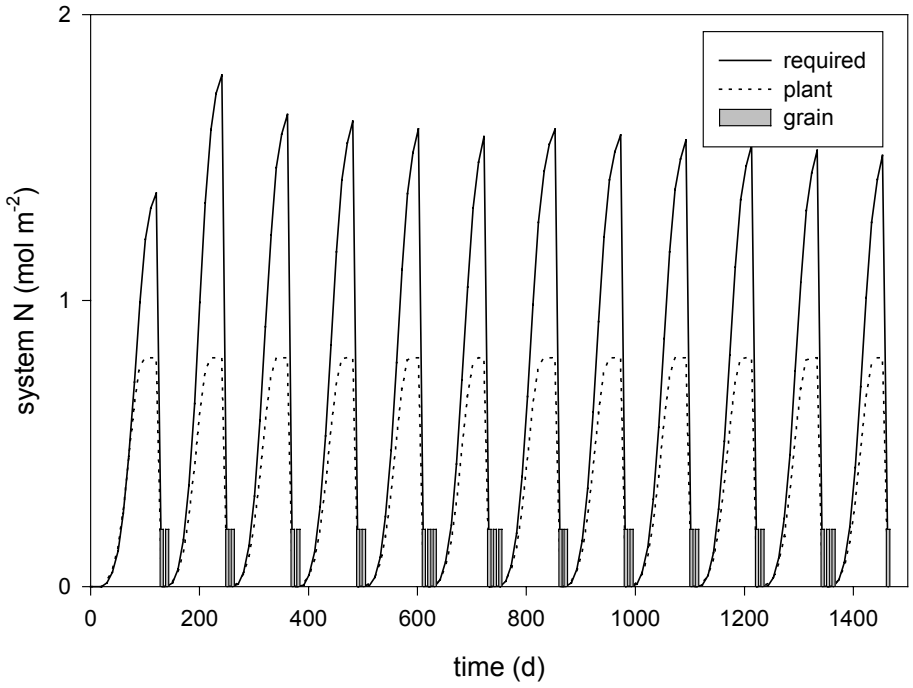

Fig.5.7.4 Simulated system fertilizer N addition, total plant N and grain N content : 4-year run of scenario 1 (triple rice, 100% straw removal, fertilizer addition for 50% potential yield).

5.8 Field data

A fundamental hypothesis of this project is that O_2 availability – or its surrogate, the redox potential E_h – plays an important role in dictating the course of SOM transformations in a periodically flooded soil. This would be of no significance if flooding, residue incorporation, and other system properties open to management did not affect E_h in the field. We therefore monitored soil E_h in the IRRI plots detailed in Section 4.4.

Figure 5.8.1 illustrates the results for the 1999 dry season (DS: Jan-Apr), in which we explored the effects of water management (continuous flooding: treatments 1 and 2; mid-season drainage: treatments 3 and 4) and straw management (removal: treatments 1 and 3; incorporation: treatments 2 and 4). In all treatments, fertilizer N was added at 150 kg N ha^{-1} (N_{150}). Here, as in all figures illustrating field data, DAT denotes days after transplant.

Figure 5.8.2 illustrates the equivalent results for the 1999 wet season (WS: Jul-Oct), in which we explored the effects of water management (continuous flooding: treatments 1 and 2; mid-season drainage: treatments 3 and 4) and fertilizer management (control: treatments 1 and 3; addition of 150 kg N ha^{-1}: treatments 2 and 4). In all treatments, straw was incorporated at a rate of 8 t ha^{-1} (S_1).

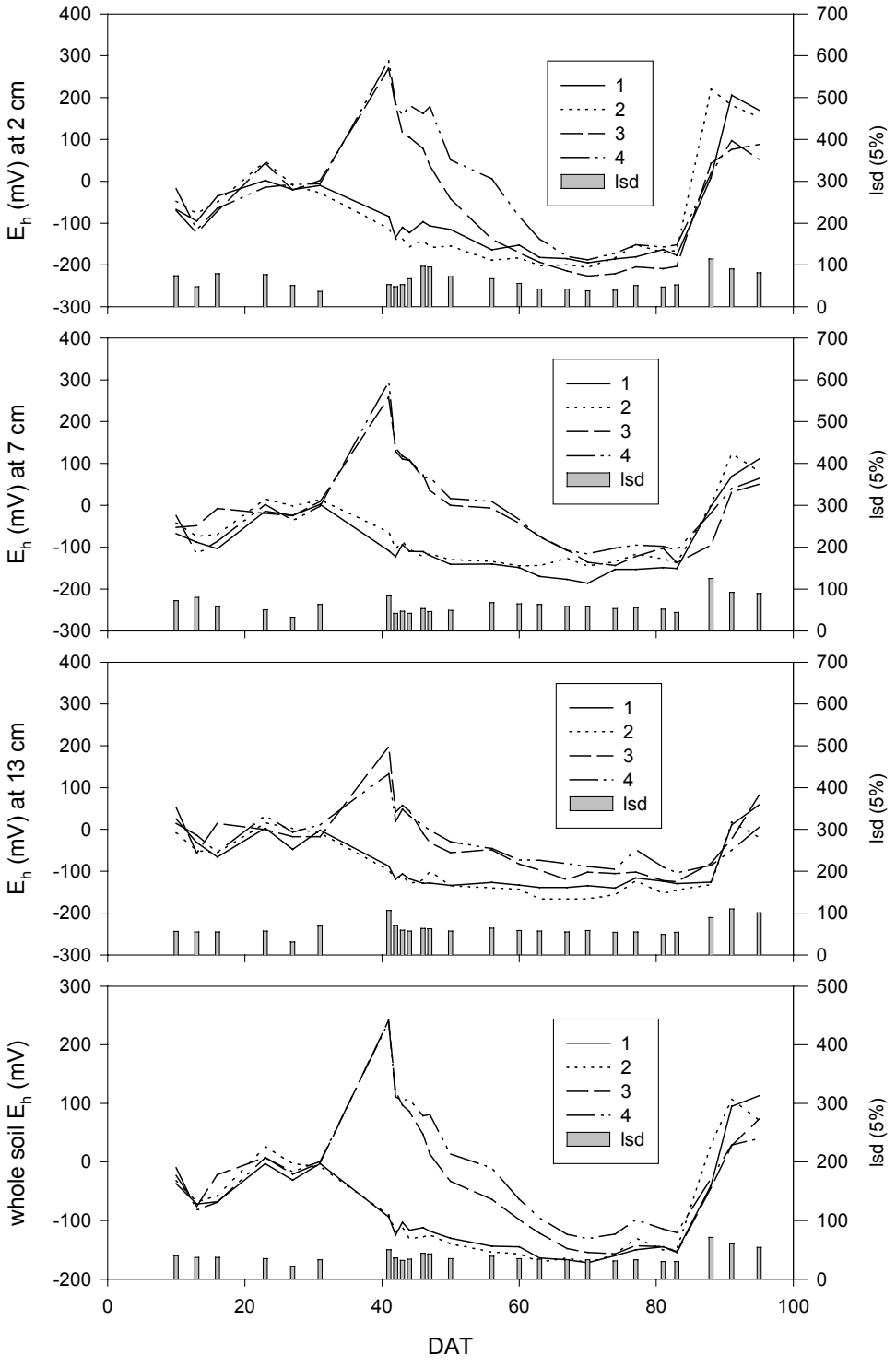

Fig.5.8.1. Soil E_h dynamics at 3 depths and the average over the whole depth : DS 1999. Treatments as in Table 4.4.1; lsd is least significant difference at 5% level.

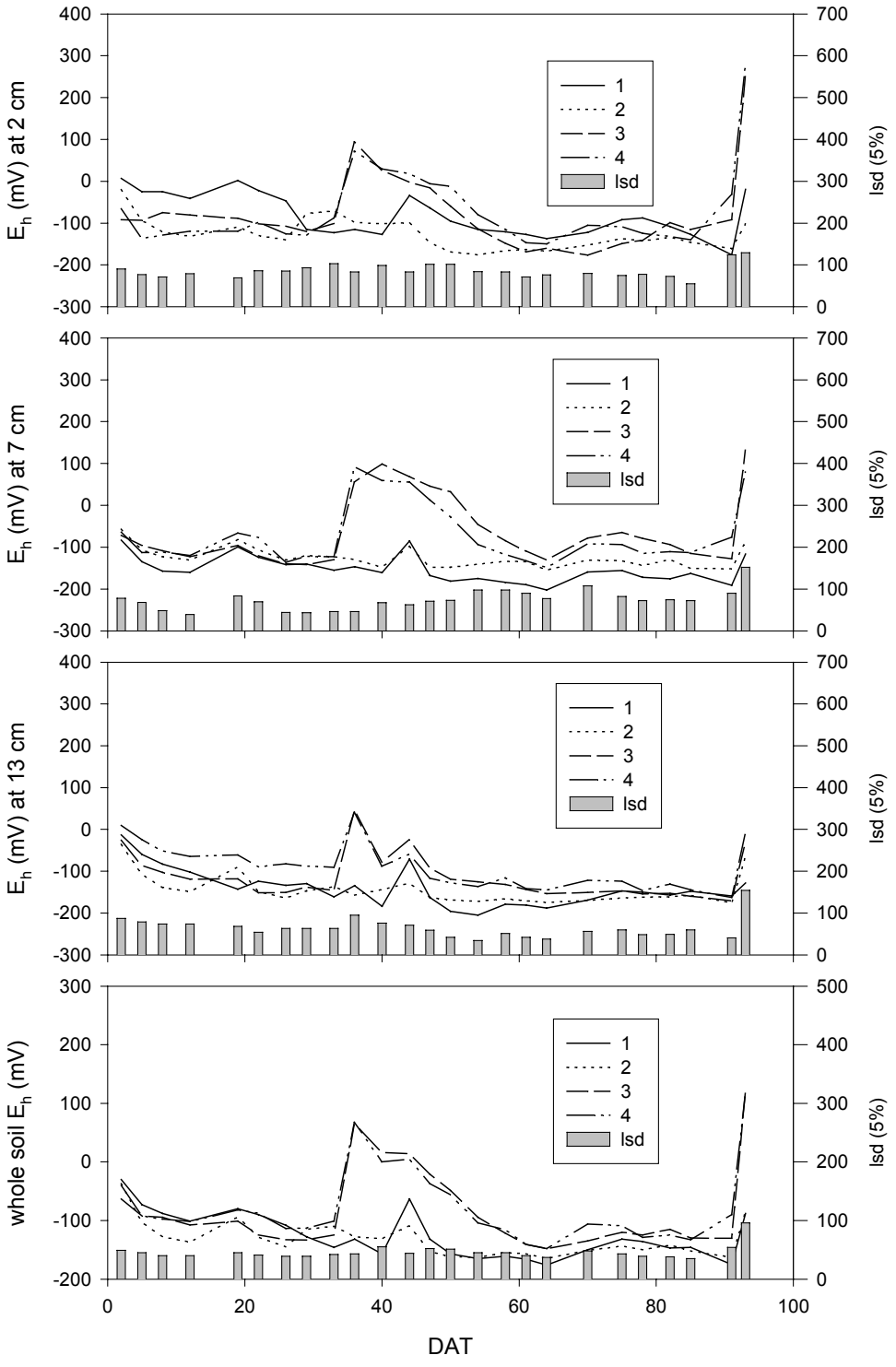

Fig.5.8.1. Soil E_h dynamics at 3 depths and the average over the whole depth : WS 1999. Treatments as in Table 4.4.2; lsd is least significant difference at 5% level.

Effect of water management on Eh

As expected, mid season soil drying (W2) in treatments 3 and 4 of both trials resulted in a remarkable rise of soil E_h, especially in the top 7 cm. The effect was more pronounced in the first trial than in the second, because drainage in the dry season (trial 1) is always likely to be more effective than drainage in the wet season (trial 2). Drainage-induced differences in soil E_h started very soon after irrigation was stopped (around 30 DAT) and lasted about 3 to 4 weeks.

Drainage treatment W0 involves a dry fallow, while treatment W2 does not. This might be expected to lead to significant differences between the initial E_hs of the 2 treatments illustrated in the above figures. It does not, presumably because any such differences disappear during the 2 weeks of flooding between land preparation and transplanting.

6. Contribution of Outputs

The project purpose (Section 3) was to create and test a model of SOM turnover and N availability as affected by flooding-induced anoxia and using the model to identify sustainable and acceptable SOM-management options. This was intended to contribute to improved management of irrigated production systems, focusing initially on rice.

The project was strategic (leading to understanding) rather than applied (leading directly to recommendations). The models SOMO and SUMO provide essential frameworks for understanding and predicting SOM cycling in occasionally flooded soils. We also established the possibility, for the first time, of measuring in-situ SOM fraction reactivity directly.

The understanding derived by this project contributes to DFID's goal to improve livelihoods of poor people through sustainably enhanced production and productivity of RNR systems in a number of ways.

Firstly DFID seeks to achieve these goals through partnerships, including CGIAR and NARS. The strategic modelling / experimental approach and experiment framework reported here is being developed further by the CGIAR and NARS as part of their R&D initiatives to enhance production and productivity. Examples of uptake achieved by the project include:

- The importance of our modelling approach to understand C – N dynamics was recognised by IRRIs fifth external programme management review 1999 – emphasising that both integrated understanding and mathematical models for flooded systems are far behind that of drained agricultural soils. The review recommended collaboration with appropriate centres of excellence to pursue this research.

  IRRI proposed, in 1999, to further develop the modelling framework outlined in this report and submitted a proposal to the German government (including IACR and AAT consultants as partners) to fund further research. The proposal was not funded.
- In Brazil, EMBRAPA Solos developed a project using their own resources that draws upon the fractionation methodology.
- The Rice Wheat Consortium / CIMMYT have included research on soil organic matter in a DFID CRF project. Through the CRF project, collaborators in India and Pakistan are developing their research capacity in this area.

Journal articles have been submitted for publication, further interpretation of results and publications are planned as part the team's active participation in international research. NRSP may wish to support the preparation of these.

Secondly, our modelling approach offers, for the first time, the prospect of testable and predictive SOM models (see background for explanation).

It is recognised that this project differs from other modelling projects funded by NRSP in that we did not aim to produce a product to be promoted and disseminated as a decision support system. This was deliberate given the strategic nature of the project.

A potential application of our model is its incorporation into system level models that describe SOM turnover or nutrient supply. This offers a way to further improve existing decision support tools that are being developed, promoted and used (by others) in a manner consistent with DFID's development goals.

The contribution of simulation models in general to DFID's development aims is subject to debate. We do not propose to enter into that debate here. However it should be noted that our strategy for promotion is likely to be cost effective and could be achieved in a number of ways. The most appropriate route will depend on DFID NRSP's judgement of the value of models.

Thirdly, measuring *in situ* reactivity of SOM fractions opens up new strategic research opportunities. It may enable the contribution of specific enzyme mediated reactions to be related to SOM turnover and nutrient cycling. Such an *in situ* assessment of soil function has hitherto not been possible. This method of assessment could be used as a tool to diagnose loss of soil function, and also be used to identify and develop ways to enhance the function of soils. Examples of the functions we hope to manipulate, degradation of organic pollutants, carbon sequestration as well as nutrient supply. Whilst such research is very much upstream, it could have great relevance to DFIDs developmental goals. However, at present our strategy is to use BBSRC central strategic grant and competitive funding mechanisms to pursue this avenue of research.

7. Publications

Arah J and Yang H 1997. Modelling soil organic matter transformations and nitrogen availability in periodically flooded soil. *INMnet Bulletin*. 1 no: 2. International Rice Research Institute, MCPO Box 3127, 1271 Makati City, Philippines.

Arah JRM. 2000 Modelling SOM cycling in rice-based production systems. pp163-181. In: *Proceedings of International Workshop on C and N Cycling in Rice Soils, April 1999.* International Rice Research Institute, Philippines.

Arah JRM & **Gaunt JL.** 2000**.** Modelling organic matter transformations in soil. In: *Proceeding of BSSS Conference. Edinburgh, Sept 1999 - unpublished*

Arah JRM Isotope tracing of C and N fluxes between measurable SOM fractions. *European Journal of Soil Science – unpublished*

Arah JRM and Kirk GJD. Modelling rice-plant-mediated methane emission. *Nutrient Cycling in Agroecosystems – unpublished*

Arah JRM. Mechanistic simulation of soil-plant-microbe interactions: opportunities and challenges. In: *Interactions in the root environment – an integrated approach, April 2000.* Plant and Soil unpublished

Gaunt JL, SP Sohi, H Yang, N Mahieu and **JRM Arah**. 2000. A procedure for isolating soil organic matter fractions suitable for modeling. In: *Proceedings of BSSS Conference. Edinburgh, Sept 1999 - unpublished*

Gaunt JL, SP. Sohi, **JRM Arah**, N Mahieu, **H Yang** and DS. Powlson. 2000.Physical fractionation of soil to obtain matter fractions suitable for modelling. pp. 89-101. In: *Proceedings of International Workshop on C and N Cycling in Rice Soils, April 1999.* International Rice Research Institute, Philippines.

Institute for Arable Crops Research. 1997. Modelling soil organic matter transformations and nitrogen availability In*: Integrated nutrient management on farmers' fields: Approaches that work*. eds. Gregory PJ, Pilbeam CJ, Walker SH. The Department of Soil Science, The University of Reading, Occasional Publication Number 1.

Institute for Arable Crops Research. 1997. Addressing problems in developing countries. pp. 45-49 *IACR Report for 1996*. IACR Rothamsted, Harpenden, Hertfordshire ISSN 0955-9051.

Institute for Arable Crops Research. 1998. Addressing needs in developing countries - Prediction of nitrogen supply. pp. 43-45 *IACR Report for 1997*. IACR Rothamsted, Harpenden, Hertfordshire ISSN 0955-9051.

Lu Y, **Arah JRM**, Wassmann R and Neue HU (1999) Simulation of CH_4 production in anaerobic rice soils by a simple two-pool model. *Nutrient Cycling in Agroecosystems – Unpublished*

Matthews RB, Wassmann R, **Arah JRM** and Knox J (1999) Up-scaling of experimental measurements of CH_4 emissions from rice fields in South East Asia using a process-based crop/methane simulation model within a GIS environment*. Nutrient Cycling in Agroecosystems – in press*

Powlson DS, Poulton PR and **Gaunt JL.** 1998. The role of long-term experiments in agricultural development. pp 1-16 *In* Proceedings ICAR National Workshop on Long-term Soil Fertility Management through Integrated Plant Nutrient Supply. IISS, Bhopal. April 1st - 4th 1998.

Sohi SP, Mahieu N, **Arah JRM** and **Gaunt JL** (1999) A procedure for isolating soil organic matter fractions suitable for modeling. *Soil Science Society of America Journal - submitted*

Swarup A and **Gaunt JL.** 1998. *Report of working group discussion, pp 326-333 In:* Proceedings ICAR National Workshop on Long-term Soil Fertility Management through Integrated Plant Nutrient Supply. IISS, Bhopal. April 1st - 4th 1998.

Other Publications not covered by FTR template

Symposium, conference, workshop posters/papers (related to communication mainly amongst researchers)

April 1998. Presentation and discussion of project at roundtable discussion / project workshop at IRRI, attended by members of IRRI's research staff involved in the Irrigated Rice Ecosystem Programme (IR2).

Arah JRM. 1998. Presentation of the depth-resolved transport-reaction model attended the final workshop of the UNDP funded Interregional Research Programme on Methane Emission from Rice Fields (GLO/91/G31). Beijing, 11-15 August 1998.

Gaunt JL. 1998. Indicators of changes in soil fertility status: Linking measurements and models. Presentation at UNIQUAIMS Workshop. IACR-Rothamsted 3rd - 8th June 1998. UNIQUAIMS is an EU funded concerted action project: Unification of Indicator Quality for Assessment of Multidisciplinary Systems.

Gaunt JL. 1999. Implications of farmer's needs for soil organic matter research. Invited presentation at Center for Development Research (ZEF) "Managing Organic Matter in Tropical Soils: Scope and Limitations". Bonn 7-10th June 1999 (invited presentation).

Gaunt JL. 1999. Invited presentation and paper to be given at BRRI / IRRI workshop on long term soil fertility experiments 8-11th March 1999. Dhaka.

Gaunt JL, DFID NRSP Research, linkages to CPP. DFID / CPP Rice Crop Protection Workshop. BRRI 6-8th March 1999.

Gaunt JL, SP Sohi, H Yang, N Mahieu and JRM Arah. A procedure for isolating soil organic matter fractions suitable for modeling. Proceeding of BSSS Conference. Edinburgh 15th – 17th Sept 1999

Dr Yang gave a lecture on SOM physical fractionation to the 'Soil and Water Biochemistry and Ecotoxicology Course'. This is a training course organised by IRRI with participants from five countries. Our fractionation protocol was distributed to the participants as a lecture note.

Manuals, guidelines, databases for non-specialist users

Models SOMO, SUMO and SOMA are available as modelmaker™ programmes. These can be obtained via:

IACR Rothamsted, West Common, Harpenden, Hertfordshire, AL5 2JQ

Dr J Arah, AAT Consultants, 15 Clerk Street, Edinburgh EH8 9JH, Scotland UK

Media presentations (videos, websites, popular press, TV, radio, etc)

Qtr 3 1997 John Gaunt was interviewed by Wrenmedia, contributing to a programme for the BBC World service. Interview covered aspects of rice production and sustainability, DFID's support was acknowledged.

8. Internal Documents

- Modelling SOM turnover in oxic/anox soils – preliminary thought – pre project Jan 1996
- Minutes of the IR2 project meeting – Feb 1998
- Modelling in R6750 – November 1998
- Documentation of Computer Interfaced Soil Incubation Controlling System – June 1998
- Development and testing of Physical SOM Fractionation Protocol in Rice Soils – June 1998
- Outline of Field Experiment for DFID Project 'Modelling Soil Organic Matter Transformations and Nitrogen Availability in Periodically Flooded Soils' – December 1998
- Copy of section 5.1.4 of 5th EPMR report – January 1999
- SOM-fraction incubation model (yang.mod) - December 1999
- Dual-compartment SOM transformation model – undated
- SOMA analysis – February 2000

Email correspondence is available for inspection at IACR, and documents can be obtained from IACR Rothamsted, West Common, Harpenden, Hertfordshire, AL5 2JQ